Advanced Combustion Systems for Next Generation Gas Turbines

Final Report

June 2002

December 2005

Joel Haynes, Jonathan Janssen, Craig Russell, Marcus Huffman

January 2006

DE-FC26-01NT41020

GE Global Research

1 Research Circle

Niskayuna, NY 12309

DISCLAIMER

This report was prepared as an account of work sponsored by an agency of the United States Government. Neither the United States Government nor any agency thereof, nor any of their employees, makes any warranty, express or implied, or assumes any legal liability or responsibility for the accuracy, completeness, or usefulness of any information, apparatus, product, or process disclosed, or represents that its use would not infringe privately owned rights. Reference herein to any specific commercial product, process, or service by trade name, trademark, manufacturer, or otherwise does not necessarily constitute or imply its endorsement, recommendation, or favoring by the United States Government or any agency thereof. The views and opinions of authors expressed herein do not necessarily state or reflect those of the United States Government or any agency thereof.

Abstract

Next generation turbine power plants will require high efficiency gas turbines with higher pressure ratios and turbine inlet temperatures than currently available. These increases in gas turbine cycle conditions will tend to increase NOx emissions. As the desire for higher efficiency drives pressure ratios and turbine inlet temperatures ever higher, gas turbines equipped with both lean premixed combustors and selective catalytic reduction after treatment eventually will be unable to meet the new emission goals of sub-3 ppm NOx. New gas turbine combustors are needed with lower emissions than the current state-of-the-art lean premixed combustors.

In this program an advanced combustion system for the next generation of gas turbines is being developed with the goal of reducing combustor NOx emissions by 50% below the state-of-the-art. Dry Low NOx (DLN) technology is the current leader in NOx emission technology, guaranteeing 9 ppm NOx emissions for heavy duty F class gas turbines. This development program is directed at exploring advanced concepts which hold promise for meeting the low emissions targets.

The trapped vortex combustor is an advanced concept in combustor design. It has been studied widely for aircraft engine applications because it has demonstrated the ability to maintain a stable flame over a wide range of fuel flow rates. Additionally, it has shown significantly lower NOx emission than a typical aircraft engine combustor and with low CO at the same time. The rapid CO burnout and low NOx production of this combustor made it a strong candidate for investigation. Incremental improvements to the DLN technology have not brought the dramatic improvements that are targeted in this program. A revolutionary combustor design is being explored because it captures many of the critical features needed to significantly reduce emissions.

Experimental measurements of the combustor performance at atmospheric conditions were completed in the first phase of the program. Emissions measurements were obtained over a variety of operating conditions. A kinetics model is formulated to describe the emissions performance. The model is a tool for determining the conditions for low emission performance. The flow field was also modeled using CFD.

A first prototype was developed for low emission performance on natural gas. The design utilized the tools anchored to the atmospheric prototype performance. The 1/6 scale combustor was designed for low emission performance in GE's FA+e gas turbine.

A second prototype was developed to evaluate changes in the design approach. The prototype was developed at a 1/10 scale for low emission performance in GE's FA+e gas turbine. The performance of the first two prototypes gave a strong indication of the best design approach.

Review of the emission results led to the development of a 3rd prototype to further reduce the combustor emissions. The original plan to produce a scaled-up prototype was pushed out beyond the scope of the current program. The 3rd prototype was designed at 1/10 scale and targeted further reductions in the full-speed full-load emissions.

Table of Contents

List of Figures

1 Introduction

1.1 Background

The trapped vortex combustion concept has been under investigation since the early 1990's, but until recently the focus has been on liquid fuel applications for aircraft combustors. The Air Force Research Lab (AFRL) initially conducted studies of cavity stabilized flames in a free stream and found certain configurations to be very stable. Following this work, a 4" cylindrical prototype combustor was developed with GE Aircraft Engines for operation at atmospheric conditions and gaseous propane fuel. The results demonstrated the TVC capability for low emissions and lean blowout stability enhancement. A second prototype was then developed for higher pressure demonstrations with liquid fuel. Complications with the liquid fuel injector design at subscale drove the research effort to begin investigating a more representative 6" rectangular prototype for liquid fuels at atmospheric pressure. This rig was used to investigate the air and fuel injection locations as well as the driver air hole locations. The preferred cavity aero design was then applied to the development of a 12" rectangular prototype for high pressure operation with liquid fuels. This prototype has demonstrated 50% NOx reductions with liquid fuels while maintaining better than 99% combustion efficiency over a much larger turndown range. Tests confirmed the applicability of the concept for aircraft and marine gas turbine engine application. The strong performance of the concept and attractive features of the design for low emission application led to the proposal of this program.

1.2 Design philosophy

Advanced gas turbines operate at higher turbine firing temperatures and pressures. An advanced gas turbine combustor must then be suitable for creating higher turbine inlet temperatures without producing excessive emissions. At high temperatures and lean conditions the Zeldovich mechanism for thermal NOx formation is the primary mode of NOx production. This relatively slow mechanism can require more than 100 milliseconds to reach 99% of equilibrium at gas turbine temperatures & pressures. Early on in this process the formation rate can be treated as a nearly linear function of time; therefore, a reduction in the combustor residence time will lead to a proportional reduction in the thermal NOx formation.

One reason the trapped vortex combustor was chosen as a suitable technology for an advanced combustor is that it has the potential to reduce NOx emissions by lowering the combustor residence time by 50%. Current state-of-the-art combustors can not be modified for shorter residence times because the additional time is needed to reduce CO emissions.

Competing against the thermal NOx formation mechanism is the CO burnout mechanism. CO must be kept to single digit ppm emission levels to meet regulations. To obtain good burnout of CO, temperatures need to be kept high at lean conditions, and good mixing of the combustion air needs to occur. The CO burnout mechanism is a strong function of temperature, so any cold regions of the combustor will retain CO

rather than reduce it to CO2. Traditionally, heavy duty gas turbine combustors have been designed with residence times greater than 20 milliseconds to provide adequate time for CO burnout. The trapped vortex combustor obtains more vigorous mixing at high temperatures at the head end which facilitates a more rapid destruction of CO.

The high temperatures associated with a diffusion flame front can contribute significantly to NOx formation in the combustor. State-of-the-art combustors have moved away from diffusion flames to premixed fuel-air designs which significantly reduce peak flame temperatures. This has proven to be the best mechanism for achieving low NOx emissions. The power generation TVC combustor incorporates fuel-air premixing as well to obtain even lower emissions than the state-of-the-art.

One drawback to fuel-air premixing has been combustion instabilities at ultra lean conditions. These instabilities involve the temporal quenching of the flame. The trapped vortex combustor has the potential for better success in this area because of the demonstrated performance in aircraft engine configurations. The cavity reaction zone helps stabilize lean flames in the main burner and has appeared to decrease combustion instabilities. This has given the TVC combustor greater flexibility in operability than state-of-the-art lean premixed combustors.

2 Executive Summary

Next generation turbine power plants will require high efficiency gas turbines with higher pressure ratios and turbine inlet temperatures than currently available. These increases in gas turbine cycle conditions will tend to increase NOx emissions. As the desire for higher efficiency drives pressure ratios and turbine inlet temperatures ever higher, gas turbines equipped with both lean premixed combustors and selective catalytic reduction after treatment eventually will be unable to meet the new emission goals of sub-3 ppm NOx. New gas turbine combustors are needed with lower emissions than the current state-of-the-art lean premixed combustors.

In this program an advanced combustion system for the next generation of gas turbines is being developed with the goal of reducing combustor NOx emissions by 50% below the state-of-the-art. Dry Low NOx (DLN) technology is the current leader in NOx emission technology, guaranteeing 9 ppm NOx emissions for heavy duty F class gas turbines. This development program is directed at exploring advanced concepts which hold promise for meeting the low emissions targets.

The trapped vortex combustor is an advanced concept in combustor design. It has been studied widely for aircraft engine applications because it has demonstrated the ability to maintain a stable flame over a wide range of fuel flow rates. Additionally, it has shown significantly lower NOx emission than a typical aircraft engine combustor and with low CO at the same time. The rapid CO burnout and low NOx production of this combustor made it a strong candidate for investigation. Incremental improvements to the DLN technology have not brought the dramatic improvements that are targeted in this program. A revolutionary combustor design is being explored because it captures many of the critical features needed to significantly reduce emissions.

In the first phase of the program a liquid fuel, rectangular TVC prototype for aircraft engine applications was converted into a natural gas fired combustor. The conversion to gaseous fuel incorporated four types of fuel injectors, one diffusion mode injector and four premixed injectors. The diffusion mode demonstrated low NOx performance and a strong cavity vortex. The premixed injectors disrupted the cavity vortex and generated high CO. The premixed injector design needed to be improved to support a strong cavity vortex.

CFD modeling of the atmospheric prototype with diffusion injectors was performed. The strong agreement between the CFD model and experimental measurements gave credibility to the modeling approach.

The premixed configurations were modeled, and the shortcomings of the designs were evident. The cavity flow field again agreed with experimental observations. High CO emissions and a weak cavity vortex were shown to be a function of the injector design.

Having anchored the modeling tool with a known geometry, the investigation for a strong cavity vortex in a power generation combustor was begun. The power generation combustor follows a can annular design rather than an annular shape studied previously; the air distributions also require a leaner head end than aircraft engine applications. The design of the main burner and cavity injectors has been studied numerically. The sensitivity of the design to various parameters has been explored, and the design was scaled to full temperature and pressure conditions of an F-class gas

turbine at 1/6 scale. The final flowfield has demonstrated a strong cavity vortex with less temperature rise than the atmospheric prototype.

Prototype 1 incorporated kinetic modeling, CFD modeling, and thermal modeling in the design phase to evaluate important performance parameters in a TVC combustor. Also in this phase, the key components of the experimental test rig and facility were engineered. Prototype 1 demonstrated the ability of the TVC combustor to reduce NOx emissions below the target performance goals, but CO emissions were excessive.

A series of design changes were incorporated in Prototype 2 using heavy application of CFD and thermal modeling. At 1/10 scale of a heavy-duty gas turbine conditions, Prototype 2c produced a 23% reduction in NOx and single digit CO emissions at full-load conditions. The emissions were reduced over 68% at part-load with wide turn-down capability. Combustion dynamics were relatively low.

Prototype 3 incorporated further enhanced design changes for a 1/10 scale combustor in an attempt to meet the 50% NOx reduction goal at full load. The prototype exceeded this goal at advanced gas turbine conditions, and produced single digit CO. At reduced firing temperatures the improvements in NOx emission were smaller and low CO required a longer residence time.

3 Experimental

3.1 Atmospheric Combustion Studies

Testing was planned for investigating the trapped vortex combustor (TVC) performance with natural gas operation. The baseline configuration required minor modifications to the existing 6" TVC rig which had been previously run with jet fuel. A total of 4 alternate rig configurations of the 6" TVC sector rig were designed, fabricated, and tested. The testing was performed at the Air Force Research Laboratory (AFRL) facility, with testing coverage supports by both GE Aircraft Engines (GEAE) and AFRL. Using the reactor network model, a detailed analysis of the test data was performed to understand the key physiochemical processes dominating the TVC emission performance. The test results were very promising by showing that NOx emissions may be reduced by more than 50% compared to the existing lean premixed gas turbine combustors.

3.1.1 Component Design

Utilizing the existing Air Force Research Lab (AFRL) 6" rectangular TVC rig, new primary and main fuel injectors were designed for gaseous fuel (CH4) for the baseline test. This rig configuration serves as a baseline as it has been prior tested with liquid JP8 type fuel. GEAE designed and fabricated hardware modifications required to convert the rig from liquid fueled to gaseous fueled as shown in Figure 3-1. All planned rig testing were performed by AFRL in their Room 151 facility located at Wright Patterson Air Force Base (WPAFB) at no direct cost to this effort. The testing was conducted at atmospheric pressure and temperatures up to 500 F with GEAE test coverage support.

The detailed design of the main and primary gaseous fuel (CH4) injectors for the baseline test are shown in Figure 3-2 and Figure 3-3, respectively. For the baseline test, fuel is premixed with air in the main starting from the IDIF inlet by introducing the cross flow plain jet from the tube periphery as schematically illustrated in Figure 3-2. The main fuel is fed through eight 0.25 in. tubes, with a sharp cone-shaped tip, having 90 ° bent. Around each tube, four injection holes are located at 45 ° from the horizontal plane in order to enhance the uniformity of fuel/air premixing level across the IDIF cross-sectional plane. The main fuel/air flow has about three inches of premixing length and injected into the main dome region of the TVC combustor as shown in Figure 3-1. It is worth noting that anchoring the main dome flow to the cooling nugget enhanced the isolation of the cavity flow based on the previous actual testing and CFD models with liquid jet fuel.

For the baseline configuration, the primary injector design utilizes the plain-jet direct fuel injection from the cone-shaped tube tip directly into the cavity. As shown I in Figure 3-3, the cone-shaped tip for the fuel injection was employed in order to enhance the fuel/air mixing (interaction) in the cavity by introducing the primary fuel at an angle to the air stream. This direct fuel injection design allows us to closely simulate the cavity combusting cases similar to the previous testing cases of the existing 6" rectangular TVC

rig configuration with liquid jet fuel. Figure 3-3 shows close-up views of the baseline primary injector design from the front and backsides of the cavity forward wall, respectively. The same amount of primary air as for the liquid-fuel cases is employed in this design using 18 air holes around the fuel injection holes as illustrated in Figure 3-3. In past years, the TVC technology has demonstrated a promising performance with liquid jet fuel for aircraft gas-turbine combustor applications at GEAE. However, the existing test data do not provide the TVC performance for ground-based gas-turbine combustor applications at scales sufficient to design an optimized TVC rig specifically for gaseous fuel. Therefore, as our first step to the current study, it is of great interest to investigate the performance of the existing 6" TVC rig for gaseous fuel by keeping many of the current configurations remained the same.

GEAE machine and sheet metal shops supported to the fabrication and assembly of the baseline configuration and adaptive hardware. The primary and main fuel injectors were manufactured to fit, with the sector in hand to assure all injector points were aligned properly.

A total of 3 alternate rig configurations were designed, focused to achieve low emissions, as described in Figure 3-4. Performance predictions were generated by GEAE and GECRD. In the overall design process, utilizing the existing Air Force Research Lab (AFRL) 6" rectangular TVC rig, new primary and main fuel injectors were designed for gaseous fuel (CH4) for the three different configurations. Configuration 1 employs the direct injection of gaseous fuel into the cavity for the primary injector and the premixing injection for the main by injecting plain jets of (CH_4) perpendicular into the incoming air stream at the IDIF inlet. For configuration 2, the premixing primary gaseous fuel injector was designed by premixing the primary air and fuel, while the main injector design remained the same as the configuration 1. Finally, configuration 3 allowed for the improved premixing level in the cavity by premixing both the driver air and primary air with fuel.

For the second configuration, 3-D Fluent CFD modeling of premixing fuel injectors was performed for determining the fuel/air mixing level within a given premixing length. As shown in Figure 3-1, only a limited space is available for the premixing of fuel with primary air without significant modifications to the existing 6" rectangular rig. Initially, four different premixing fuel injector designs for the primary injection were proposed. The optimum design was carefully downselected based on the fuel/air mixing level at the injector exit plane predicted by 3-D Fluent CFD models. The downselected premixing primary injector is shown in Figure 3-5. The fuel is injected through the eight holes on the cone-shaped tube inside the air shroud. The cone-shaped tube was chosen in order to prevent the possible flow recirculation. The first four of those eight fuel injection holes are located near the cone base, whereas the remaining other four holes are located further downstream. These two sets of fuel injection holes are staggered to each other, and thus enhance the uniformity of the mixing level on the exit plane.

Figure 3-6 shows the CFD predicted fuel/air mixing level at the exit plane of the premixing primary fuel injector at FAR = 0.03136 and fuel split = 0.5. For the main fuel injection, same as the baseline configuration, the fuel is premixed at the IDIF inlet by injection of plain jets of (CH_4) perpendicular into the incoming air stream.

The overall schematic drawing of configuration 3 is illustrated in Figure 3-7. The forward and aft driver holes are closed up, and two types of the cavity premixing injectors have been designed: one is the forward premixing injector, the other is the aft premixing injector. The schematic drawings of the injectors are shown in Figure 3-8. For the forward injector, both the forward driver air and primary air are premixed with fuel and injected into the cavity as four separate jets from each forward wall. The aft injector allows the aft driver air to premixed with fuel and to inject into the cavity as four separate jets from each aft wall.

Configuration 3 required permanent hardware modifications to the forward cavity wall and aft-liner plenum in order to fit the fwd and aft premixing injectors, respectively, to the TVC 6" rig. Note that changing the hardware configuration from 1 to 2 does not require permanent hardware modification, since the primary injectors of configurations 1 and 2 are readily interchangeable. The intent for the testing at WPAFB is to quickly investigate the TVC performance for gaseous fuel using the existing 6" TVC rig without major hardware modifications. Thus, it is not necessary that the three configurations designed in the current work are the optimum designs for the ground-based gas-turbine combustor applications. In past years, the collaborated TVC testing team effort between WPAFB and GEAE has demonstrated very promising performance for aircraft combustor applications in terms of the low emissions with a short combustor length. Therefore, it was planned to investigate the performance of the available 6" TVC rig for gaseous fuel by keeping many of the current configurations remained the same. After the planned testing at WPAFB, prototype combustors employing new designs were built and evaluated over a variety of conditions, specifically for the ground-based applications.

Similar to the premixer of the configuration 2, the air entering the forward and aft injectors of the configuration 3 is partially blocked by the fuel participating in the premixing process in the premixer passage. A flow circuit model has been developed and applied to estimate the percentage of the air blockage in both the forward and aft premixers. The model is based on the conservation equations of mass, species concentration, momentum, and energy using a lump-parameter analysis. The model has a predictive capability of estimating the effect of the fuel injection on the air mass flow rate over the range of operating conditions. It should be noted that the total pressure drop is fixed at 5%. Based on the model results (Figure 3-9), the cross-sectional area of the air passage of the premixers was designed to account for the effect from fuel injecting into the premixing. Since a broad range of fuel splits will be investigated in the planned testing, it is a difficult task to design a single-orifice premixer compensating for all testing points. The fuel split denotes the ratio of the cavity fuel mass flow rate to the total fuel mass flow rate. Based on the pre-test prediction results (discussed in the next section), fuel splits less than 0.4 have been determined to be the targeting design points because of the low emissions. Using the flow circuit analysis, the air blockage by the fuel in the premixer was estimated to be less than 2% for the fuel split below 0.4 as shown in Figure 3-9.

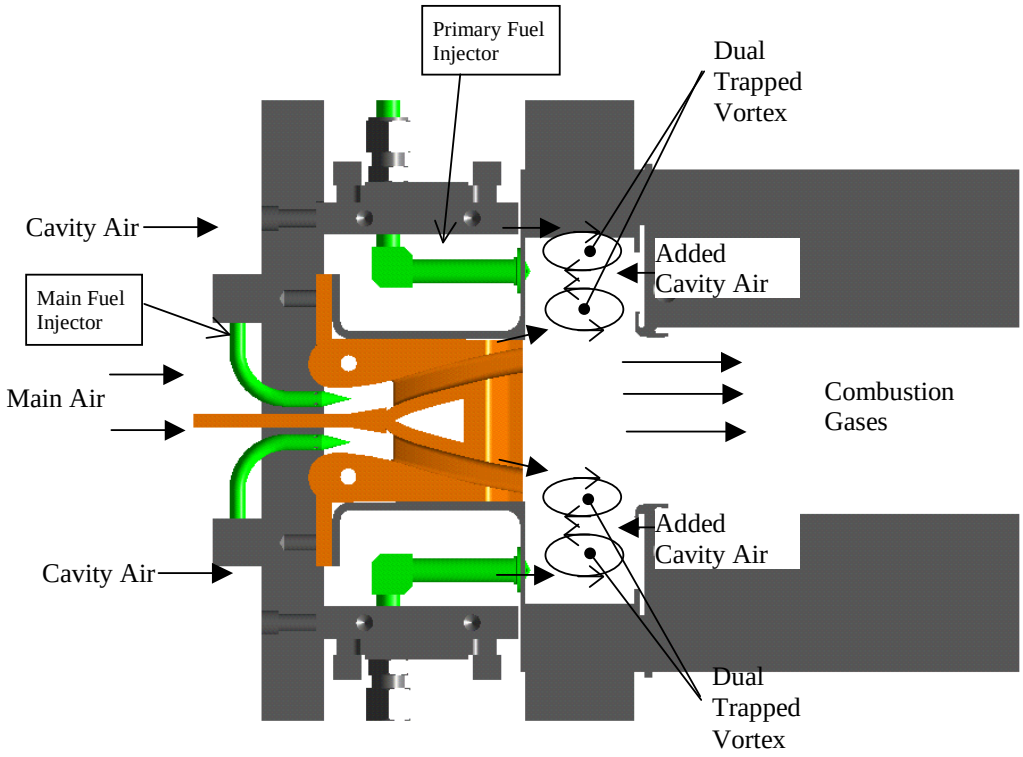

Figure 3-1 Baseline configuration of 6” rectangular TVC sector

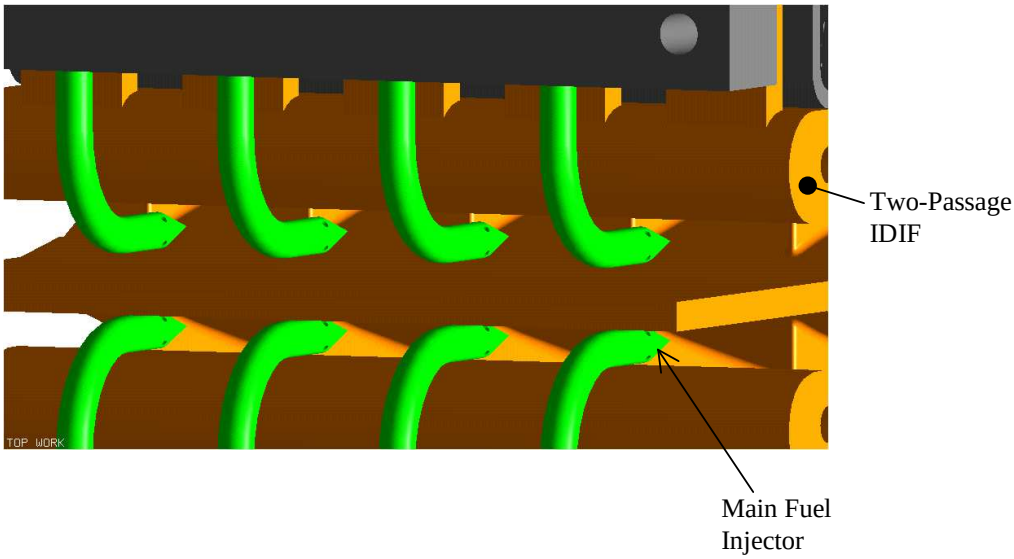

(a) Back View

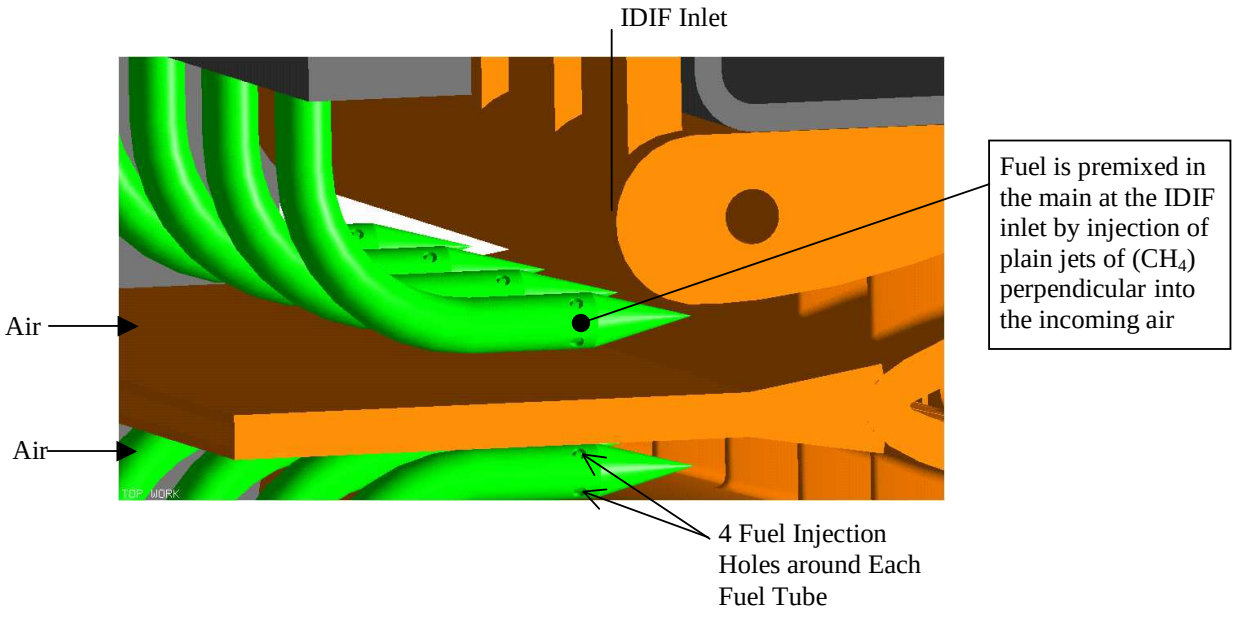

(b) Side View

Figure 3-2 Close-up view of main fuel injectors (a) Back and (b) Side views

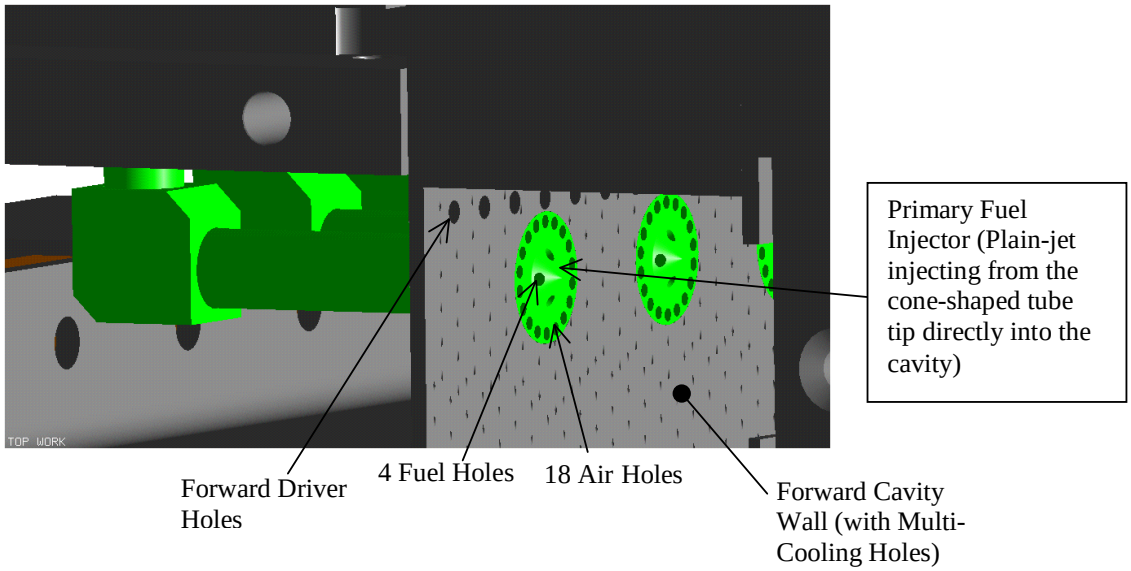

(a) Front side of forward cavity wall

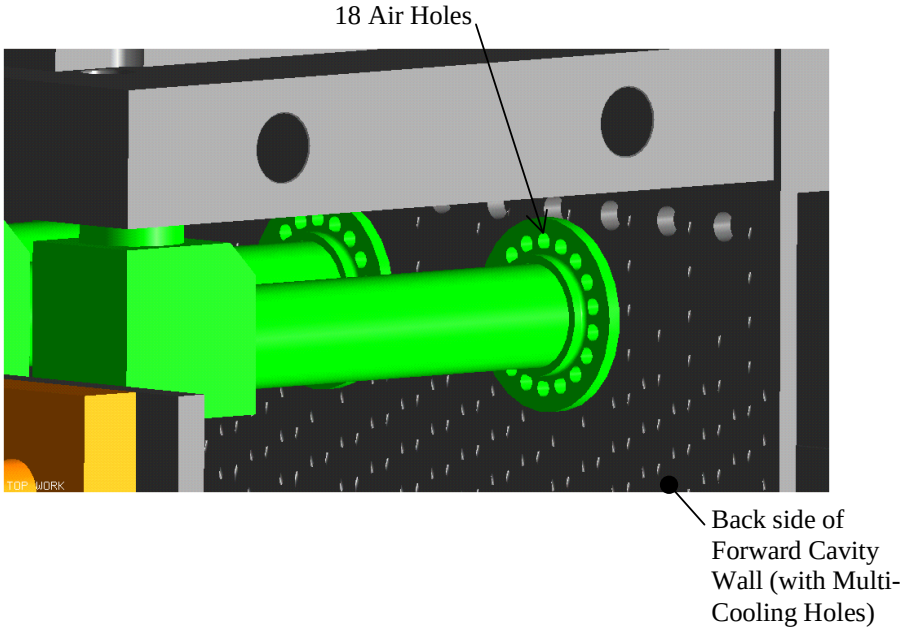

(b) Back side of forward cavity wall

Figure 3-3 Close-up view of primary fuel injectors (a) Front side of forward cavity wall and (b) Back side of forward cavity wall

Baseline	Primary Injector	plain jet direct injection from a cone-shaped tube into cavity
	Main	premixed plain jet in cross-flow
Configuration 1	Primary Injector	direct injection of gaseous fuel
	Main	premixed injection with plain jets perpendicular into the incoming air stream
Configuration 2	Primary Injector	premixed air and fuel injector
	Main	same as configuration 1
Configuration 3	Primary Injector	improved premixing
	Main	improved premixing

Figure 3-4 Atmospheric test rig configurations

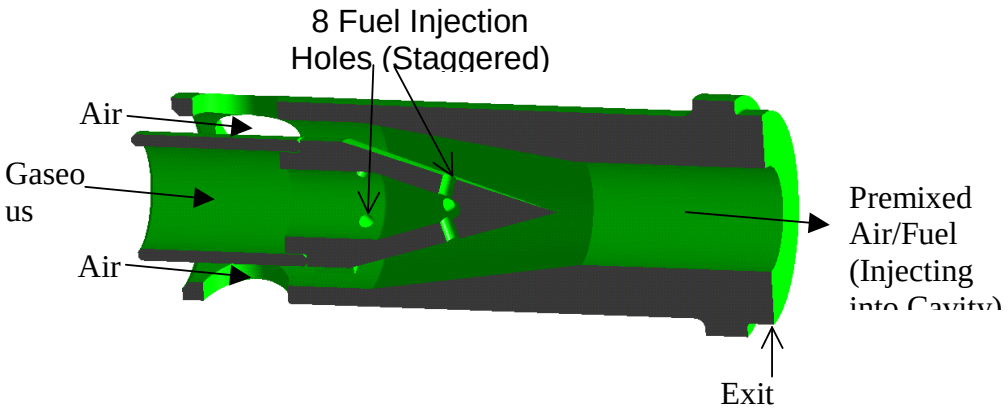

Figure 3-5 Cut-out view of primary premixing fuel injectors of configuration 2

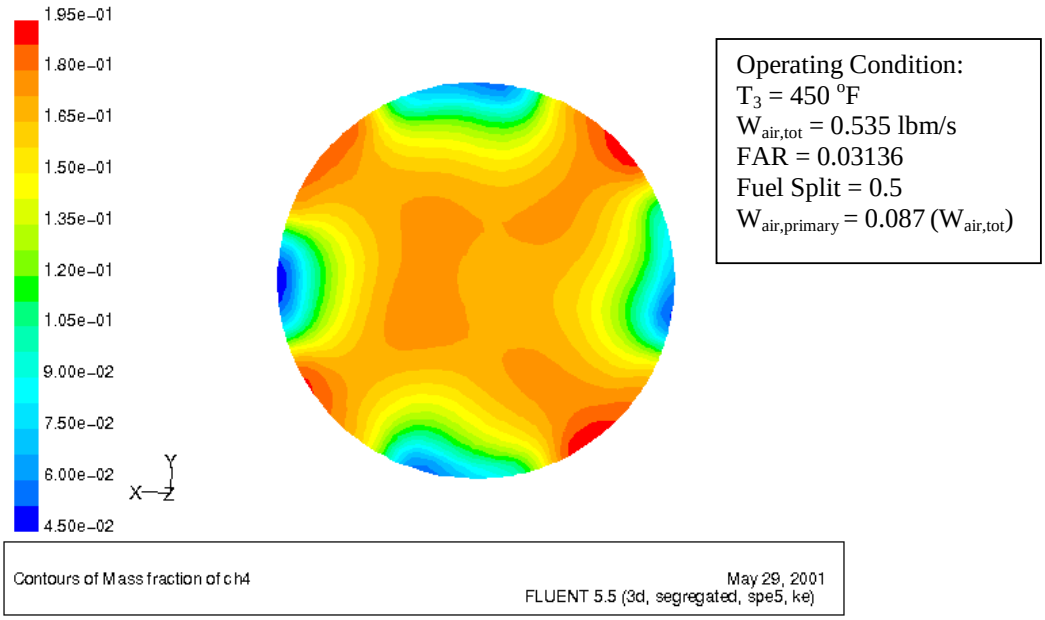

Figure 3-6 CFD prediction of fuel/air mixing level at injector exit plane of primary premixing fuel injector of configuration 2

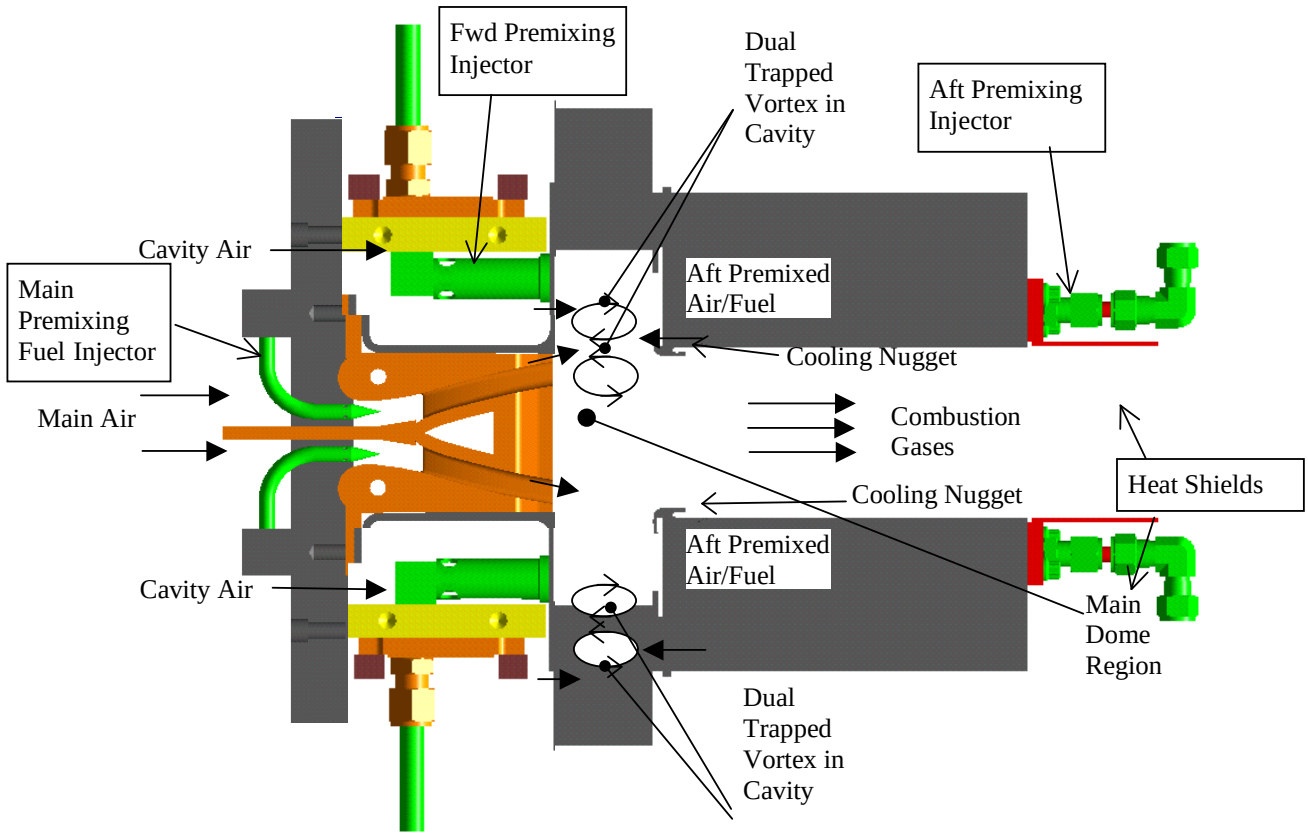

Figure 3-7 Schematic drawing of gaseous fuel injection 6" TVC configuration 3

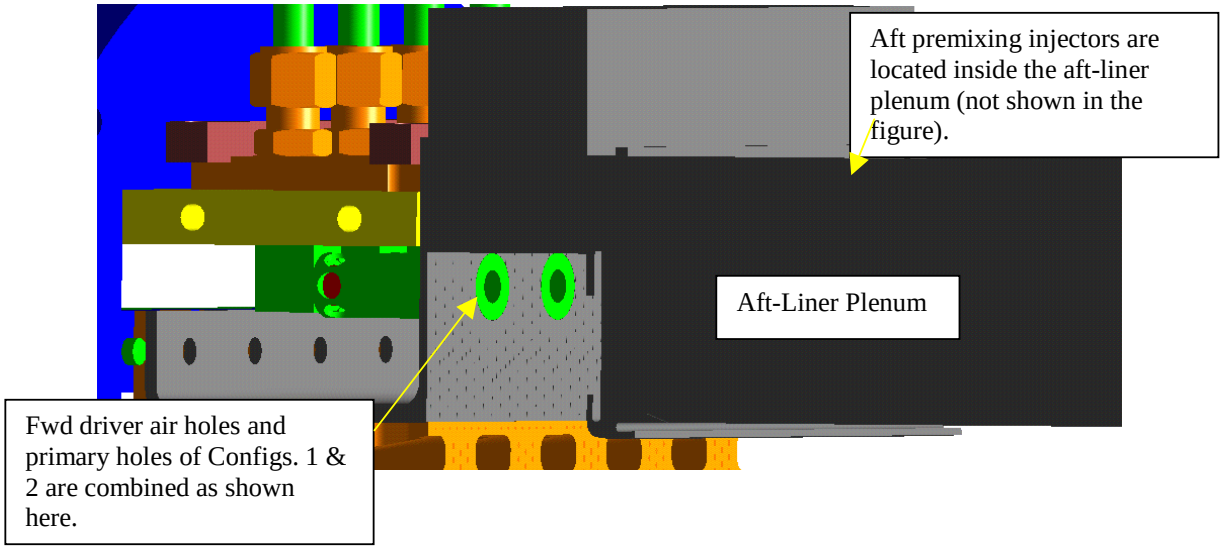

(a) Fwd Premixing Injectors placed in outer cavity wall of 6” TVC rig.

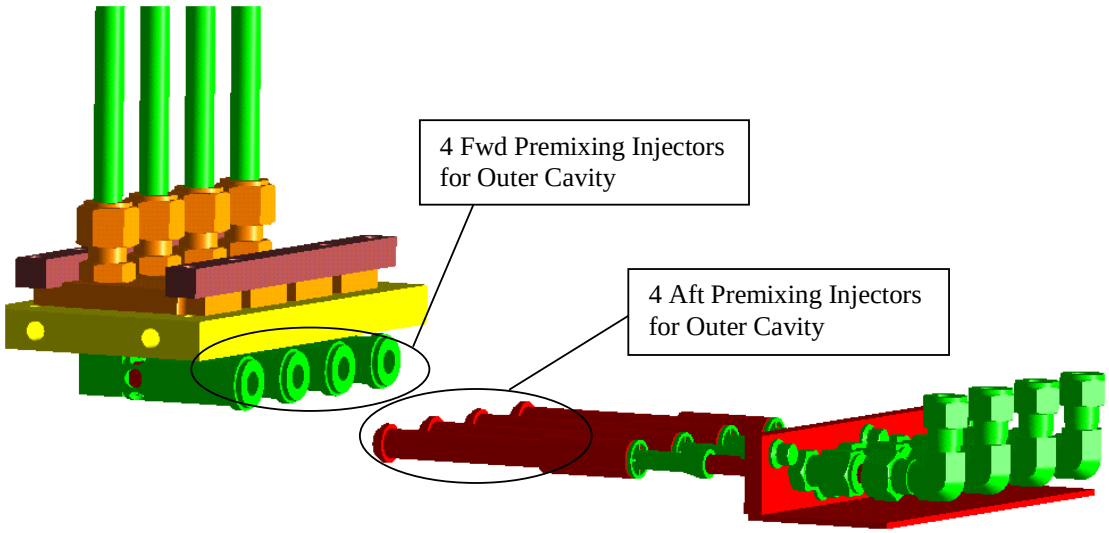

(b) Fwd and Aft Premixing Injectors without 6” TVC Rig.

Figure 3-8 Close-up view of fuel injectors (a) Fwd Premixing Injector (b) Aft Premixing Injector

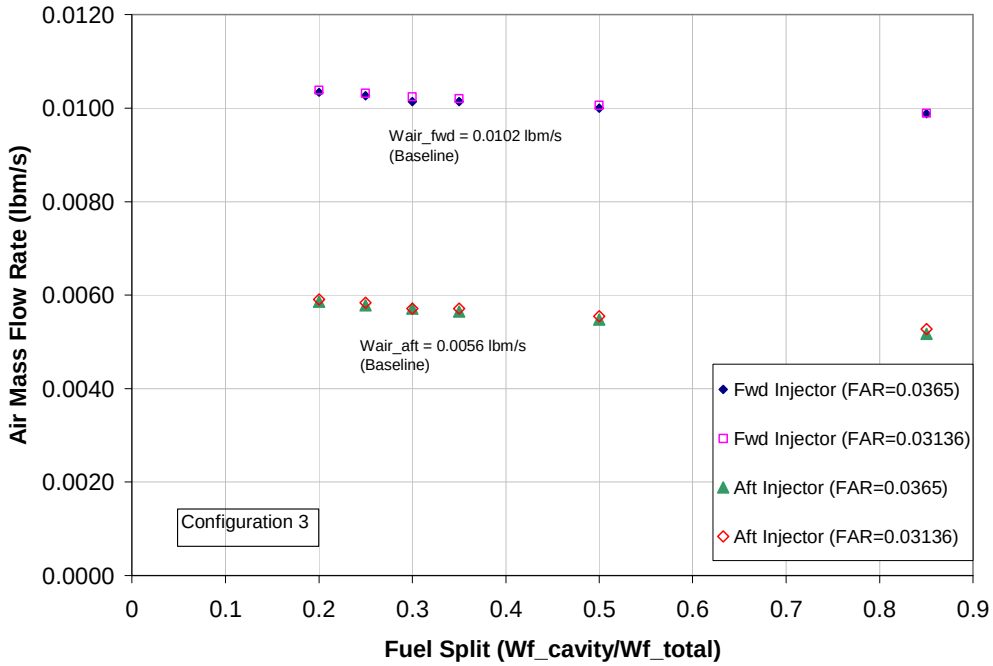

Figure 3-9 Effect of fuel injection on air mass flow rate in the fwd and aft premixing injectors of configuration 3

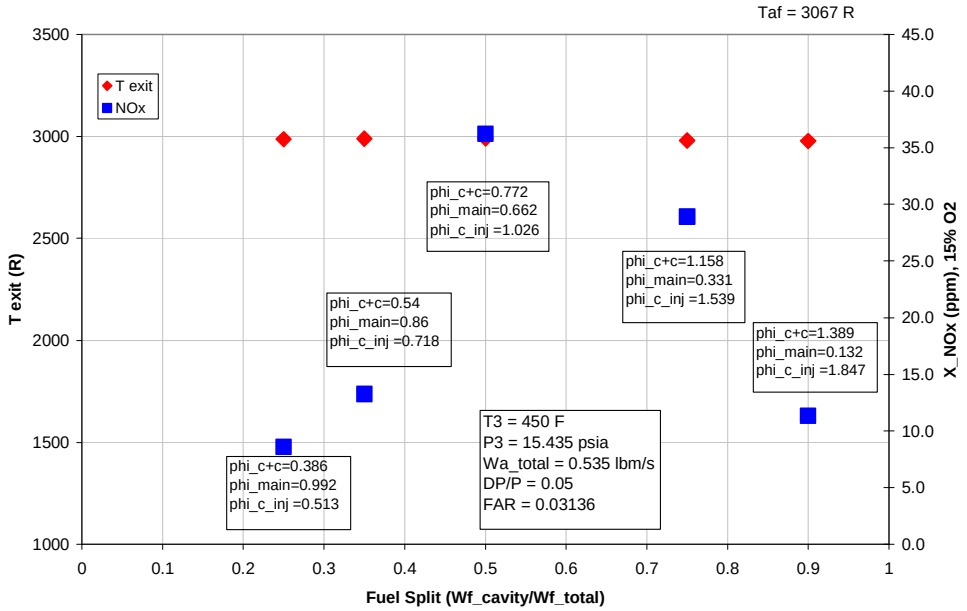

Figure 3-10 Predicted exit temperature and NOx by reactor network model over the range of fuel splits for FAR = 0.03136 for configuration 3

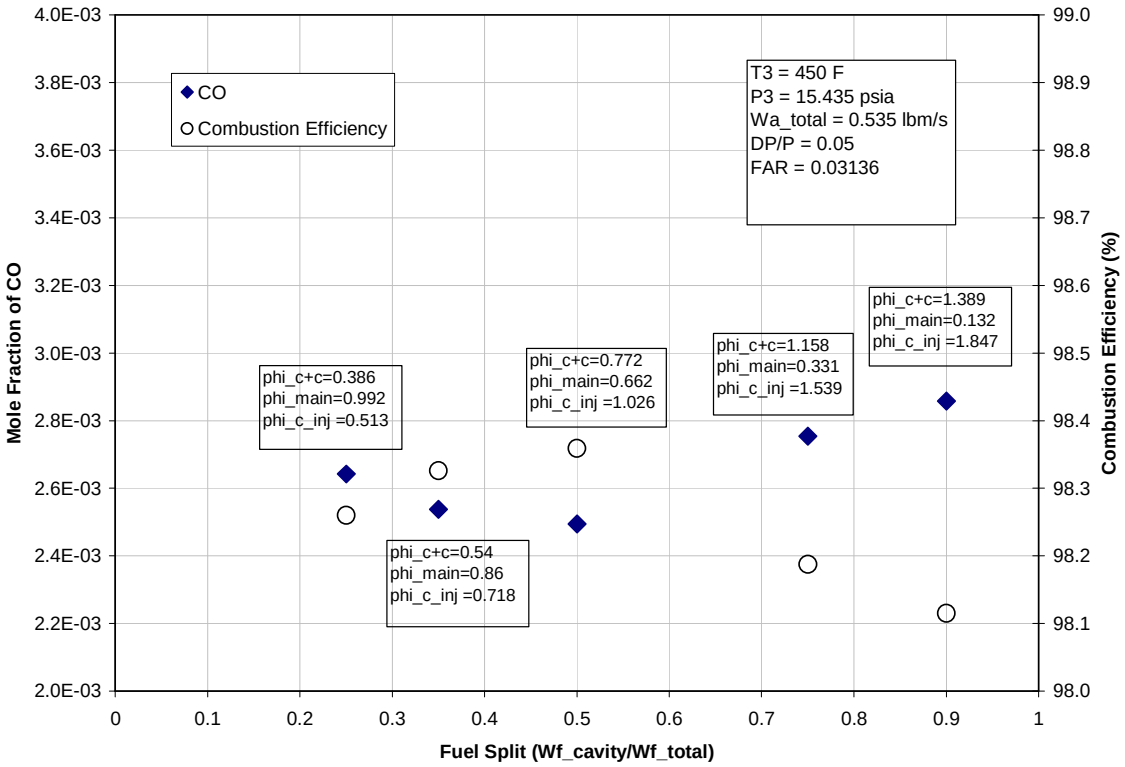

Figure 3-11 Predicted CO concentrations by reactor network model over the range of fuel splits for FAR = 0.03136 for configuration 3

3.1.2 Kinetics Modeling

A kinetics design tool was developed to guide the design and sizing of components. This model was used to investigate the effect of the fuel split between the cavity and main sections of the combustor on NOx production and lean blow out. A reactor network was developed to capture the emissions signature of the 6" rectangular rig with a premixed main burner and a diffusion fuel cavity injector.

Chemkin

A network reactor modeling tool built on the CHEMKIN II code was used to analyze the kinetics of the reactor. The modeling tool supports perfectly stirred reactors, plug flow reactors, and non-reacting elements. The reactors are characterized either by their volume or their residence time for a specified mass flow rate entering at specified temperature and pressure conditions. The code accounts for finite rate elementary chemical reactions in the reactor using a hybrid Newton/ time-integration method. An in house reaction mechanism for hydrocarbon combustion was used to study the combustion of natural gas composed of 95.6% methane and other minor species in air.

Zone Model

The modeling tool was used to construct a six zone model of the trapped vortex combustor. The cavity was modeled as two reactors: a PSR, zone 1, and a non-reacting element, zone 2, shown in Figure 3-12. Zone 1 represents the fuel and air in the primary and secondary vortices and zone 2 represents the cooling air that doesn't participate in combustion in the cavity. The main burner is represented by a PSR and a PFR. The PSR, zone 3, captures the near field mixing & reaction zone of the main burner jets. The PFR, zone 4, represents the bulk flow as it carries the products of combustion downstream. The combustion liner cooling air does not participate in the PFR and simply dilutes the final mixture. It is modeled by a non-reacting element, zone 5. The average exit conditions are captured by a non-reacting element, zone 6.

The mass flow leaving one reactor can be split between multiple reactors in the network. Fuel is supplied to zones 1 & 3 according to the fuel split specification. Air is supplied to all 5 upstream zones maintaining the cavity and main air splits. The air flow is further subdivided between zones 1 & 2 and between zones 3 & 4. Zone 1 has a minimum phi value representing the change in reaction zone volume with fuel addition. The residence time in zone 2 is proportional to its air fraction. The main burner has a fixed residence time for zone 3 to capture the lean blow out characteristic. It also has a minimum phi value which is used to calculate the cavity volume under low fuel flow conditions. The partially reacted mixture from zone 1 flows into zone 2 and the main PSR, zone 3, for flame stabilization. The products of zone 2 & 3 flow into zone 4. Zones 4 and 5 flow into zone 6 and are mixed to determine the average exit conditions. The total volume of the combustor is known and the mass flow distributions to the cavity, main burner, and combustion liner cooling air are known.

Design tool

The design tool incorporates the zone model into the network modeling tool to conduct simulations of the reactions in the trapped vortex combustor. The design

parameters of the zone model can be independently varied according to the simulation conditions. A six sigma design of experiments (DOE) was conducted to examine the influence of various parameters on the combustors emission performance. By comparing the simulated emission characteristic with the experimental data, the parameter settings for the model were refined, and the physical basis for the model tested. In the simulations the fuel split between the cavity and the main burner was examined over the range for each configuration of the model. The fuel split ranged from 100% cavity fueling to lean blow out of the main and cavity burners.

The critical geometrical design characteristics were explored using in a Design Of Experiments (DOE) study. A fractional factorial test plan enabled the evaluation of the main effects of these characteristics with an optimal number of runs.

In the first DOE, two parameters were examined at three levels. The split of the products from zone 1 into zones 3 and 4 was set to 25%, 50%, and 75% into zone 3. The residence time of zone 3 was set to 0.3 ms, 0.8 ms, and 1.3 ms. Figure 3-13 shows the corresponding results. The NOx emissions spanned a narrower range when a smaller percentage of the zone 1 products were put into zone 3. Furthermore, the NOx sensitivity to the split was increased with increasing residence time. So, the lowest emissions were realized with low split and low residence time, but the sensitivity only around 10 ppm.

In the second DOE the reactor limit values were explored. The zone 1 reactor minimum phi was set to 0.6, 0.75, and 0.9, and the zone 3 reactor minimum phi was set to 0.6, 0.75, and 0.9. Figure 3-14 shows the model was insensitive to the zone 3 reactor limit, changing only a few ppm. However, the zone 1 reactor minimum was significant in that it led to the formation of the distinct local minimum for the reactor network. The curvature was also seen in the experimental data. The minimum represents the lowest fuel flow rate for sustaining the full cavity vortex. Below this point, the main burner begins to form NOx faster than the leaning out of the cavity can reduce it. When the cavity reaches the lean blow out point, the main burner is contributing to higher NOx emissions than occurred at the local minimum.

In the third DOE the lower limit for zone 3 residence time was examined. The zone 3 residence time was reduced to: 0.2 ms, 0.1 ms, and 0.05 ms while maintaining a 25% split of the zone 1 products into zone 3. The minimum phi for reactor 3 was set to 0.3, 0.4, and 0.6. The results are shown in Figure 3-15. Again the results were relatively insensitive to the setting for reactor 3. The Zone 3 residence time however demonstrated a small effect on emissions until lean blow out was triggered. The NOx emissions were eliminated when the cavity failed to light because the zone 3 residence time was too small. As the lean blow out point was approached, CO emissions would rise and temperature would fall.

In the fourth DOE the air splits in the system were varied as shown in Figure 3-16. The split of the zone 1 products to zone 3 were varied from 25% to 100%. The increase in the split increased the slope of the change in the NOx and increased the range. The air fraction to the main burner has a dramatic effect on the overall NOx curve, reducing it by over 5 ppm / % main air. Decreasing the air to the cavity also reduced the overall NOx by more than 2 ppm/ % cavity air except near the high cavity loading limit where it reduced the inflection and raised the NOx at 100% cavity fuel.

The conclusion from this initial study was that the % main air is the most significant parameter in reducing overall NOx and that the zone 3 residence time needs to

be maintained relatively high to prevent the early on-set of lean blow out. The model captured the presence of a local minimum as observed in the experiments reflecting the physical change in the vortex size as the lean blow out limit is approached.

The multi-zone model has not captured the full emission characteristics of the atmospheric rig tests. The inflection the NOx emissions was demonstrated as well as the lean blow out point. However, the emissions magnitude was not matched. Earlier emissions modeling studies matched the magnitude but failed to capture the lean blow out point and the inflection in the NOx emission characteristic. More complex network models have the ability to capture the emission performance of the combustor, but they are fine tuned for a specific flow field. The next step would be to investigate models of increased complexity, which capture critical features of the flow field, but this is beyond the scope of this investigation.

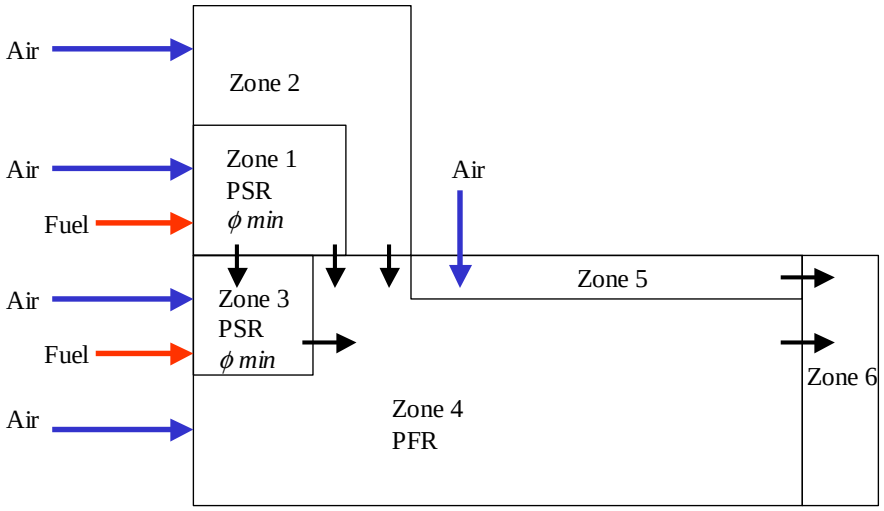

Figure 3-12 Atmospheric study Chemkin zone model

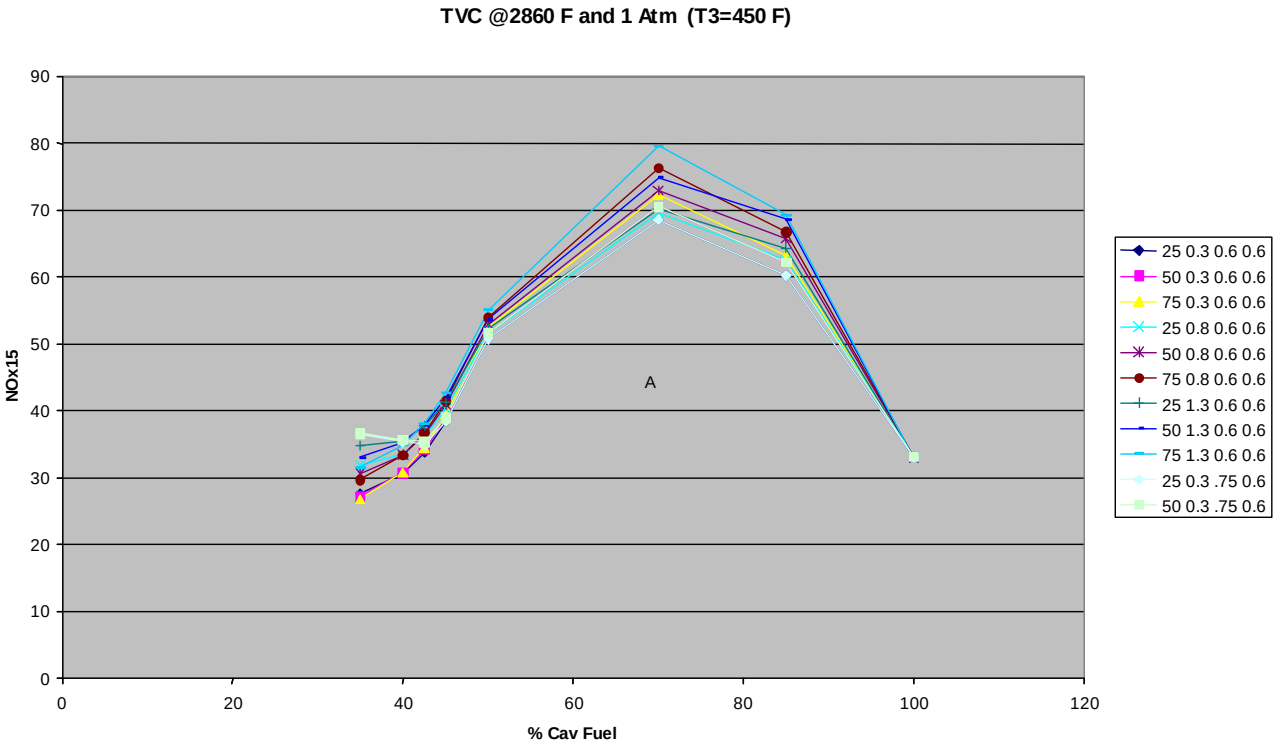

Figure 3-13 Atmospheric study modeling of NOx15 versus % cavity fuel for residence times of 0.3 ms, 0.8 ms, and 1.3 ms

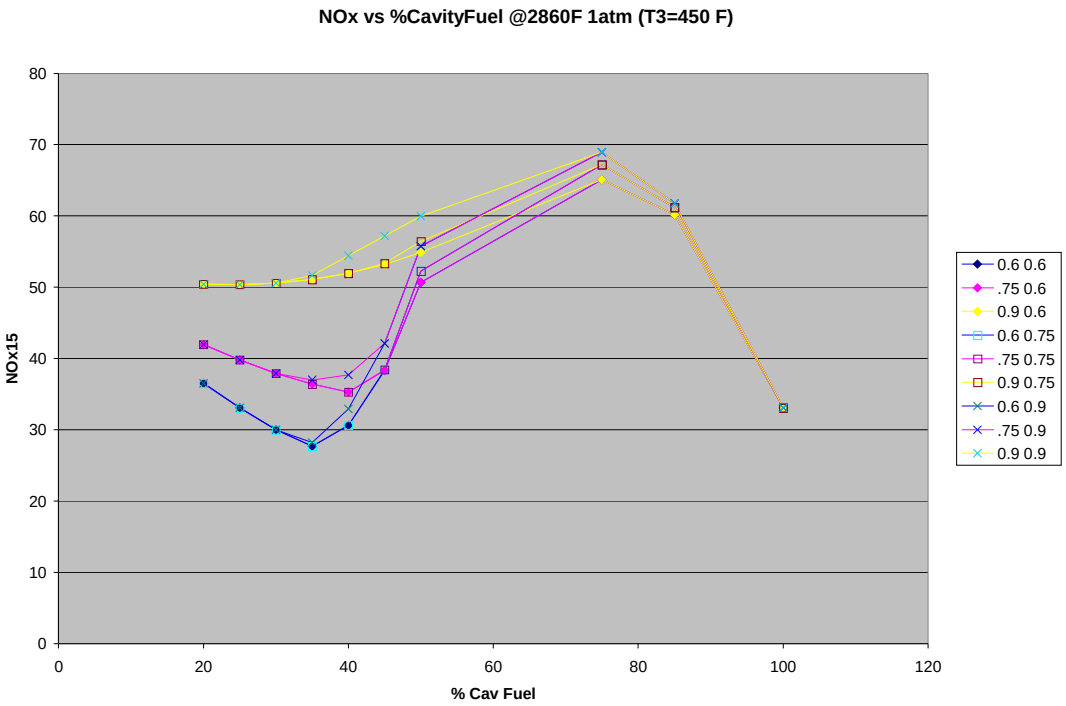

Figure 3-14 Atmospheric study model of NOx15 vs. %cavity fuel split given zone 1 and zone 3 reactor minimum phi set to 0.6, 0.75, and 0.9

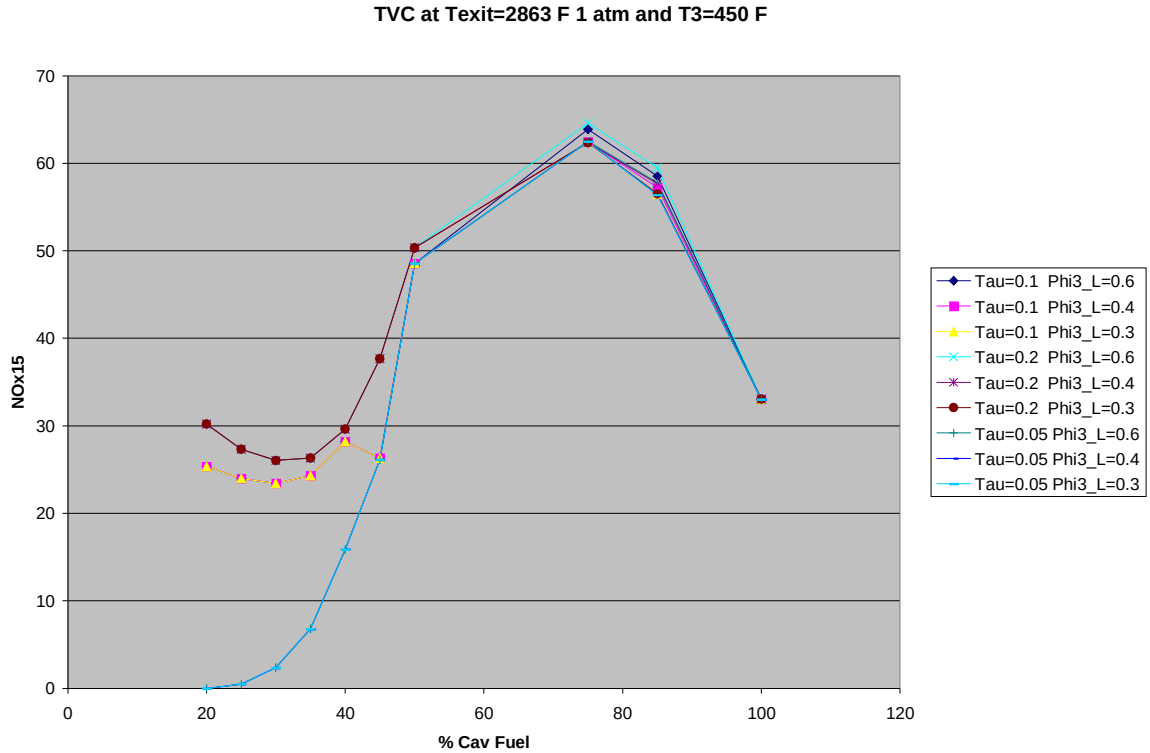

Figure 3-15 Atmospheric study model of NOx15 vs. %cavity fuel with zone 3 phi set to 0.3, 0.4, and 0.6)

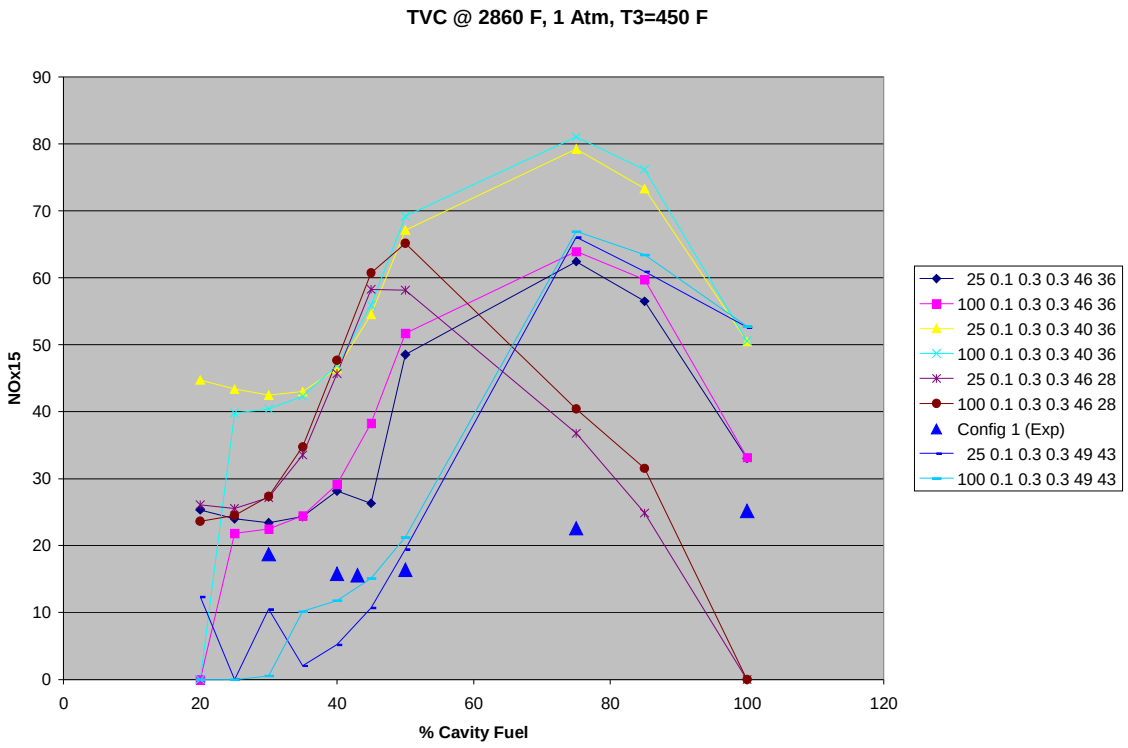

Figure 3-16 Atmospheric study model of NOx15 vs. %cavity fuel with varying air splits

3.1.3 Flow field Design CFD

3-D Fluent CFD analysis of the gaseous fuel injection TVC 6" rig was performed using a GE developed Laminar Flame Model (LFM). 400K grid models were generated to numerically investigate the performance of the gaseous fuel injection TVC rig configuration 1. In the main, the fuel is premixed at the IDIF inlet by injection of plain jets of (CH_4) perpendicular into the incoming air stream (shown in Figure 3-17a), whereas the direct injection of gaseous fuel into the cavity is employed for the primary injector. Due to the difficulties associated with the combustion modeling, the IDIF passage was solved separately from the TVC combustor. The grid model for the single cup, upper half of the bi-passage IDIF is shown in Figure 3-17b. The pressure boundary condition was used for the IDIF air inlet boundary specification, whereas the velocity boundary condition was used for the fuel inlet boundary specification. The CFD prediction for the premixing level at the IDIF exit plane is shown in Fig. 6c for T3 = 450 °F, P3 = 15.5 psia, FAR = 0.03136, and fuel split = 0.5. The air/fuel mixing at the exit plane is not perfectly uniform, but to a certain extent has achieved sufficient uniformity to improve the premixing level compared to the existing configurations of the 6" TVC rig with a simple hardware modification.

Figure 3-18 shows the grid model for the single-cup, upper half of the 6" TVC rig configuration 1 with the coordinate system attached. The center plane is specified at z = 0, whereas two other planes specified at z = 0.3" and 0.6" for the illustration purpose as shown in Figure 3-19 through Figure 3-21. Results of the CFD case with LFM are shown in Figure 3-19 through Figure 3-22 for T3 = 450 °F, P3 = 15.5 psia, FAR = 0.03136, and fuel split = 0.5. The predicted IDIF exit plane information is employed as the inlet boundary condition for the TVC combustor model. For the configuration 1, the direct fuel injection is used for the cavity (Figure 3-18). The primary injector design utilizes the plain-jet direct fuel injection from the cone-shaped tube tip directly into the cavity. This direct fuel injection design allows us to closely simulate the cavity combusting cases similar to the previous testing cases of the existing 6" rectangular TVC rig configuration with liquid jet fuel.

As shown on the center plane, a noticeable resident time is required for the fuel/air mixing and reactions to take place in the cavity under atmospheric pressure and T3 = 450 °F. At a fuel split of 0.5, the equivalence ratio for the primary air and fuel is 2.545, thus it is extremely fuel rich near the primary injector in the cavity. Results also show that the fuel, injected into the cavity as well as into the inner and outer IDIF passages, may be quenched along the aft liner cooling. Also, the model predicts one strong vortex in the cavity with a weaker vortex near the main/cavity interface. At fuel split = 0.5, the premixed fuel of the IDIF continuously burns in the main dome region of the combustor as shown in Figure 3-19 through Figure 3-21. At z = 0.3" (Figure 3-20), it can be seen that the vortex in the cavity enhances the air/fuel mixing and flame stabilization in the cavity. Since the plane at z = 0.3" aligns with the IDIF exit, the "cold" jet entering the main region can be clearly seen (Figure 3-20). Figure 3-21 shows the flame in cavity transporting down to the main dome at z = 0.6". On this plane, the model predicts that the vortex in the cavity is very weak, and the vortex near the cavity/main interface, shown in Figure 3-19 and Figure 3-20, no longer exists. Overall, the flame is well contained in the cavity and transports down to the main, serving as the

heat source for the main during the continuous combustion process. Figure 3-22 shows the exit temperature contour for the single-cup, upper half of the 6" TVC exit plane. A center peak temperature profile is predicted (along z direction). Also, the highest exit temperature is predicted to be between the liner wall and the line of symmetry.

Figure 3-23 shows the CFD model predictions for the combustor exit temperature and NOx for four different fuel splits at T3 = 450°F, P3 = 15.5 psia, and FAR = 0.03136 for the configuration 1. Unlike the DRA-2 model results, the model predicts significant incomplete combustion over the operating condition range investigated (combustion efficiencies ~ 60 to 80%). The predicted combustor exit temperature is noticeably less than its adiabatic flame temperature (T_{af} = 3067 °F) as shown in Figure 3-23. It must be noted that DRA-2 model results shown in Figure 3-10 and Figure 3-11 are for the configuration 3 where the driver air and primary air are all premixed with the fuel in the cavity. At fuel split = 1.0, the DRA-2 model predicted that the fuel does not burn in the combustor under atmospheric pressure and T3 = 450°F since $\phi_{\text{fwd\&aft premixer}}$ is too rich in the cavity. About 98% combustion efficiencies were predicted at fuel splits less than 0.9 using the DRA-2 model. As expected, the CFD model predicts the lower NOx as the combustion efficiency decreases. It is worthy noting that the higher NOx is predicted at fuel split = 0.5 compared to that of fuel split = 0.75, while the combustion efficiency is about the same between these two cases. This trend has also been predicted by DRA-2 model (Figure 3-10). In past years, the cavity optimization rig was used under Air Force Contract F33615-93-c-2505 for jet fuel applications and tested under atmospheric pressure and T3 = 500°F in the Room 151 at WPAFB. The test from the previous work showed that the combustion efficiencies over a FAR range from 0.0139 to 0.0359 with fuel splits > 0.9 were above 90%. It is difficult to draw a conclusive argument about the predicted NOx formation over the range of fuel splits under atmospheric pressure from the CFD analysis. Test data from the current gaseous fueled rig configurations are needed for model validation.

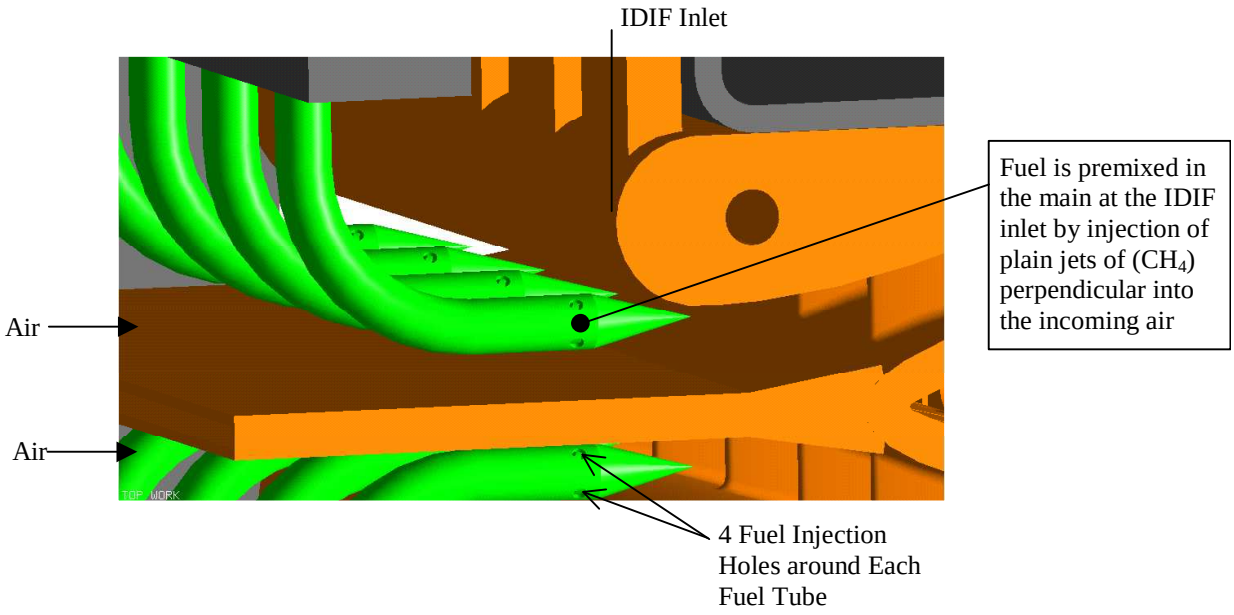

(a)

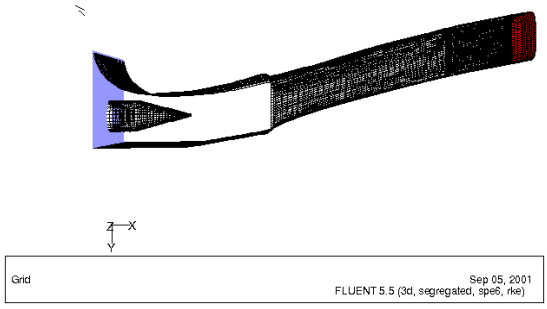

(b)

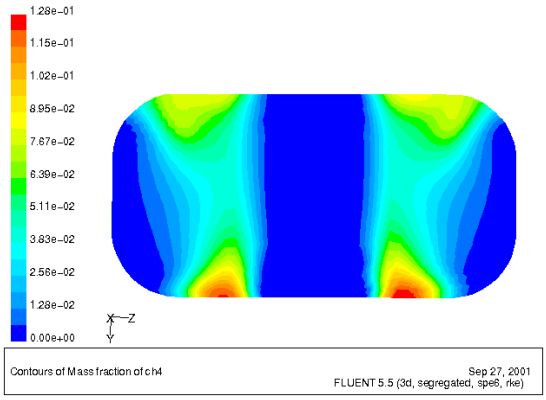

(c)

Figure 3-17 Bi-passage IDIFs (a) main fuel injectors with bi-passage IDIF, (b) CFD grid for single cup, upper half of IDIF, (c) CFD prediction for fuel concentration on the IDIF exit plane at T3 = 450 °F and P3 = 15.5 psia (FAR = 0.03136, fuel split = 0.5) for configuration 1

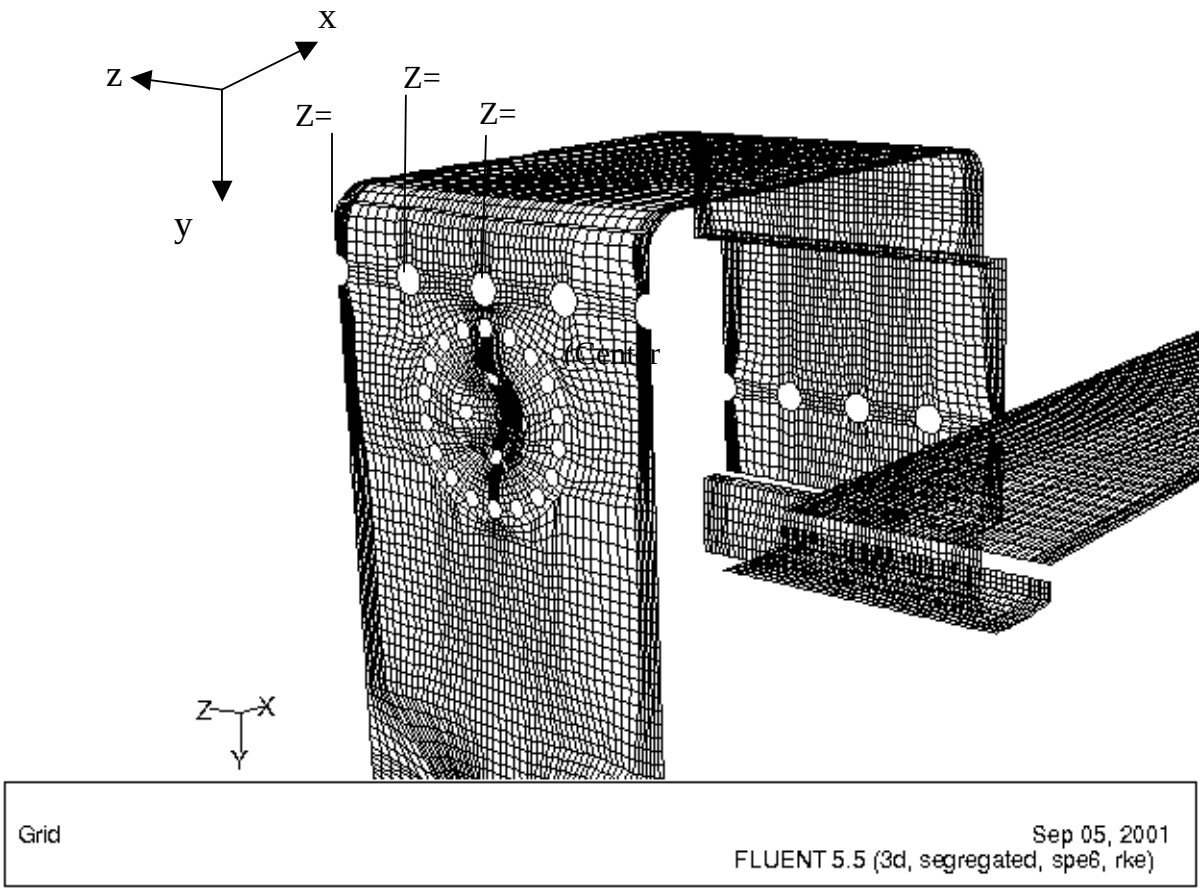

Figure 3-18 CFD grid model for single cup, upper half of 6” TVC rig configuration 1

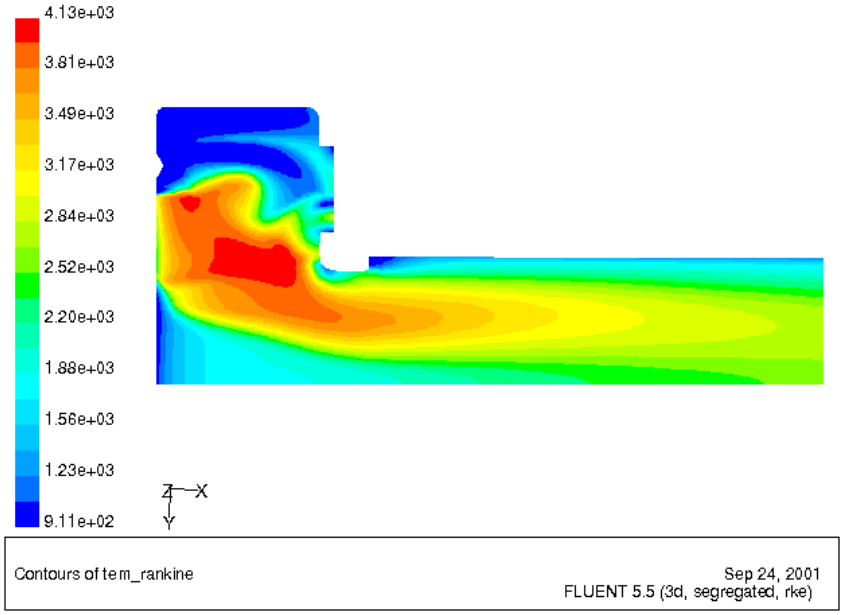

(a)

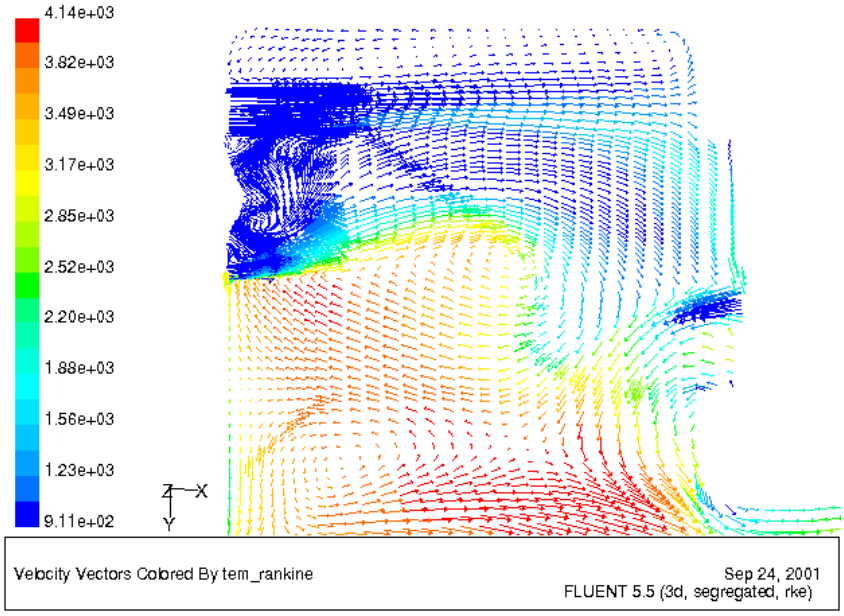

(b)

Figure 3-19 CFD Predicted temperature profile using the laminar flame model (LFM) at T3 = 450 °F and P3 = 15.5 psia (FAR = 0.03136, fuel split = 0.5) for 6" TVC configuration 1. (Plotted plane: In-line with the primary injector, center plane, z = 0")

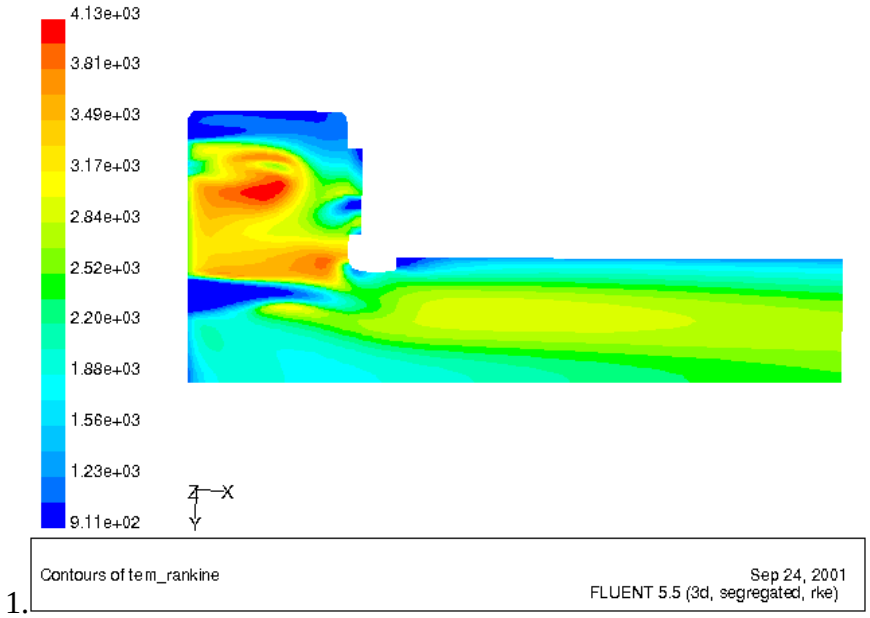

1.

(a)

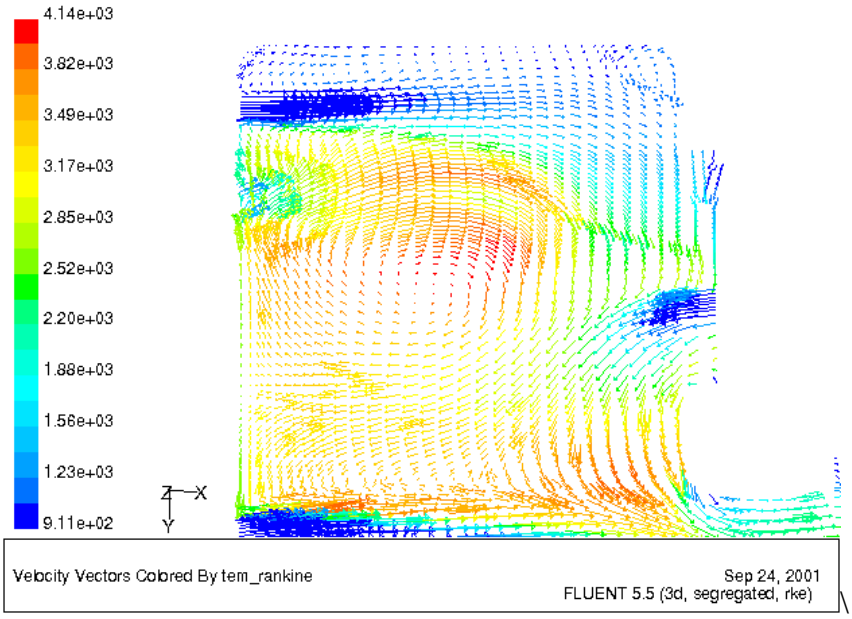

(b)

Figure 3-20 CFD Predicted temperature profile using the laminar flame model (LFM) at T3 = 450 °F and P3 = 15.5 psia (FAR = 0.03136, fuel split = 0.5) for 6" TVC configuration 1. (Plotted plane: In-line with the driver hole next to the center plane, z = 0.3")

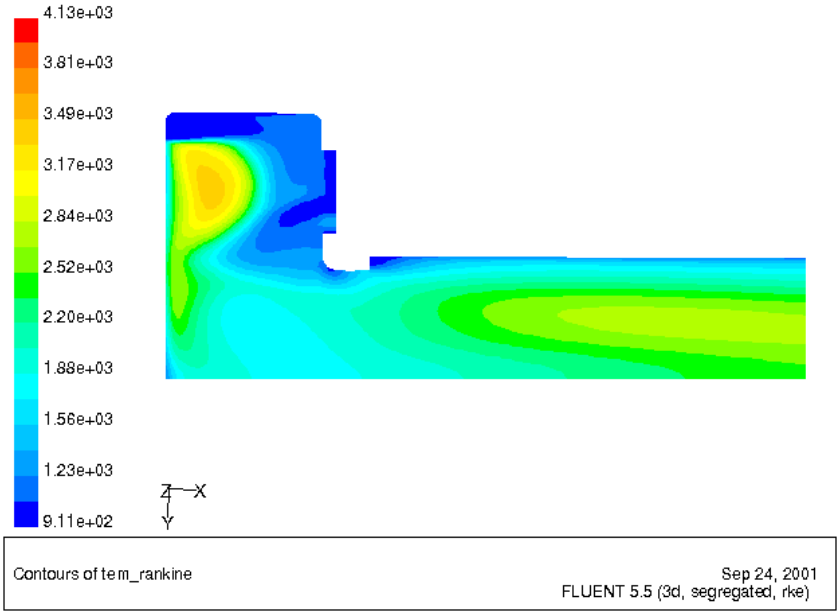

(a)

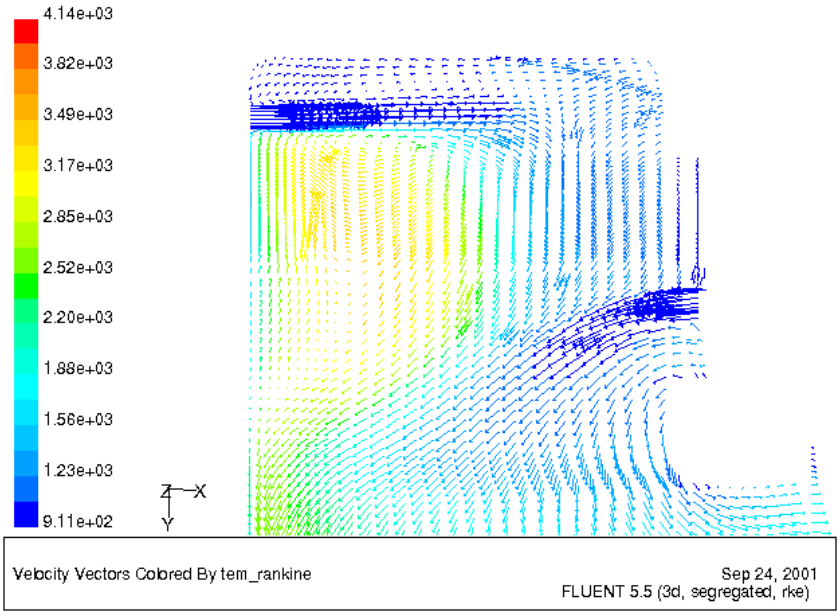

(b)

Figure 3-21 CFD Predicted temperature profile using the laminar flame model (LFM) at T3 = 450 °F and P3 = 15.5 psia (FAR = 0.03136, fuel split = 0.5) for 6" TVC configuration 1. (Plotted plane: In-line with the second driver hole from the center plane, z = 0.6")

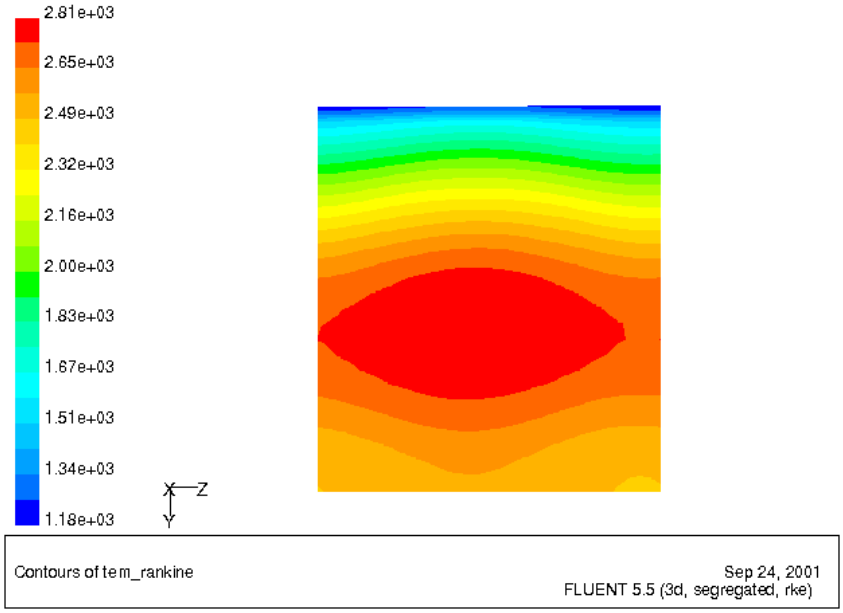

Figure 3-22 CFD Predicted exit temperature contour using the laminar flame model (LFM) at T3 = 450 °F and P3 = 15.5 psia (FAR = 0.03136, fuel split = 0.5) for 6" TVC configuration 1

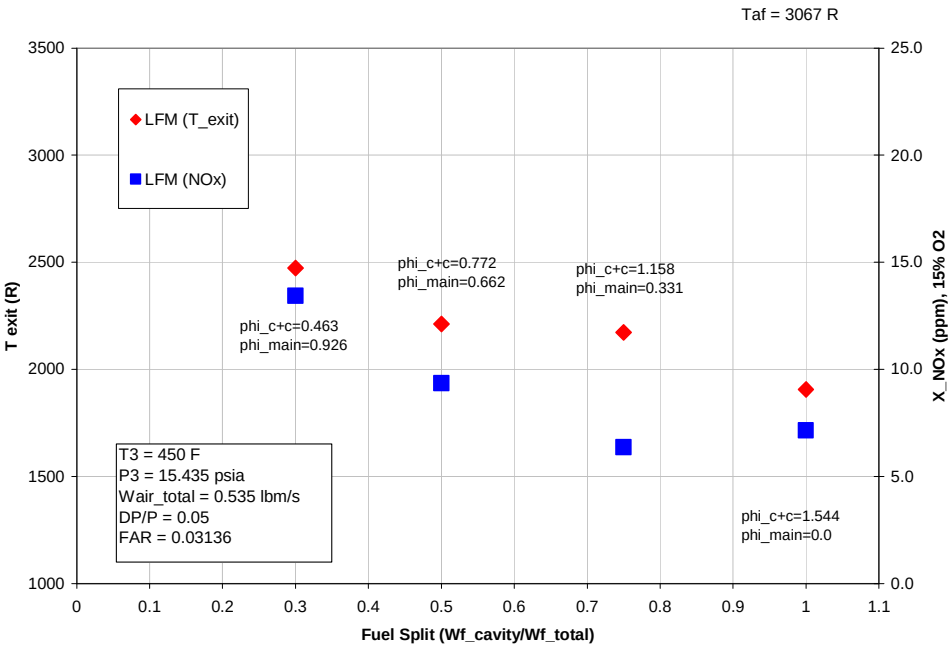

Figure 3-23 Predicted exit temperature and NOx by CFD model using the laminar flame model (LFM) over broad range of fuel splits for 6" TVC configuration 1

3.2 Prototype 1

The goal of this research effort is to design a combustion system with 50% lower NOx emissions and comparable CO to today's state-of-the-art premixed combustion systems. Low dynamics, high turndown, and acceptable thermal performance are also goals of the program. Early demonstrations of the TVC combustor with natural gas have demonstrated some promising preliminary results, but a more detailed investigation is being conducted here. In the evaluation plan of Prototype 1, three distinct prototype geometries are studied. However, through the process of conducting Design of Experiments, many design variations are investigated.

A Quality Function Deployment (QFD) was performed to rank the trapped vortex combustor design parameters with top level performance parameters, i.e. critical to quality (CTQ) factors. Figure 3-24 shows the results of the study. The ranking totals for each of the design parameters are given in the bottom row of the chart. The top ranking parameters to be investigated are highlighted in color on the bottom row.

All prototypes are designed with the dark blue features: visual access to the combustion zone, tunable injector fueling modes, and cavity fuel split controls. The first prototype will be used to explore the light blue characteristics as well: injector orientation, premixing length, corner design, and the number of main burner rings. These will be explored in a systematic manner using fractional factorial design of experiments.

According to the current assessment of the design parameters, the second prototype will differ significantly from the first prototype with regard to the cavity volume. The best light blue characteristics will be incorporated, but will also be the subject of further study.

The original intentions were to select the best performing prototype with regard to the top level system requirements and their rankings for scaled-up evaluation. Since combustor scaling is largely limited by facility capabilities, reduced pressure experiments were planned to determine the performance of a larger scale prototype. Demonstration of the flow field scalability as well as the critical combustion kinetics would reduce the risk of taking the design to full scale. The first prototype is a 1/6 scale design, and the evaluation plan called for a 50% increase to ¼ scale with the last prototype. However, this plan was not realized in these experiments. Instead, the second and third prototypes were 1/10 scale designs.

Combustion System Requirements

Product Requirements

Customer Expectation	Importance	Visualization	Injector Fueling Mode	Cavity-Main Fuel Split	Injector Orientation	Premixing Length	Corner Design	# Main Burner Rings	Main Burner Ports/Injector Ratio	# of Fwd Drivers	# of Aft Drivers	Aft Driver Radial Location	Cavity Volume	Cavity Aspect Ratio (L/H)	Cavity Shape	Cavity Injector Location	Prototype Scale		Total
T3 (combustor inlet temp)	4																		0
T3.9 (combustor exit temp)	5												M				H		60
P3 (compressor discharge pressure)	4												H				H		72
dP/P (combustor pressure drop)	3														M	L			12
Tau_TP (transition piece res. time)	4																		0
V3.9 (combustor exit velocity)	3																		0
NOx Emissions	5	M	H	H	M	M		L	L	L	L	L	H	M	L	L	L		235
CO Emissions	4	M	M	H	M		L	M	L	L	L		H	L	L	H	M		192
Turndown	3	H	L	H	H			M	M	M	M	L	H	M	M	M	L		180
Dynamics	4		H	M		H		L	L				L	L	L	M			116
Thermal Performance	4	H	L	M	L		H					M			H		L		144
Total		90	100	132	58	51	40	30	22	18	18	20	163	32	67	65	105		

Figure 3-24 Prototype 1 quality function deployment diagram

3.2.1 Component Design

The TVC performance is sensitive to the design of both the main burner and the cavity injectors. Several permutations in the basic design were incorporated into the test plan to evaluate this design sensitivity. Two designs were chosen for the main burner, injector premixing location, and diffusion circuit orientation.

The main burner designs of the annular TVC followed the approach of earlier designs with non-swirling bluff body stabilized flames. However, in this prototype the annular configuration reduces the main burner ports to a proportionally smaller space and a circular pattern. This configuration requires more air to be introduced near the center of the main burner rather than on the perimeter. As in earlier designs the main burner ports are paired with each cavity injector. A leading factor in the combustor design requirement as determined by a Quality Function Deployment (QFD) study was the number of main burner rings. The two designs featured three and two rings respectively. Both designs had the same target of 50% flow split and incorporated premixed fuel with the main air. The premixed fuel is introduced well upstream through a fuel manifold. The center of each main burner features an effusion air-cooled face.

The cavity is fueled by gaseous fuel injectors. The injectors were designed to introduce the fuel in either a diffusion mode or premixed mode or a combination of the two. The premixing circuit can introduce the fuel at two different stations. Each location has eight fuel injection holes through the outer wall at two axial positions in the tube containing the premix air. The first station is around 10 duct heights upstream and the second station is around 60 duct heights upstream. The fuel mixes with the non-swirling air over this distance before being injected into the cavity.

For the diffusion mode the injector has four fuel jets emitting directly from the tip into the cavity. The jets are equally spaced and set at a 30 degree angle to the horizontal. The orientation of these jets relative to the main burner and cavity outer wall is believed to be significant on the results of modeling studies. Two jet orientation configurations were proposed.

3.2.2 Flow Field Design CFD

A CFD model was developed as a design guide to determine the presence and strength of the cavity vortex structure. The baseline cavity geometry was transformed into a can-annular design, and target combustor exit temperature was set at 2900F at a pressure of ~270 psi. Target combustor total pressure drop was 5%.

CFD models were created to determine and test the scaling parameters which were used to transform a successful rectangular TVC design to a can-annular TVC. Target injector, main, and driver hole velocities were taken from the baseline Cartesian design. Passage hydraulic diameters were determined from the target pressure drop and velocity at flow temperature. Results of each can-annular design were compared to the baseline Cartesian design in terms of formation and size of the cavity vortex.

Modeling Tool: The 3D CFD solutions are generated with Star-CD with user defined reaction rates and detailed chemistry. A parametric approach is used to define and model the chemically reacting flow field. Geometrical definition typically starts with an Excel spread sheet definition which governs the 1D scaling and design of experiment concepts which are then incorporated into the 3D CFD model.

CFD Sub-models: The CFD model uses a standard k-e turbulence model. All flow properties, including specific heat, viscosity, and conductivity are functions of temperature taken from the CHEMKIN data base. A 5-Step chemical kinetic mechanism is used for the oxidation of methane and carbon monoxide. The reaction rate for each cell was determined by the minimum rate established from the chemical kinetic time scale and the turbulence time scale (eddy break-up)

Geometry definition: The can-annular prototype CFD model is assumed to be symmetric about the forward injector centerline and a circumferential plane between injectors. The typical model size is approximately 270,000. A mesh sensitivity study was performed in which each cell within the CFD model was refined by 2X2X2. Comparison of the results of the flow field and exit conditions indicating that the coarse model was suitable.

Computational Facilities: The CFD solutions were performed on a dedicated Linux cluster in which a typical converged solution was obtained in less than 6 elapsed hours. The solutions were obtained with Star-CD's V3.105A double precision executable.

In the first phase of combustor evaluation CFD modeling had a strong correlation with experimental observations and detailed measurements. The demonstration of CFD as a viable modeling tool for the TVC flowfield, makes it a valuable research tool in the design of the prototype combustor. Critical to the design's success is the establishment of a robust cavity vortex for mixing and stabilization. Flow field modeling was used to determine the impact of different design parameters on the flowfield.

The effects of the outer main flow exit angle on the cavity vortex were studied to determine the impact on the location and size of the cavity vortex. The main burner jet is angled toward the cavity corner. The baseline design had a flow angle of 11 degrees

from the liner centerline. Simulations were performed at flow angles of 9 and 13 degrees from the liner centerline, a variation of plus or minus 2 degrees. Results indicated that outer main flow angles between 9 and 13 degrees produced nearly identical cavity vortex structure. The flow is deflected out of the cavity by the vortex when the angle is increased. Surprisingly, the flow leakage around the cavity corner showed little change when the angle was decreased. These results demonstrate the robustness of the design relative to the angle of the main jet.

Next, the impact of injector orientation on the flowfield was examined for two injector orientations. The diffusion fuel circuit of the injector introduces fuel at four points. A CFD model of the combustor was operated for both cases. A preferred orientation was chosen based on the CFD results. This orientation showed improved delivery of fuel, enhancing combustion in the main jets and flame stability.

A fundamental difference between the atmospheric combustion experimental studies and the sub-scale prototypes is in the air distribution of the system. The atmospheric studies prototype had 13% less head end air than the prototype target. Moving more air to the head end in the prototype reduced the peak flame temperatures in the cavity and main. The impact of this change on the cavity vortex structures was observed to be small in the models. The primary and secondary vortices both show a temperature rise, albeit several hundred degrees less. The lower head end flame temperatures are believed to be important for lowering the overall NOx emissions from the TVC combustor.

The combustor flowfield predicted by CFD was shown to have a strong correlation with the experimental flowfield in the atmospheric combustion studies investigation. In this phase of the program CFD has been used to design the flowfield for the prototype combustor. A critical feature of the flowfield is the presence of a strong, high-temperature, primary vortex in the cavity. The presence of a secondary vortex is also desirable for increased stabilization of the main burner.

The sensitivity of the design to various design parameters has been investigated. The CFD model reflects the relative changes in the flowfield as the boundary conditions are changed. A flowfield design with a strong central vortex has been modeled and will be developed into the first prototype design. Visual observation of the cavity flowfield will be used to observe the size and location of the vortex in comparison to the CFD model. Additional modeling will be performed to determine flowfield changes with flow split.

3.2.3 Thermal Modeling

The scope of the thermal/mechanical design effort is to ensure the structural integrity of Trapped Vortex Combustor components. All combustor components exposed to hot gas flows need some degree of cooling. This is because the temperature limits of the alloys used are well below that of the gases they must contain. These temperature limits can be due to the onset of excessive oxidation, the degradation of strength properties, or to thermally induced stresses. For the purposes of the rig testing, oxidation is not an issue due to the "short" time at operating temperature. Controlling thermal stresses can require limits on both maximum temperatures and temperature gradients.

Existing combustor-cooling designs, field experience, best practices and lessons learned are employed in the design of the TVC rig. "Controlled convection" refers to forced convection with a specific device to control the flow velocity. This was employed between the combustion liner and Hula Seal Collar. "Passive convection" refers to forced convection but with no effort to control the flow velocity with a separate device. This was employed on the backside of the cavity. The combustor forward wall and outer wall were effusion cooled according to the best practices of the WPAFB prototype. The aft wall of the combustor was slot cooled. TBC was employed on all combustor hot surface to increase their temperature limits / life. In designing the cooling system the spallation temperatures of the TBC were considered a max temperature.

A simple assessment of the combustion liner heat transfer was made to determine the design requirements. Flow velocity and flow rate were examined for a variety of conditions to determine the best design. Figure 3-25 shows the results of the analysis for the best design with a flow velocity of 133 ft/s and a passage height of 0.027." The collar was extended over the length of the combustion liner to extend the controlled convection over its entire length. The combustion liner also had backside impingement cooling holes at the upstream end to cool hot-spots downstream of the corner.

Cooling of the cavity surfaces was evaluated in a progressive manner as shown in Figure 3-26. Heat transfer correlations were used to first approximate the cooling effects on a given surface. Then a finite element model was constructed to give a 3D picture of the surface temperatures. A design sensitivity study was then conducted on different parameters to determine the best cooling hole size and spacing for the flow available. The study conferred that an H/d = 8 would be sufficient for 0.020" cooling holes on the outer wall. The study also indicated that 3 rings of 150 cooling holes of 0.020" diameter would work best for cooling the corner.

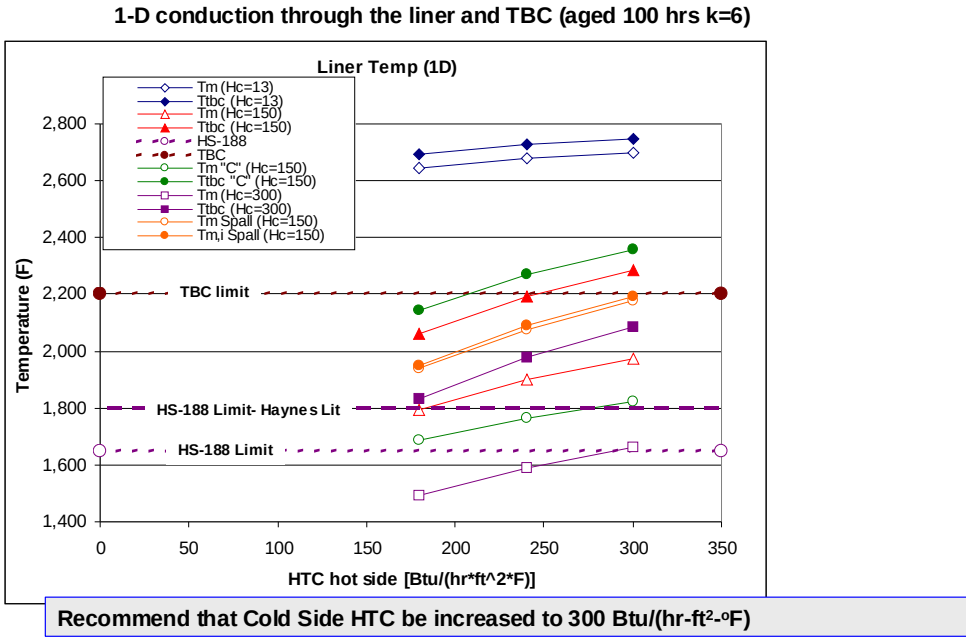

Figure 3-25 Prototype 1 liner cooling analysis

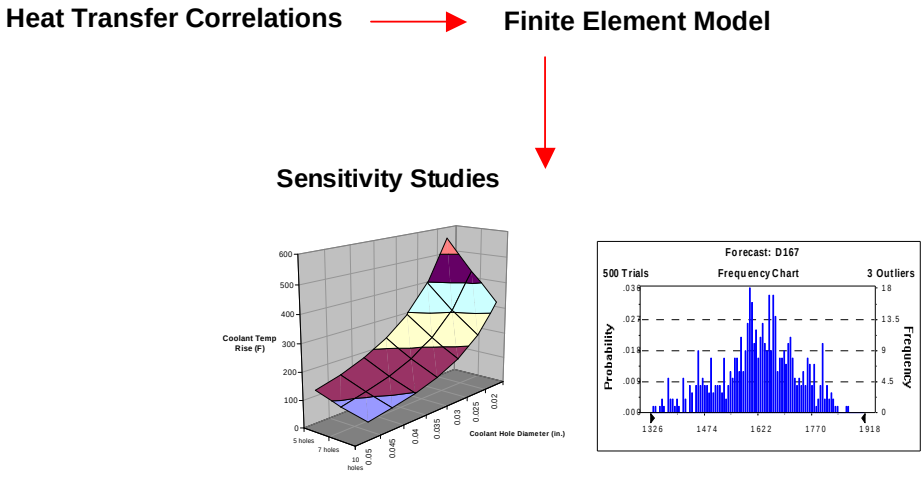

Figure 3-26 Prototype 1 cavity cooling analysis

3.2.4 Combustion Test Rig

Air & Gas Supply

The GE Global Research combustion test facility is capable of simulating the combustor inlet conditions of a heavy-duty gas turbine or an aero-derivative. Sub-scale prototypes and component parts of large-scale machines can be evaluated at this facility with a 16 lb/s maximum air flow capability. Compressor discharge pressures can be simulated up to 40 atm. of pressure using a boost compressor, and inlet air temperatures up to 1100 F can be evaluated using a gas fired heat exchange preheater.

Natural gas from the local utility is supplied to the test facility for combustion tests. The gas is periodically analyzed to determine its composition and heating value. A high pressure boost compressor can supply 600 psi natural gas to an experiment at flow rates of at least 0.25 lb/s. A storage plenum is integrated into the system to ensure that the gas supply pressure remains relatively steady.

Pressure Vessel

High pressure combustion tests are conducted within a test vessel rated for 350 psi. and 1050 F operation. The vessel is made of 316H stainless steel components. Two sections of 16" pipe, a 28" and a 38" pipe, make up the body of the vessel which houses the combustor shown in Figure 3-27. A 16" flange is held between the two vessels. Compressor air is supplied to the vessel through a 4" pipe connected to the top of the first vessel. An over-pressure rupture disk is attached to the second 4" pipe connected to the second vessel. The test piece connects to a water cooled 16" flange assembly which injects high pressure water into the hot products and transitions to an 8" exhaust pipe. The downstream end of the exhaust pipe connects to a flow control valve which is used to regulate the backpressure in the vessel.

Flow metering & Control

Accurate evaluation of the flame temperature is important to any investigation of NOx emissions. Exit temperature profiles can be evaluated with an emissions probe, but closure with metered flow measurements is also performed to ensure experimental accuracy. Furthermore, combustor control depends on the internal fuel splits, so steps are taken to resolve these distributions.

Because of the importance of these measurements, a Six Sigma project was undertaken to evaluate the accuracy of the flame temperature measurement based on flow rates. In a Pareto evaluation of the sources of error, measurements of the fuel heating value and the heat release transfer function ranked lower than errors in phi. The accuracy of individual fuel and air flow rates is the single most important factor in this calculation. A statistical tool was developed to properly size the flow metering system and obtain a clear understanding of the systems ability to evaluate flame temperature.

The air flow to the test vessel is metered using a large and a small flow orifice on the cold flow. With independent control of the flow through the orifices, a wide range of air flows can be measured with 3% accuracy and 95% confidence. All of the air supplied to the test vessel participates in combustion.

The fuel is supplied to the combustor through three different circuits: main burner fuel manifold, injector diffusion fuel manifold, and injector premixed fuel manifold. With the use of a venturi an individual fuel stream can be measured with 2% accuracy and 95% confidence. Figure 3-28 shows the fuel metering schematic for the test hardware. Venturi were positioned to measure the specific flows for which the greatest accuracy was desired. Other flows could be calculated from this basis set, but errors would accumulate in the other calculations. The total fuel flow to the rig is metered independently so that the flame temperature can be calculated as accurately as possible. The fuel flow to the main burner is calculated to get an accurate estimate of the premixed flame temperature. The total cavity fuel is measured to assess the overall flame temperature in the cavity. The injector premix fuel is metered to determine the split between premixed and diffusion fuel with 3% accuracy and 95% confidence.

The combustor geometry is divided into two zones to facilitate better visualization of the cavity flame during operation. This requires the combustor manifolds to be divided into two sections. Figure 3-28 shows the branching of the fuel circuits just before the combustor. The fuel metering system can meter the fuel flows with 1.7% accuracy when fueling only half of the combustor.

The fuel flow control system is also detailed in Figure 3-28. The fuel flow to the main burner, injector diffusion circuit, and injector premixed circuit are controlled independently. Each circuit can be turned on and off, and each has its own flow control valve. There are also manual and actuated shut-off valves for the total fuel flow for the rig as well as a control valve for the same function. The manifold branches can also be shut-off with a manual valve so that only half of the combustor is fired.

The air is supplied continuously to the rig during compressor operation. Air from the compressor is directed to the rig through a system of actuated and manual 6” valves. The air flow control valves are located upstream of a pre-heater and enable turndown of the overall flow. Downstream of the test rig is located a control valve where the water cooled products of combustion are restricted to establish vessel pressure.

Overview of flow path

After the air enters the test vessel through the 4” pipe to the vessel, it is annularly distributed by a manifold with 8 holes into the central part of the vessel. A thin walled reverse flow liner then directs the air to the opposing end of the test vessel. From that end the air can flow along the length of the combustor cooling its walls and supplying air to the combustor at various locations. Figure 3-29 shows the combustor air flowpath and a schematic of the hardware components. The combustor test section is cantilevered from the 16” flange. It connects to a simulated transition piece consisting of an inlet and ceramic lined duct. Sample probes pass through the vessel at the entrance of the transition piece and at a downstream position which represents the total combustor residence time.

Reverse flow liner

The reverse flow liner is a SS 316 rollup that is cantilevered from the inside of SS 316 ring. This ring is held in position with 12 radial bolts that extend into the outer wall of the 16” chamber. The reverse flow liner is used to increase the convective cooling of

components by forcing the cooler inlet air to flow over the entire assembly en route to the head end of the combustor.

Head end mounted combustor

The TVC combustor assembly will be constructed on four thread rods that are cantilevered from the head end flange. This allows for easy combustor modifications, by removing only the head end flange, while leaving the downstream components undisturbed.

Transition piece

The transition piece is used to carry the combustion byproducts out of the test vessel. It was constructed from a stock 10 inch SS316 pipe that had a ceramic liner cast within it. The transition piece is rigidly bolted to the downstream flange of the vessel. Figure 3-30 shows this assembly. There are two 3/8" diameter radial openings that allow for sample probes to enter the flow path. The sample probes are located at the exit of the combustor and at the position representing the transition piece exit of an F-class combustor. These probes have large external actuators, which allow them to transverse the flow field, and therefore had to be carefully aligned with external ports in the vessel. Custom sealing assemblies were designed for the 10" pipe to minimize the leakage around the probes into the combustor products.

The transition piece is attached to the combustor assembly with a custom made double hula seal that is welded to the combustor exit piece. The hula seal allows for thermal expansion of components in the axial direction while maintaining a small leakage area.

Water cooled exhaust

The hot products leaving the transition piece enter a water cooled flange assembly. The water is injected into the hot products through 8 holes around the outside of the 8" pipe in the center of the assembly. The water flow rate is regulated to provide sufficient cooling to the products to protect the downstream control valve.

Pressure control valve

An 8" pipe connects the water cooled assembly to a downstream control valve. The control valve restricts the flow of the cooled products and regulates the pressure of the vessel. The temperature of the valve is monitored for adequate cooling. With this arrangement any combustor test condition can be simulated.

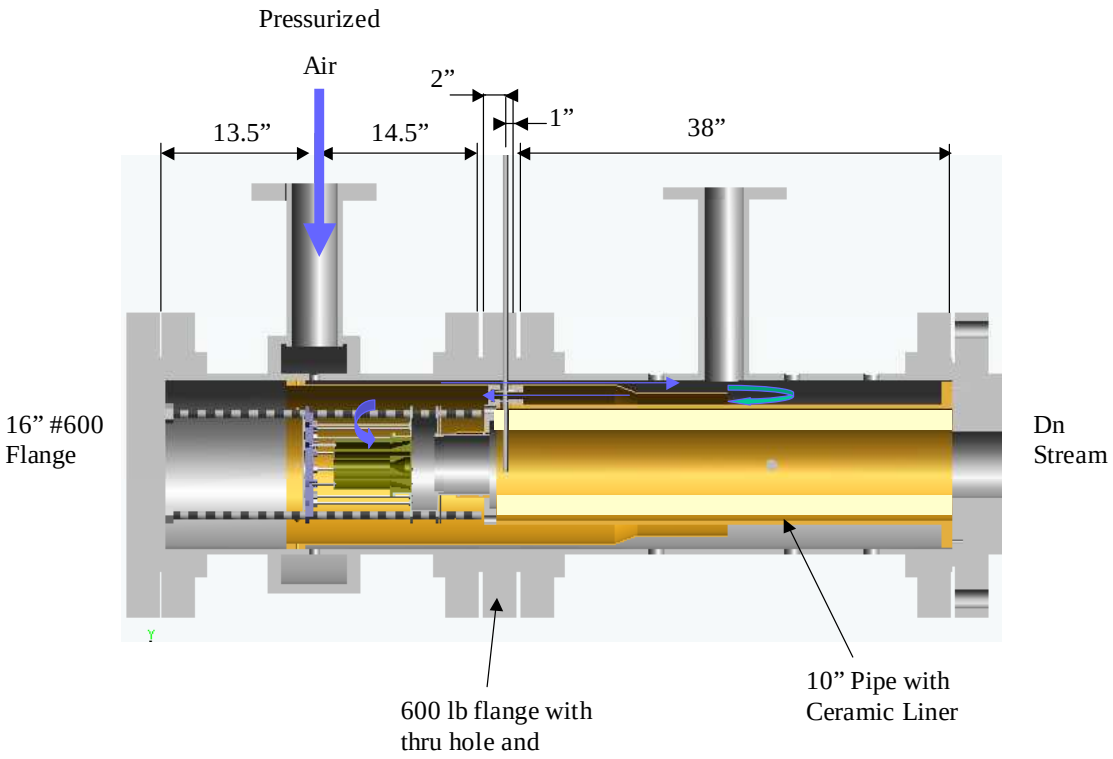

Figure 3-27 Pressure vessel layout

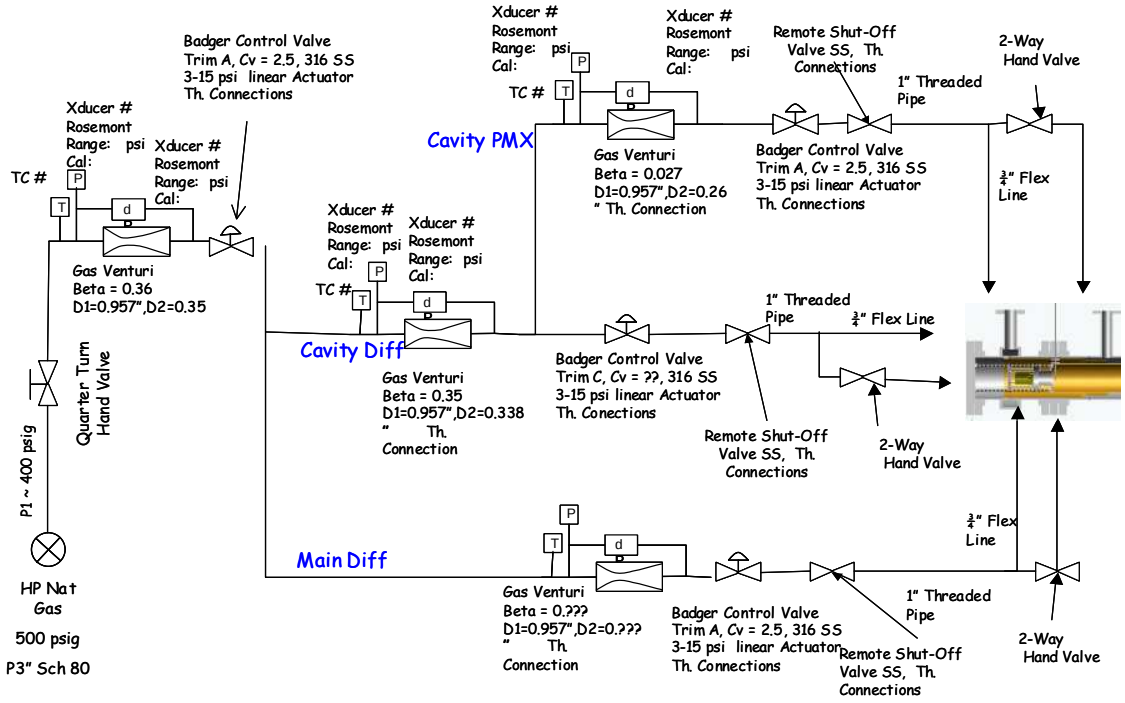

Figure 3-28 Fuel metering schematic

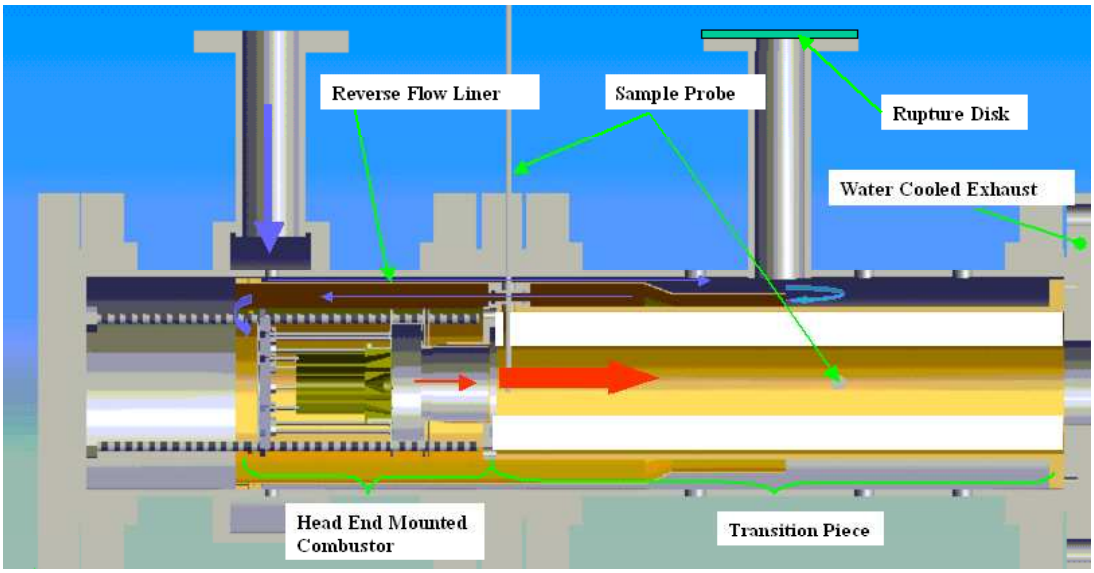

Figure 3-29 Prototype 1 combustor flowpath

Figure 3-30 Ceramic combustion liner inside of test vessel

3.2.5 Combustor Components

The combustor body was held from four threaded rods that are cantilevered off the head end flange. Figure 3-31 illustrates a cross section of the combustor body. By using a series of eared rings secured to the threaded rod, the combustor body is assembled by sandwiching sections together. This provides for modularity in the design to facilitate parametric design studies.

Main Burner

The main burner consists of a patterned area for premixed fuel and air to pass. The center of the burner is a bluff body with an effusion cooled surface. Fuel is premixed with the main burner air in an annular passage leading up to the exit. Figure 3-32 shows the fuel and air premixing tube for the main burner. Stabilizing this lean mixture is the responsibility of the cavity vortex.

Injectors & Manifold

The injectors are custom made and will allow for the both premix and diffusion experiments to be run. The downstream side of the injectors seat against the back of the forward wall, while the upstream end is rigidly connected to a split manifold (not pictured) with Swage Lock fittings. Figure 3-33 shows the upstream injector hardware. The manifold has been designed so that half of the injectors can be fuel at a time, this allows for the better visualization of the combustion zone.

Forward Wall

The forward wall is constructed from Haynes 188 alloy. It has three concentric bolt circles. The first set seats the injector, the second set is for the cavity driver jets, and the last allows the forward wall to be bolted to the outer wall and the eared ring. The cavity size was determined following reduced drag criteria for the vortex. [1]

Outer Wall

The size of the outer wall dictates the vortex cavity aspect ratio and size. The length of the cavity was kept at an aspect ratio of 1.2 times its height to promote the formation of the vortex and strong interaction with the main flow. [1] [2] The outer wall is constructed from four individual pieces. Parts that will be located in the combustion zone are fabricated from Haynes 188 alloy, while the outer flanges will be made of Hastelloy X. Figure 3-34 is the outer wall, showing a port for visual access with a camera.

Aft Wall Assembly

The aft wall assembly consists of the three parts, the aft wall, the corner ring and the corner ‘L’. The aft wall and the corner ‘L’ are manufactured using Haynes 188 alloy. The corner ring will have backside cooling slots and therefore can manufactured using a material with a lower temperature rating, Hastelloy X.

Combustion Liner

The combustor exit is constructed from a heat-treated Haynes 188 alloy rollup. The combustor liner is welded to the corner holder which is welded to the aft wall

assembly. On the down stream side the combustion liner is fitted with a double hula seal which minimizes leakage. The inside of the liner is coated with TBC.

Hula Seal, Collar & Flange

The hula collar and flange have been fabricated from SS316. The downstream end of the flange bolts to the ceramic lined transition piece. The combustor exit then slips inside the collar where it is held in radial position by the hula seal. It is however free to move axially to accommodate any thermal expansion experienced by the components. The hula seal is shown in Figure 3-35, with the assembled hardware.

Non-reacting tests were performed at atmospheric conditions to determine the effective areas of each air passage of the trapped vortex combustor test rig. This information provides the percentage of air that goes to each major zone in the rig including combustion air, cooling air, and sealing leakage air. The experimental results are compared to theory and the air split information is programmed into the data acquisition software to calculate flame temperatures in the combustion regions for combustion testing. Also the information gives an indication how much cooling and leakage air is used.

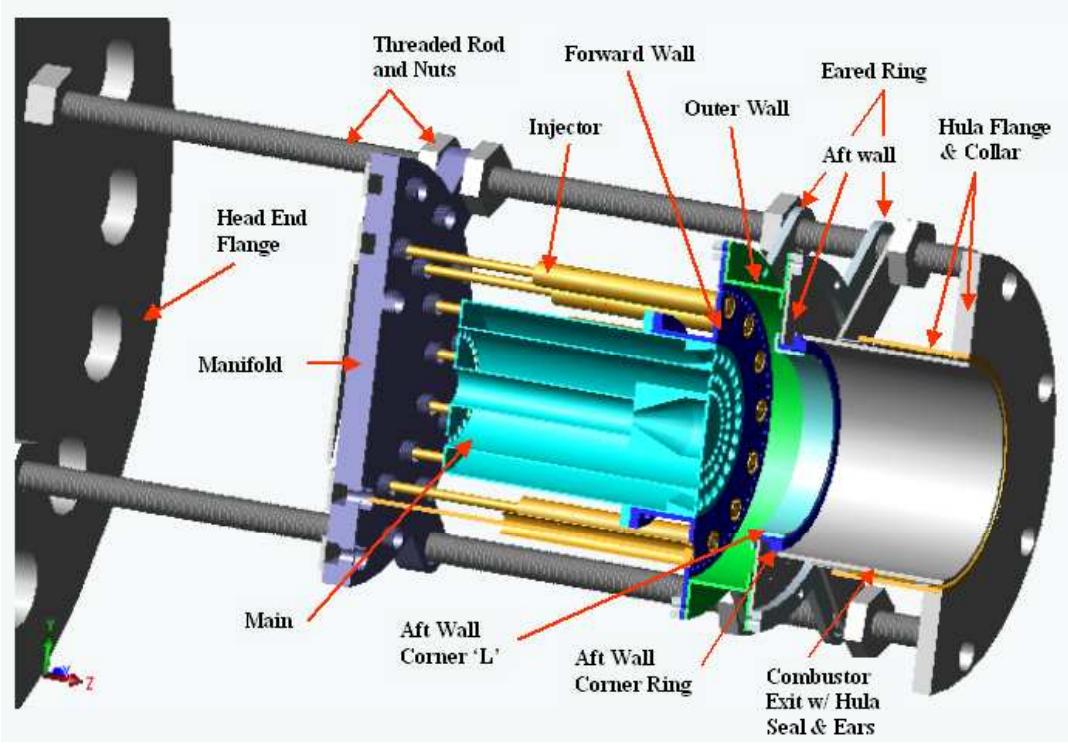

Figure 3-31 Prototype 1 combustor components

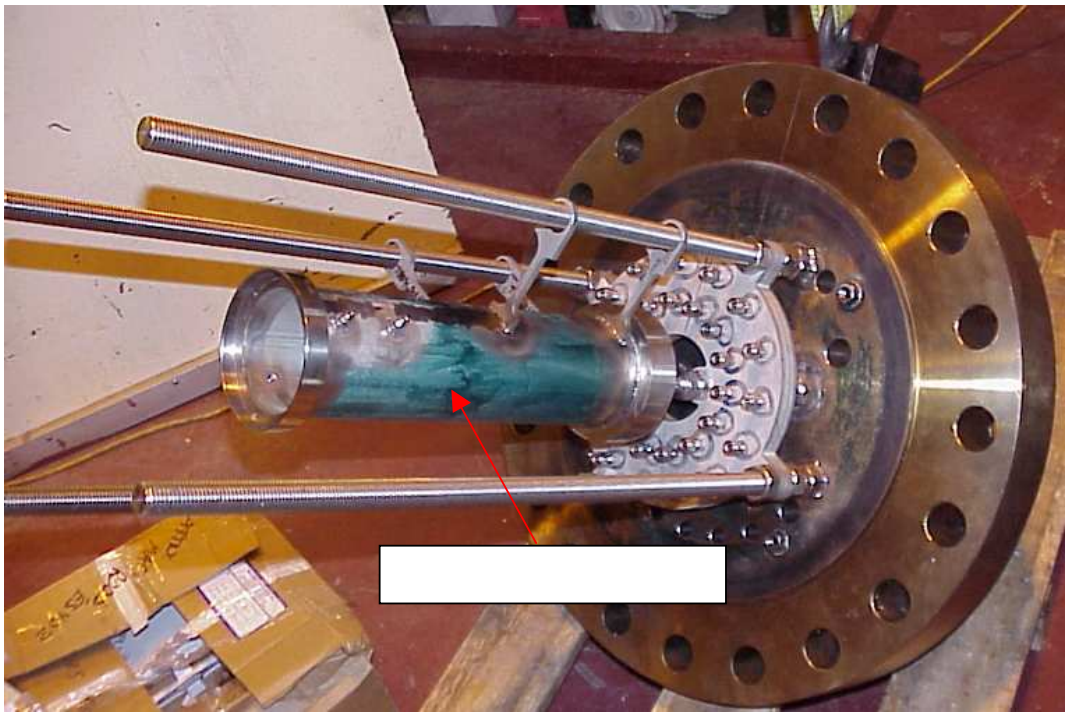

Figure 3-32 Prototype 1 main premixing section assembled on head end flange with fuel injector manifolds

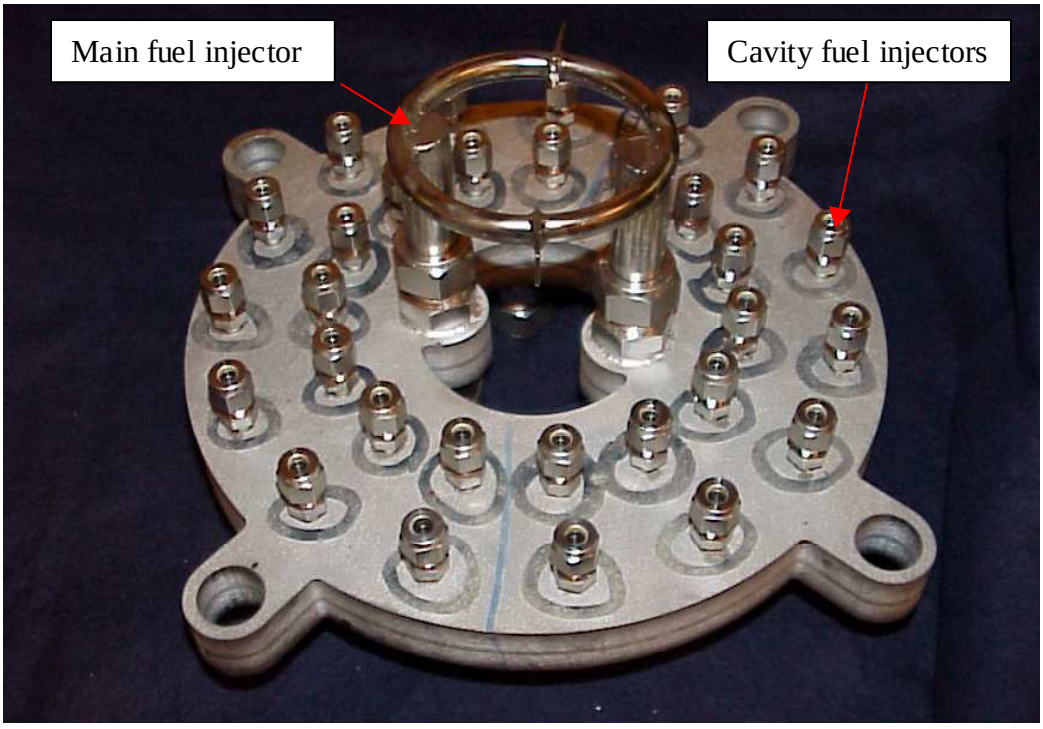

Figure 3-33 Prototype 1 fuel injector manifolds

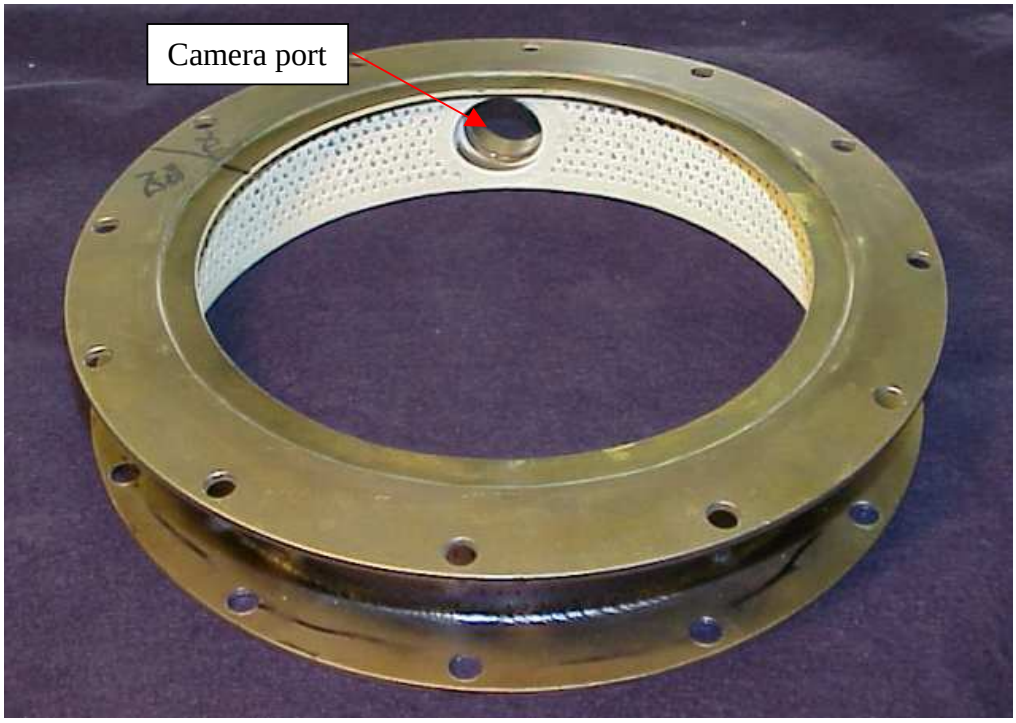

Figure 3-34 Prototype 1 outer wall showing camera port

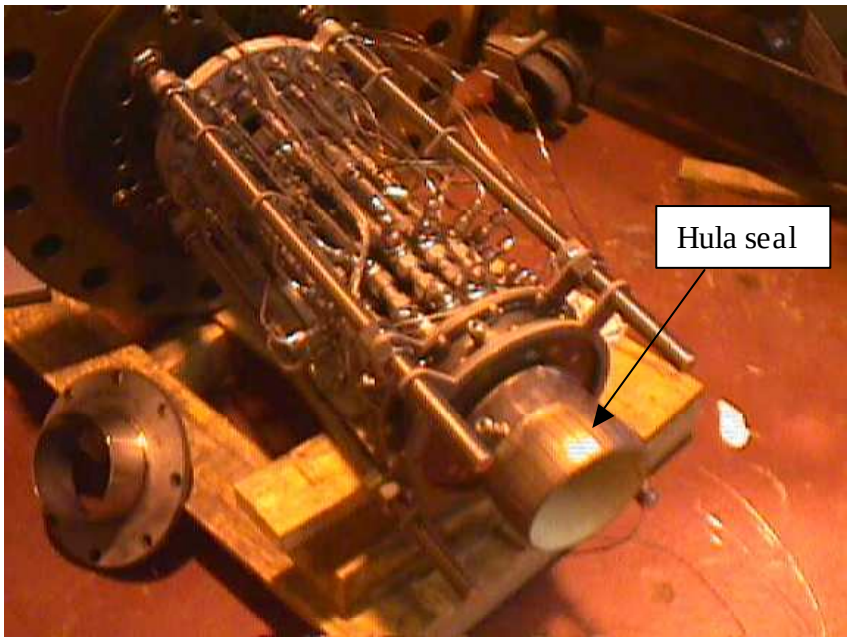

Figure 3-35 Prototype 1 assembled experimental hardware showing hula seal

3.2.6 Instrumentation

Gas sampling

The capability to collect and analyze gas samples is critical to the demonstration of a low emissions combustor. In the TVC combustor gas samples are taken at two locations. The upstream location corresponds to the exit of the combustor into the transition piece. Emissions at this location are also representative of those in an aero-derivative when the proper inlet conditions are maintained. Further downstream in the transition piece the second sample is collected. This location represents the exit of the transition piece into the turbine when the proper inlet conditions are met. Both gas sample probes can be traversed radially across the full width of the combustor. The annular design is not expected to have a significant tangential profile at the downstream position. Profiles will be measured to verify this assumption and verify closure with the fuel metering system. The profiles can be used to determine radial temperature gradients and emission gradients as well.

In the experimental facility gas samples are collected in the combustion zone through a water-cooled probe. Pressure in the vessel drives the flow through the sample line; the flow rate is regulated by a valve downstream. The sample is then delivered to the analyzer bay through a heated line. Dry samples are obtained by means of an ice bath condenser; wet samples come directly from the heated line.

The analyzer bay consists of several instruments. Each is connected directly to the data acquisition system for real time recording. The CO analyzer has ranges of 0 to 100, 0 to 500, and 0 to 1000 ppm. The NO/NOx analyzer has ranges of 0 to 10, 0 to 25, 0 to 100, and 0 to 250 ppm and takes a dry sample. The O2 analyzer operates on a 0 to 25% scale and can be used to determine the fuel-air ratio and diluted temperature of the upstream combustion process. The CO2 with a 0 to 10% scale can be used for the same purpose. An unburned hydrocarbon analyzer has a 0 to 5% range and is used to confirm fuel flow continuity as well as unreacted fuel concentration.

Temperature Measurement

The TVC combustor hardware is heavily instrumented with thermocouples to monitor critical part surfaces and determine thermal performance of the cooling system. Figure 3-36 shows the location of thermocouples on the combustor transition piece. Three are located by the flange interface with the water cooled section to monitor wall temperatures in this low flow region. Three are located in the vicinity of the downstream sample probe to check for hot gas leaks or breakdown of the ceramic in that area. Four are located around the upstream sample probe to check for ceramic breakdown at the inlet. These thermocouple will be scanned by the data acquisition system every few seconds, and a temperature history will be stored for each experiment.

The combustor is instrumented with thermocouples at several critical surfaces. Figure 3-37 shows the location of these. Three TC's are located on the combustor wall below the hula seal to monitor exit liner temperatures. Two are located on the hula seal collar to determine the effectiveness of the cooling flow. Three are located at the start of the hula seal to monitor hot spots. The cavity corner, aft wall and outer wall each have three TC's evenly spaced to monitor part temperatures. The forward wall has TC's near the weld for the main burner holder. At least three of the injectors are equipped with

flashback TC's in series with a fuel shut-off alarm. The main burner is equipped with the same detection and alarm system. The other injectors will have flashback TC's to monitor the temperature but will rely upon a software alarm.

Pressure Measurement

Critical pressure and delta pressure measurements are taken at strategic locations in the combustion system.

Figure 3-38 shows the critical locations where pressure is monitored for the Prototype 1 hardware. Locations include the air supply pipe, the reverse flow liner, the combustion entrance, and the cavity, main, and transition piece combustion zones.

Dynamic Pressure Measurement

In premixed combustion systems coupling between the heat release and pressure waves can grow to create significant pressure dynamics within the combustor. The cavity vortex of the TVC combustor is expected to have a stabilizing effect on the combustion instabilities, but the combustion dynamics will be monitored to justify this claim. Three high response dynamic pressure transducers will be connected to the rig. One will be located in the combustion liner and two will be located 90 degrees apart in the cavity. With this arrangement axial, tangential, and bulk modes of dynamics can be measured.

The signals from the high response pressure transducers will be processed by a high speed data acquisition system and signal analysis software. The frequency and amplitude of the dominant modes will be stored at regular intervals by the data acquisition system. More detailed data files can be generated over short periods of time for test points of special interest.

Optical Access

Visual access of the flame in the TVC combustor is the easiest way to evaluate the strength of the cavity vortex. To facilitate this a camera port is mounted on the wall of the cavity as shown in Figure 3-39. Furthermore, the combustor design allows for it to be fired on only one side. The camera is positioned to look at a right angle to the first injector to be fired in this mode. The adjacent injectors will create a background image, but most will be blocked by the curvature of the combustor.

The camera is a 2.54mm diameter miniature camera housed in a water cooled jacket. The camera housing has a quartz window for optical transparency and is sealed to prevent leakage. The combustor has a quartz window with a compression fit to prevent leakage across the opening. The camera is aligned the window on the combustor to view the top of the cavity to near the centerline.

The camera can also provide information on hot sections in the combustor design, and alert the operator to over temperature conditions. The camera has visual access to the top side of the forward wall and aft wall and corner. It also has visual access to one-quarter of the cavity outer wall. The flame attachment location on the main burner may be determined, and the thermal design of the corner will be evaluated.

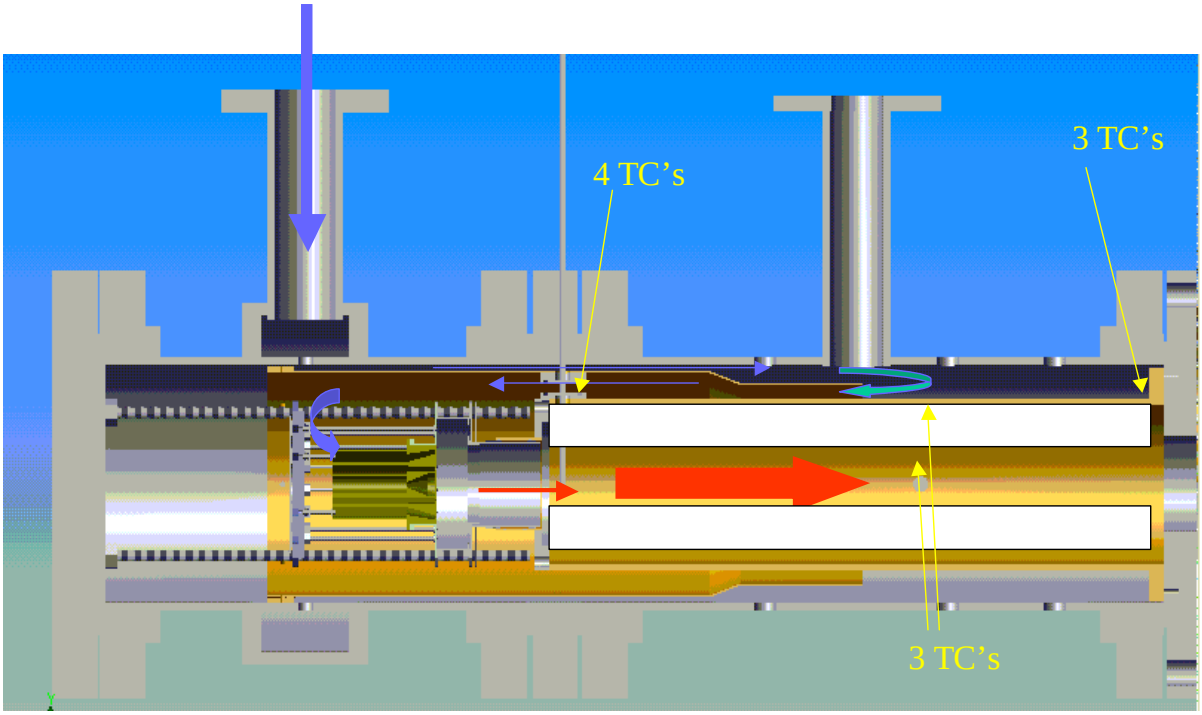

Figure 3-36 Thermocouple instrumentation on the test vessel for Prototype 1

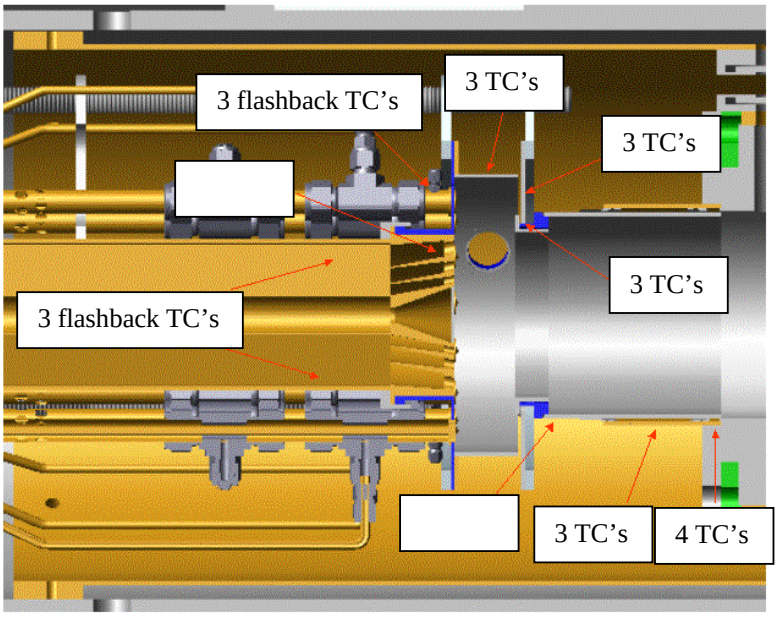

Figure 3-37 Prototype 1 Thermocouple instrumentation locations

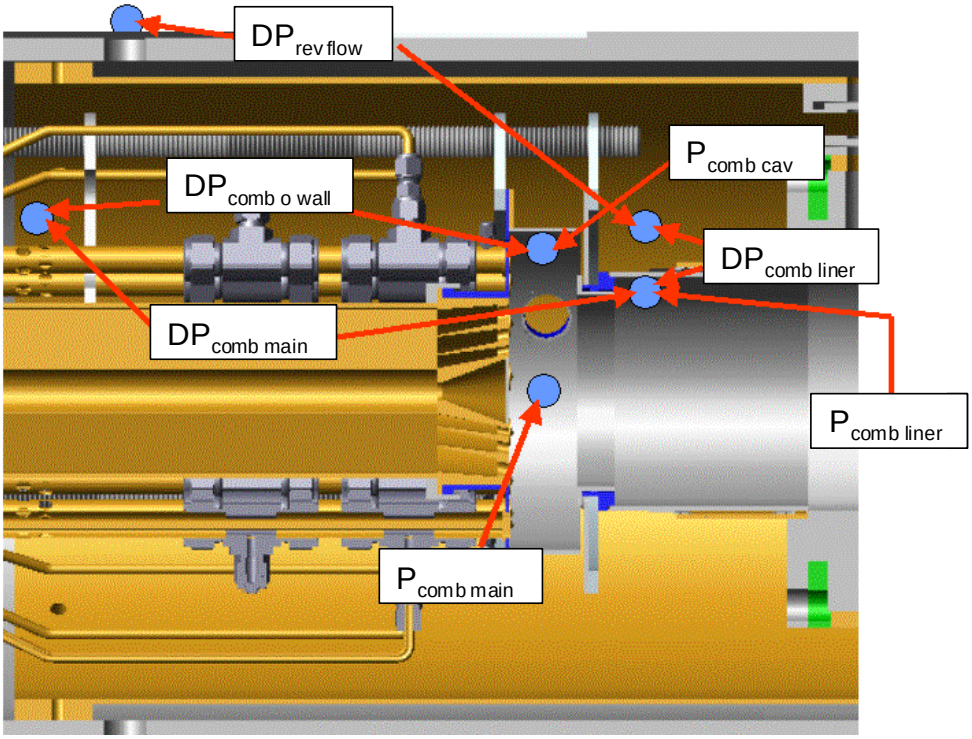

Figure 3-38 Pressure instrumentation locations

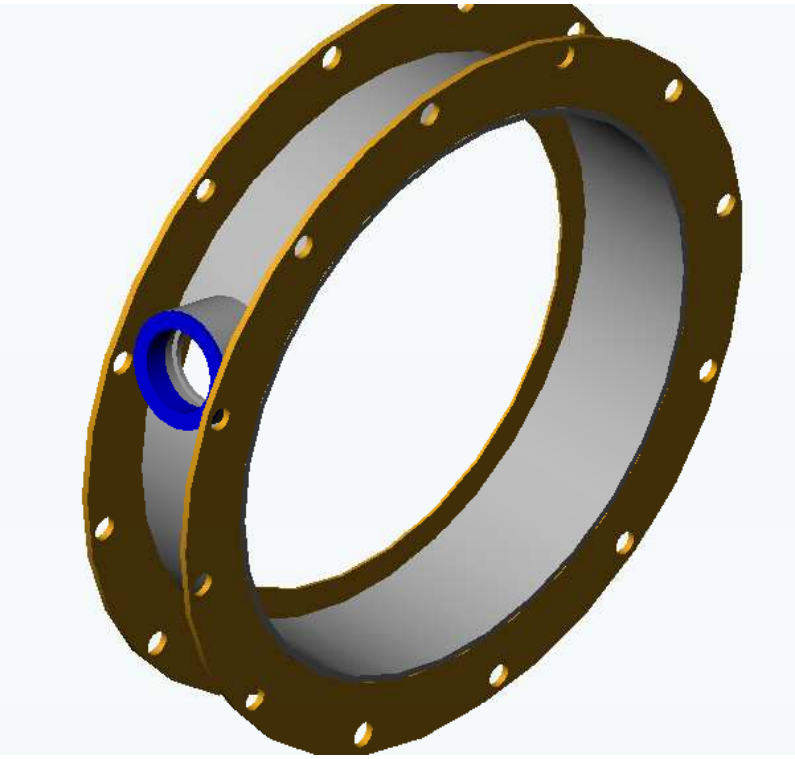

Figure 3-39 Prototype 1 optical port

3.3 Prototype 2

Several enhancements were made to the trapped vortex combustor design during this design phase. First, as an extension of Prototype 1, design changes were proposed and validated by CFD modeling to improve the vortex structure in the cavity. This design is termed Prototype 2a1. However, the emissions results were unsatisfactory. As a result, several design concepts changed in the next prototypes. In Prototype 2a2, the cavity and main premixer designs were changed. The 15 cavity fuel injectors were replaced with an annulus with 25 slots. The main premixer design changed from concentric holes to 15 radial slots. For Prototype 2b, less outer wall effusion cooling was used, and the forward wall was redesigned to accommodate thermal growth issues with Prototype 2a2. Further, the 2b design included cavity premixer analysis, resulting in a change in the cavity premixing section. Due to more thermal issues on the forward wall, extensive redesign was performed for Prototype 2c. Additionally, this design included the elimination of the aft fuel driver ports and a further reduction in cooling. Combustion tests were performed and emissions data was obtained from Prototypes 2a2, 2b, and 2c.

3.3.1 Component Design

Prototype 2a1 was designed following the design effort of Prototype 1, with the goal of strengthening the cavity vortex and reducing emissions. Using the QFD evaluation of the design criteria, the leading design parameter was selected for study in Prototype 2a1. The combustor cavity volume ranked highest, far above cavity aspect ratio, shape, and injector location. Changes in any of these parameters required a significant change in the prototype hardware and could not be studied without a significant design and manufacturing effort.

Prototype 2a2 also incorporated a change in the combustion liner because of the thermal performance limitations encountered in the evaluation of Prototype 1. This change was added after the evaluation knowing there was still adequate time to incorporate the change. The 2-cool combustion liner was selected because of its ability to cool the liner with very small clearances. The sealing flange and transition piece had to be resized based upon the changes in the design.

Following the aerodynamic design study it was decided to reduce the cavity effusion air. This was accomplished by sealing the cavity effusion walls with a stainless sheet. The sheet covered the span of the cavity, but TC's were place on the outer effusion wall surface to monitor the temperature during evaluation. The wall temperatures were monitored during evaluation.

A cross-sectional schematic of Prototype 2a2 is shown in Figure 3-40. The forward wall was designed in two sections, an inner piece for the main burner and an outer ring for cavity fuel injection.

Prototype 2b incorporated more significant changes to the combustor design than prototype 2a2 as a result of additional efforts to improve the turndown performance while maintaining low NOx. Based on aerodynamic considerations the land area of the main burner needed to be increased, the injectors needed to have a more uniform

circumferential fuel distribution, and the cavity cooling and air distributions needed to be changed. Additionally, Prototype 2b was targeted to have no step downstream of the cavity corner to make it more representative of a realistic design.

The most challenging change in the new design was the removal of injectors. The intent was to introduce the fuel into the cavity in a fashion that would mimic a driver hole, from a flow standpoint, while maintaining two distinct fuel circuits. Ideally the fuel would enter the cavity at the same radial position regardless of the operating mode, diffusion or premix. Unfortunately, such a design would be very expensive to develop because it would require complex fuel circuits, switching mechanisms and a purging system. Alternatively, a system with two separate 75-hole arrays, on concentric bolt circles, was developed. The radial spacing between circuits was dictated by the thickness of the wall dividing them and worked out to be approximately 0.15 inches. Separate manifolds feed the inner diffusion circuit and the premix circuit. This reduced the tubing requirement and simplified the design, in comparison to Prototype 1. The complex manifold used to feed the injectors of prototype 1 was replaced with a system some strategically located tubing and Swagelock fittings. The forward wall was fabricated from a 0.5 inch thick piece of SS316 stock plate. The circular flow passages were machined on a lathe prior to having the holes laser drilled. The outer premix tube was machined from thick walled SS304 tubing, while smaller diameter piece of SS316 tubing was EDM'ed to create the inner premix tube. All tubing and manifold covers were fabricated from SS316.

The outer wall, main premixer, and corner piece from prototype 1 are reused in prototype 2b. The corner holder had to be modified to accommodate the 2-cool sleeve and the smaller flow area associated with the removal of the backward facing step. The decreased exit diameter also required that the hula seal's mating flange and down stream ceramic liner be resized. This simplification in the design change also required the combustor scale to change to 1/10 of a full can.

Prototype 2c was designed to reduce thermal stress issues. Material thickness was added to the forward wall. Also, the design for Prototype 2c incorporated the main slots and cavity slots on the same forward wall.

Effective area tests were performed with Prototypes 2b and 2c to determine air flow splits to the combustor. As seen from the test results, cooling air was reduced considerably from Prototype 2b to Prototype 2c.

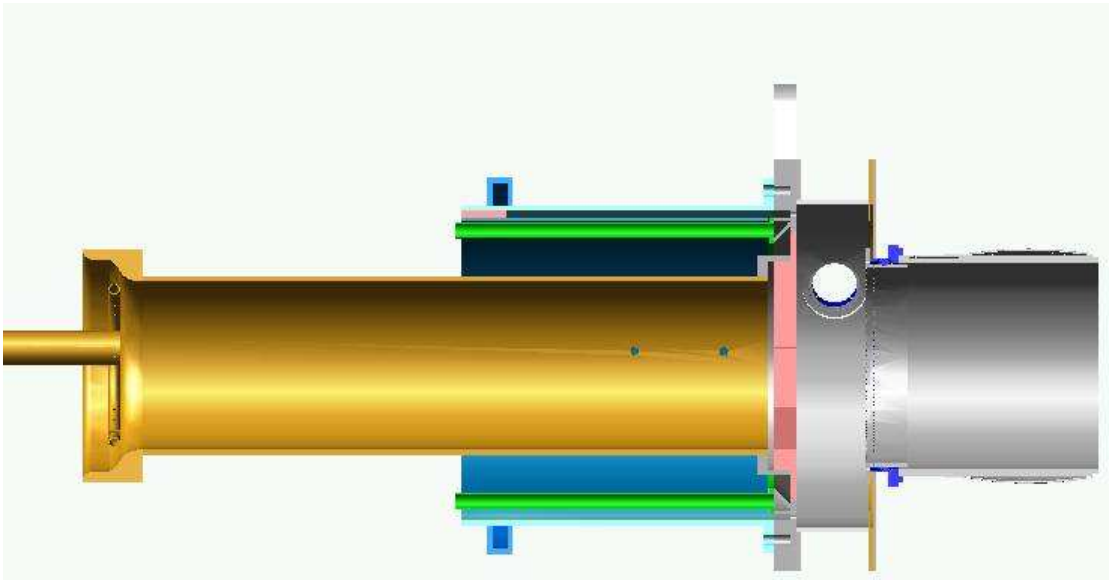

Figure 3-40 Prototype 2a2 cross-section

3.3.2 Kinetics Modeling

The chemical kinetic model performed for Prototype 1 was extended for Prototype 2. Several iterations of reactor zones and air splits were modeled. A list of the zone modifications is given below. A figure of the zones for Model 11, the best performing model, is shown in Figure 3-41.

TVC-new-5 Adjustments for setting lower limit on zone 3 size, cooling air from 5 to 4, and bypassing air from main to 5 for high cavity fuel percentages.

TVC-new-6 Added Zone 4b, corrected for the volumes (no longer using half reactor calculations). Zone 4b receives only input from main and cooling air. Small percentage of air from 1 and 3 go to 5.

TVC-new-7 Main zones remain the same as in 6. In cavity, zone 1 is non-reacting and zone 2 is a PSR reactor. The fuel and some air is injected into zone 1. This jet entrains enough air until the zone reaches a specified phi-target value. This then goes into zone 2 where it reacts. In the program, the fuel is actually injected in zone 2 to indicate the presence of an ignition source.

TVC-new-8 The logic for the sizes of the cavity zones remains the same as in Model 7. A maximum phi is specified then for zone 2. The excess cavity fuel then passes downstream into zone 4. A correction was made to zone 3 volume which also probably effected Model 7 results.

TVC-new-9 Two new PSR reactors created. One in front of what used to be zone 4b and the other between what used to be zone 3 and zone 4a. The numbering of the zones was changed so that now the zones number 1-9 as shown in the figure. The order the zones are input into CHEMKIN was also changed when this was discovered to have an impact. Now, lower numbered zones always flow into higher number ones.

TVC-new-10 Made Zone 7 have the exact same composition as 3 by sending a portion of the cavity to Zone 7 well. Other Zones and connections remained the same. This was done to prevent Zone 7 from blowing as quickly as cavity fuel increased. Also no flow from Zones 2&3 to 4.

TVC-new-11 Changed the Zone 7 to received more main fuel than main air. This was done to make the zone richer and prevent it from reach lean blowout as quickly as cavity fuel increased. This was physically validated by looking at simulations of the main fuel/air injectors which seemed to show a greater concentration of fuel on the bottom.

TVC-new-12 Made percentage of cavity air a variable. Set the lower limit (at low cavity fuel) to agree with experimental data on lean blowout. Increased at high cavity fuel by taking away air from the main. This helped to smooth out zones 7 & 8 temperatures by taking away air from the main when these zones were lean.

TVC-new-13 Made phi2 and fuel burned in 2 a function of cavity fuel %. The equation for phi2 was of the form phi2=c2*x/(c1+x) 2 where x was % cavity fuel. c1 and c2 where solved by setting phi2=.419 at 25% (LBO) and phi2=.8 (max) at 100%. The equation for mass of fuel burned in 2 was of the form m_fuel2=c4*x/(c3+x). c3 and c4 where solved by setting m_fuel2 equal to all the fuel present in the cavity at 25% and at 100% saying 38.2% of the air was in the cavity and using the phi2max.

TVC-new-14 Made percentage of cavity air a discontinuous function. Lower limit is set as before to have lean blowout occur with between experimentally determined 25-30% cavity fuel. Cavity air stays at this value until phi2max is reached. At this point, cavity air linearly increases to an input Xcavfinal value at 100% cavity fuel. From this point to 100% cavity fuel, the fuel burned in the cavity also linearly increases to maintain phi2max. Excess fuel not burned in the cavity is dumped into zone 5.

TVC-new-15 The way zone 2 volume is calculated is changed. Instead of it relating to jet entrainment of air in zone 1, now the residence time of zone 2 is specified as an input. This is also generally a shorter value than before, similar in length to tau5 instead of tau 6 or 8. The volumes of zones 1 and 2 are then calculated from this residence time. Also, the % main air and % main fuel through zones 7 & 8 were later set to be the same.

Model 11 yielded the best performance of all 15 models as compared to Prototype 2 data. The resulting data from Model 11 is given in Figure 3-42 and Figure 3-43. In this model the NOx curve inflection point occurs near where the temperature curves of Zones 6 and 8 cross. Due to there relatively long residence time and high temp, Zones 6 and 8 tend to be the primary NOx production zones (along with maybe zone 2). Zone 8 tends to start off hot and get cooler, while zone 6 starts off cool and gets hotter. Since the NOx production increases exponentially with temperature, the min overall NOx production will over when both temperatures are equal. This is assuming equal mass flow and residence time in both zones. In reality, zone 8 has less flow than zone 6, but this effect is linear and not as dominant as the temperature effect.

This reactor network model shows that lean blowout occurs in the cavity when the cavity phi= 0.419. Experimental data from Prototype 2 data shows that blowout in the cavity occurs when phi in the cavity equals approximately 0.3-0.37. Since this is not a higher phi than the lean blowout phi, it is determined that lean blowout in the cavity is due to lean blowout from mixing all the fuel with all the air. Thus there may be no lower phi limit on Zone 2. The question then becomes how much air participates in the reaction in Zone 2. Since the model says the lean blowout for the reaction occurs at phi= 0.419, this is assumed to be correct. Then, from the experimental data we know how much fuel is injected in the cavity when it blows out. Thus the amount of air participating the cavity reaction may be calculated by using phi of .419. This percentage of the total air will then be the percentage of air in the cavity used by the model (at lean cavity conditions).

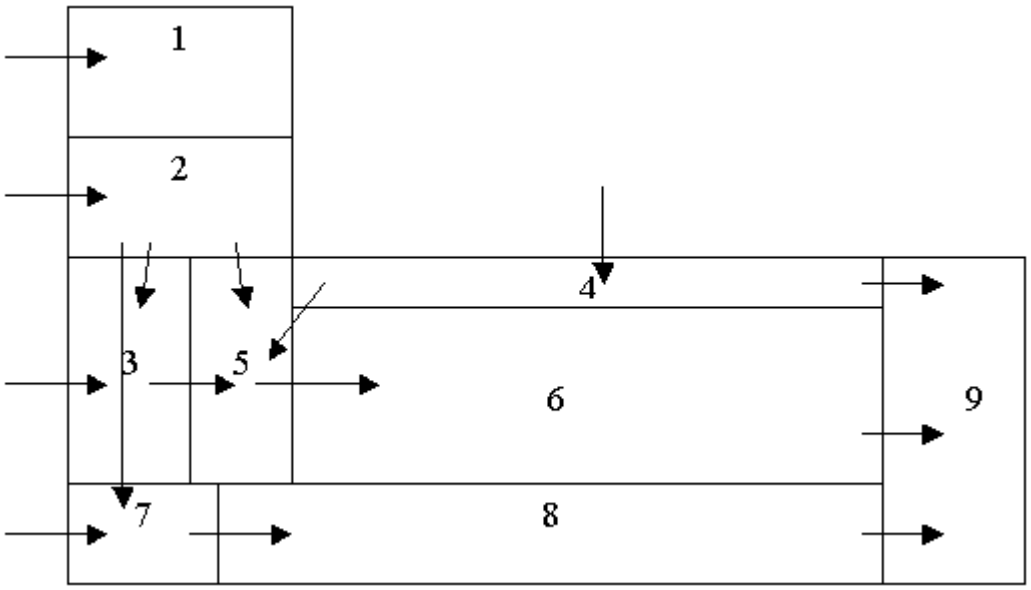

Figure 3-41 Prototype 2 network reactor Model 11

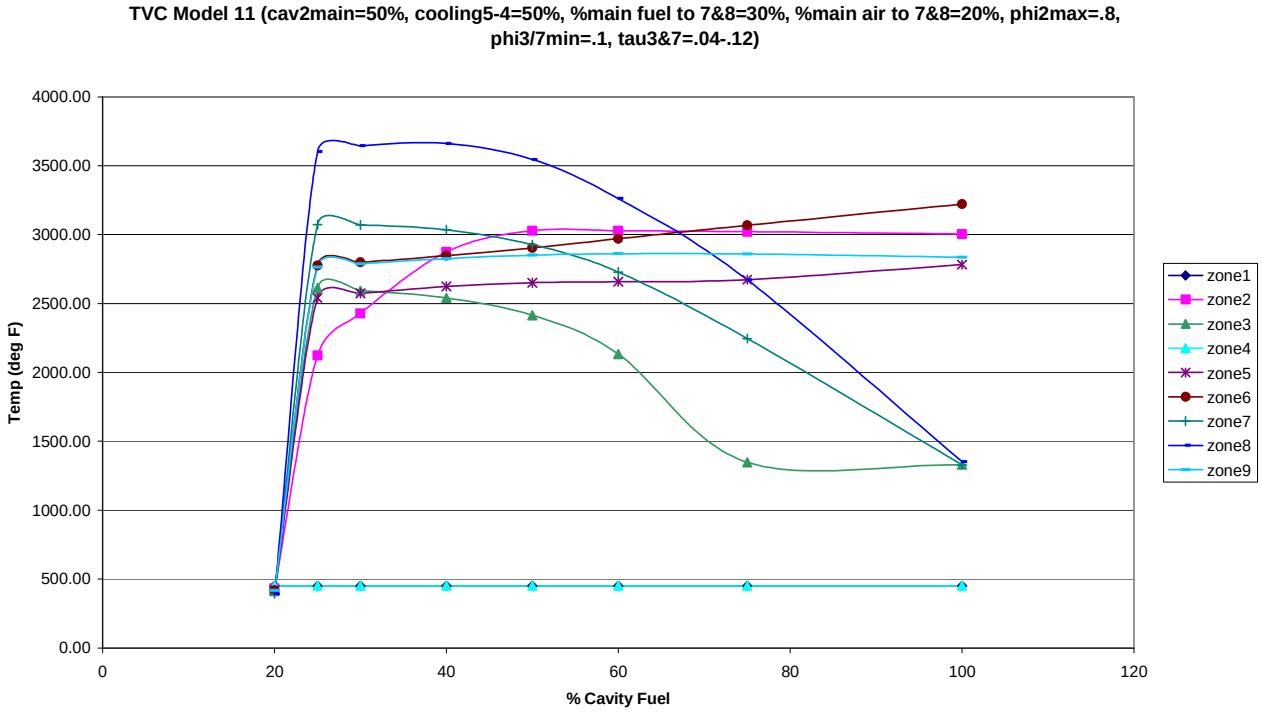

Figure 3-42 Prototype 2 network reactor Model 11 Temperature vs. % cavity fuel

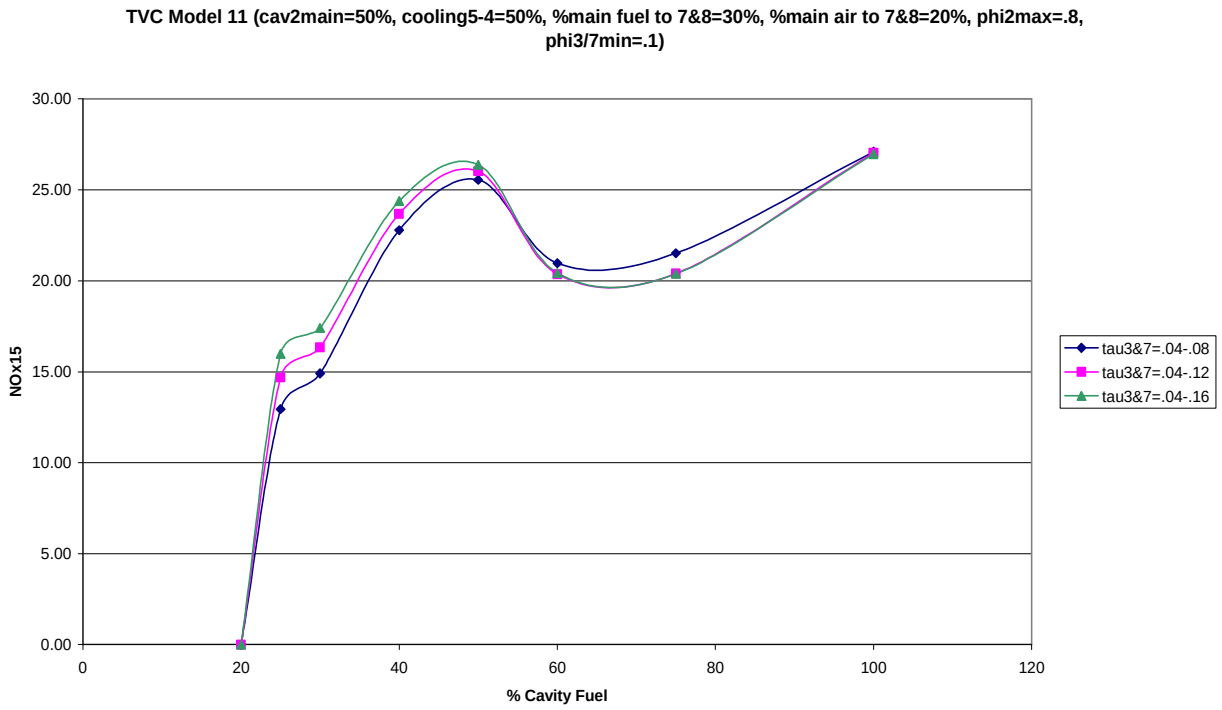

Figure 3-43 Prototype 2 network reactor Model 11 NOx15 vs. % cavity fuel

3.3.3 Flow Field Design CFD

The effect of closed aft driver holes on the temperature field at the mid-plane of the TVC combustor located at 84° was examined. Closing the aft driver leads to a significant reduction in temperature in the aft wall vicinity. This is due to the fact that by closing the aft driver forces more air to go through the forward driver slots and the main premixer, thereby leaning the fuel-stoichiometry in the vortex cavity. This leaning of the fuel-air stoichiometry leads to overall lower temperature in the vortex cavity. The case with closed aft driver hole demonstrates a strong robust vortex. Thus, it is clear that closing of the aft driver hole does not negatively impact the vortex aerodynamics. The impact of aft driver closing and the resulting leaning of the vortex cavity on NOx emissions predicted at the transition piece exit plane are shown in Figure 3-46. As seen in Figure 3-46, closing the aft wall driver leads to a three-fold reduction in NOx emissions. This significant reduction in NOx emissions is due to the leaning of the fuel-air stoichiometry in the vortex cavity, which reduces peak temperatures in the cavity. This reduction in peak temperatures lowers the production of NOx. The effect of aft wall driver on the CO emissions is shown in Figure 3-47. Clearly, as seen in Figure 3-47, closing the aft driver holes lowers the CO emissions also. Based on these results, it can be concluded that by closing the aft driver holes, the fuel-air stoichiometry in the vortex cavity is leaned out further, thereby leading to a significant improvement in the emissions performance without any negative impact on the aerodynamics.

In the results shown above, a perfectly premixed forward driver was assumed. To evaluate the effect of perfect premixing on the NOx emissions performance, the forward driver premixer was explicitly included in the model. This evaluation was conducted to determine the levels of NOx entitlement that can be achieved by using forward driver with perfect or a near-perfect mixing performance. The effect of unmixedness in the forward driver premixer on the NOx and the CO emission performance is shown in Figure 3-48. A perfectly premixer forward driver has the potential of reducing the NOx emissions by around 1.2 ppmvd. Furthermore, Figure 3-48 also demonstrates that a perfect forward driver premixer does not negatively impact the CO emissions performance.

To evaluate the concept of aft wall fueling, a CFD model of the TVC with a premixed aft wall driver was conducted. The rationale behind the aft wall fueling concept was that by fueling from the aft wall, better participation of fuel with air would be obtained. This would lead to a better mixing and localized leaning of fuel-air stoichiometry, thereby leading to reduction in NOx performance. Fueling using aft driver reduces the amount of leakage air that bypasses the cavity vortex and escapes around the corner. This increases the fuel-air participation in the vortex and leads to a more flatter and more uniform temperature profile at the transition piece exit. This reduction in the temperature non-uniformity and the increased participation, leads to a further reduction in NOx emissions. The magnitude of this NOx reduction, as predicted by the CFD model is of the order of around 1 ppmvd.

The results discussed so far were obtained prior to testing and thus a direct comparison between the predicted and the measured results could not be made. This necessitated a detailed validation of the TVC CFD model, such that the CFD model can be used with increased fidelity and confidence to suggest design changes and further

optimize the TVC performance. A controlled set of experiments was conducted and detailed temperature, O_2, CO_2, and NOx profiles were measured at transition piece exit to provide data for the CFD validation exercise. The experiment was conducted for a exit cavity fuel split of approximately 35%. The match between the predicted and the measured temperature is fairly good; however, there is a slight asymmetry in the measured profile that is not predicted by the CFD model. It is hypothesized that the airflow distribution in the experiment was circumferentially non-uniform, which could have led to the observed asymmetry in the temperature profile. As the sector CFD model assumed asymmetry, the asymmetry present in the experimental data could not be reproduced. The asymmetry seen in the temperature profile is amplified and clearly visible in the NOx profile. For reasons discussed above, the asymmetry in the NOx profile is not predicted by the CFD model as it does not include any asymmetry of air flow field as it enter the combustor. Even though the profiles are not exactly reproduced by the model, the CFD predicted flux averaged NOx corrected to 15% O_2 at the transition piece exit is 17.1 ppmvd, which compares very favorably with the measured value of 16.0 ppmvd. Similar comparison for predicted and measured O2 and CO2 profiles at transition piece exit is shown in Figure 3-49 and Figure 3-50 respectively. As seen in these figures, it is clear that barring the asymmetry observed in the experimental results, the predicted and the measured profiles do agree fairly well.

Given the discrepancy caused by flow asymmetry the CFD model was considered to be validated to the greatest extent possible. This model can be used to predict aerodynamic and emission performance of new TVC configurations and thereby aid the rapid design and optimization of TVC concepts. Furthermore, besides evaluating the impact of design features on TVC performance, the validated CFD model can be used to further optimize the design and also aid in the scale-up process for scaling the TVC from a prototype scale to a full-scale combustor.

In conclusion, a robust modeling tool was developed which captures the main flow field characteristics and can provide design guidance on emission performance. The modeling results indicate that improvements to the premixer performance and aft wall injection air can improve emission performance. Furthermore, experimental data indicates asymmetry in the flow field, and reducing this in the subsequent design will further benefit NOx and CO performance. A next generation prototype, which incorporates ideal premixing, needs to be evaluated to demonstrate the performance entitlement.

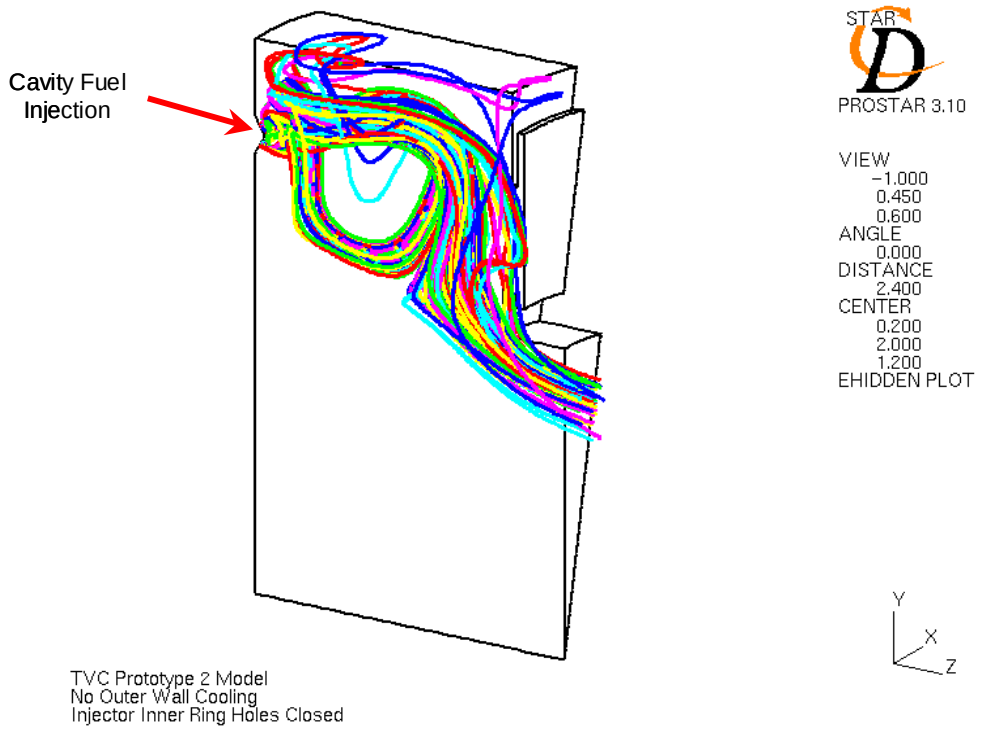

Figure 3-44 Prototype 2a1 Case 8 particle trace of cavity fuel with cavity outer wall effusion cooling turned off and inner ring of cavity premix air injector holes closed

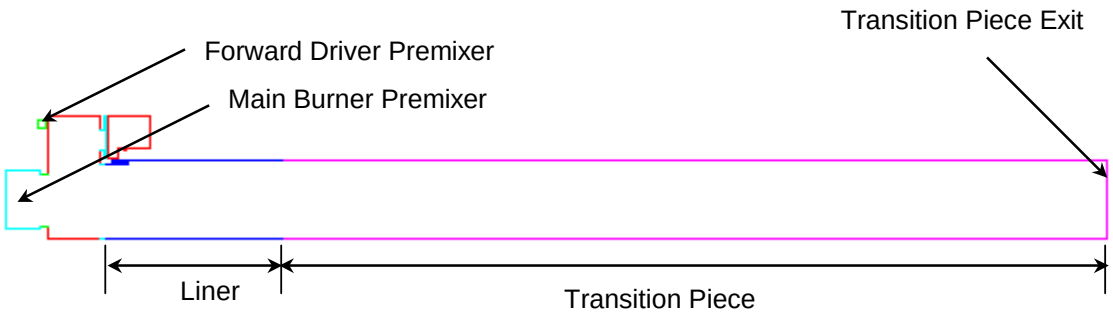

Figure 3-45 Prototypes 2a2, 2b, and 2c computational Domain of the Trapped Vortex Combustor CFD Model

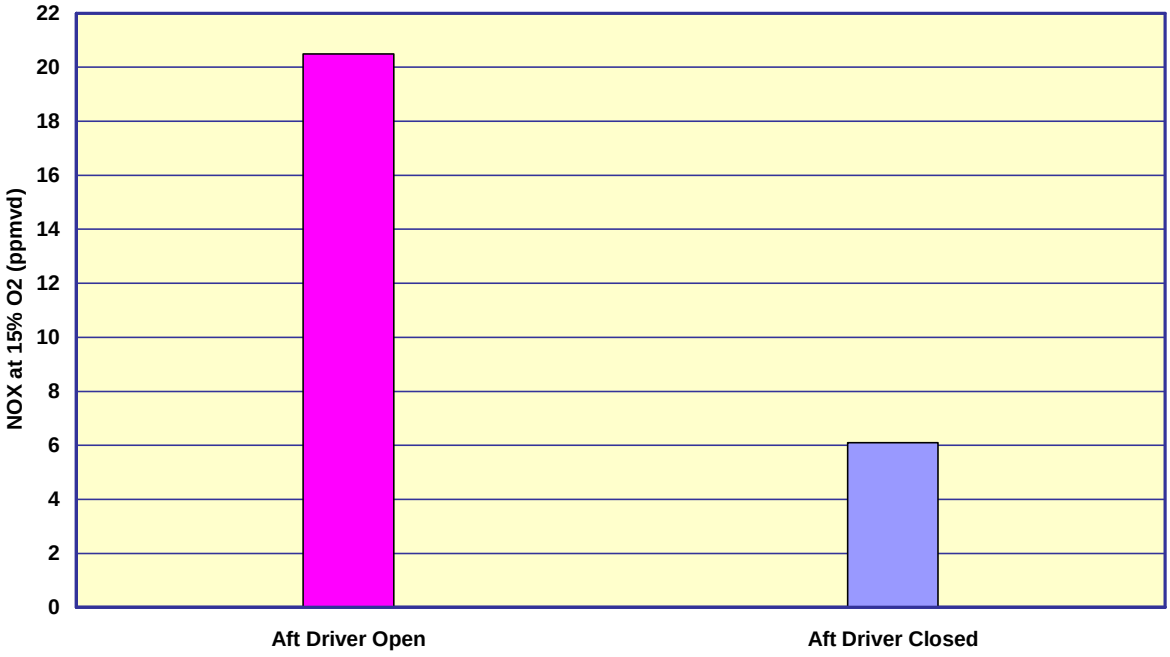

Figure 3-46 Effect of Aft Driver Holes on Predicted NOx Emissions at Transition Piece Exit for Prototype 2b

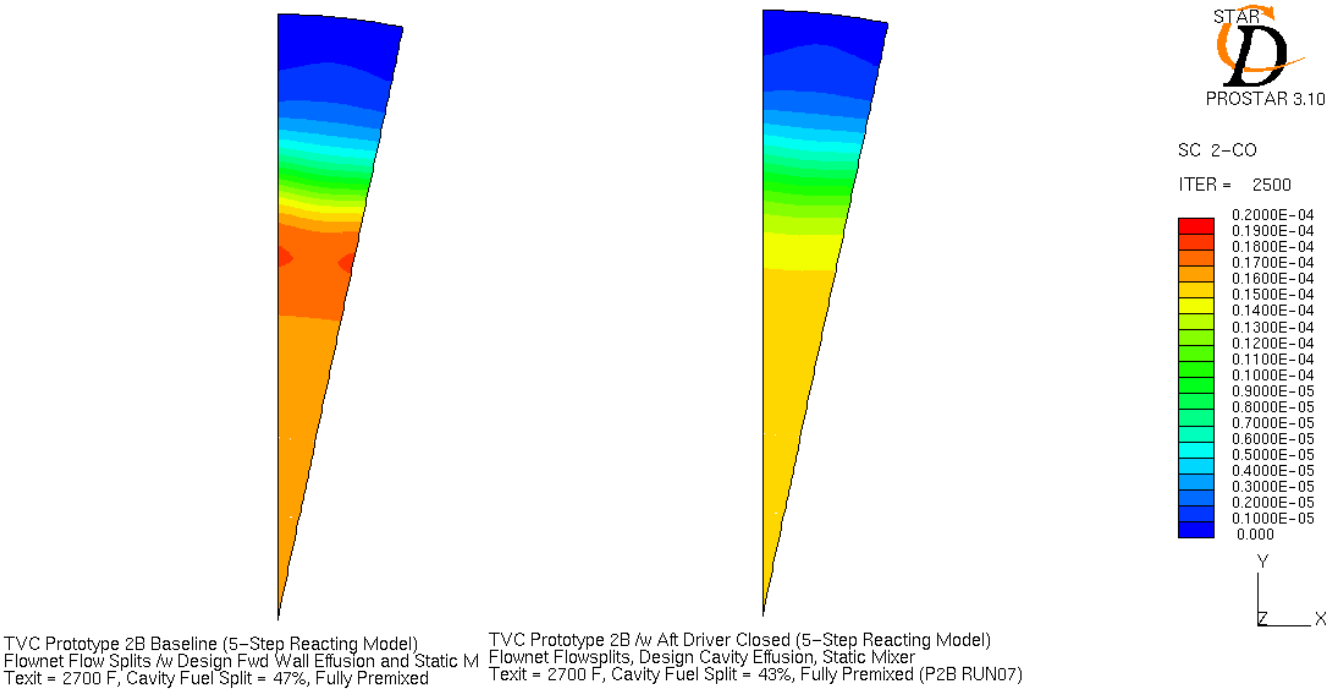

Figure 3-47 Prototype 2b effect of Aft Driver Holes on CO Emissions Predicted at Transition Piece Exit – (a) Aft Driver Holes Open (b) Aft Driver Holes Closed

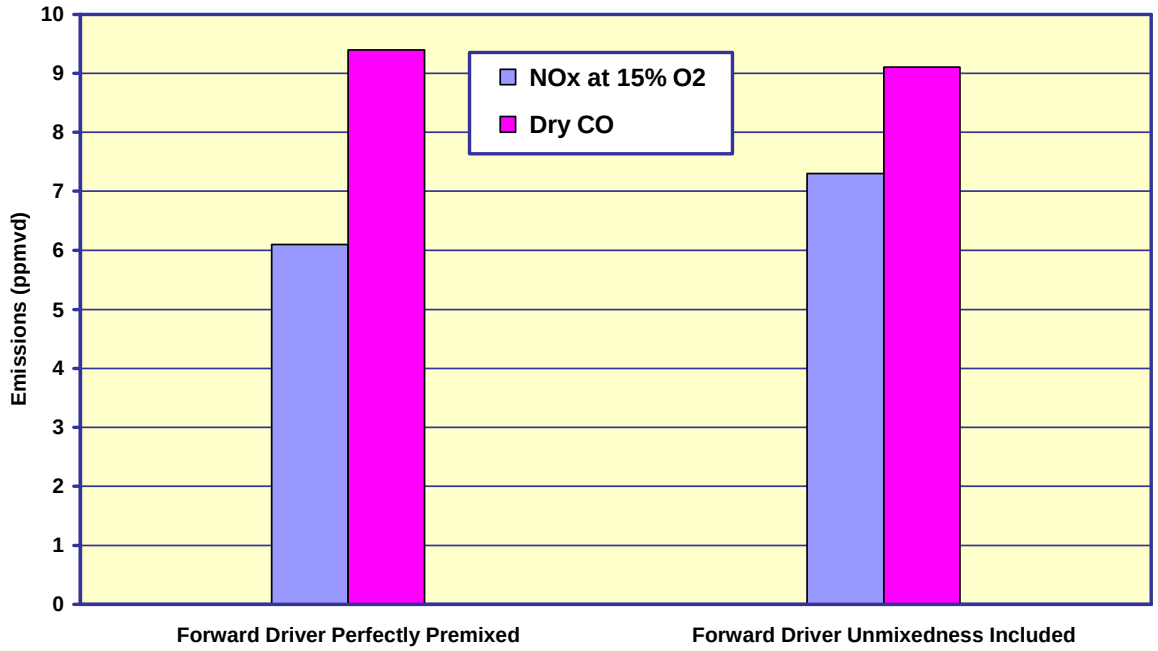

Figure 3-48 Prototype 2b effect of Forward Driver Mixing on NOx and CO Emission Performance

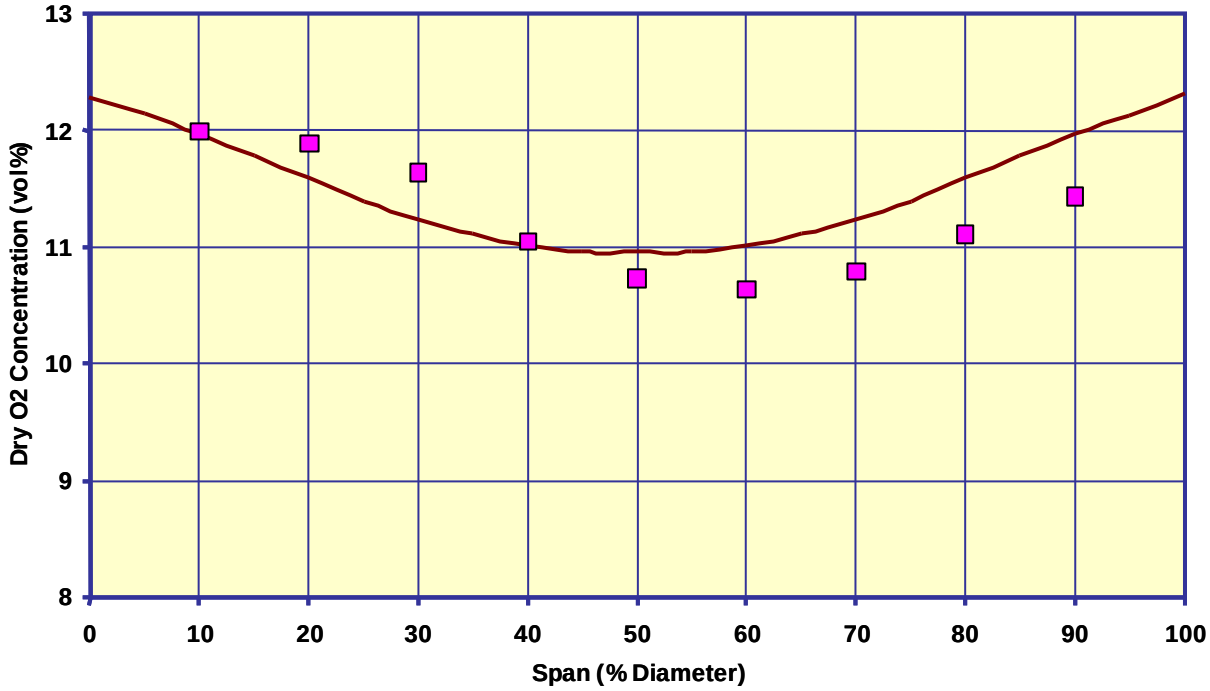

Figure 3-49 Prototype 2b comparison Between Predicted and Measured O_2 Concentration Profile at Transition Piece Exit

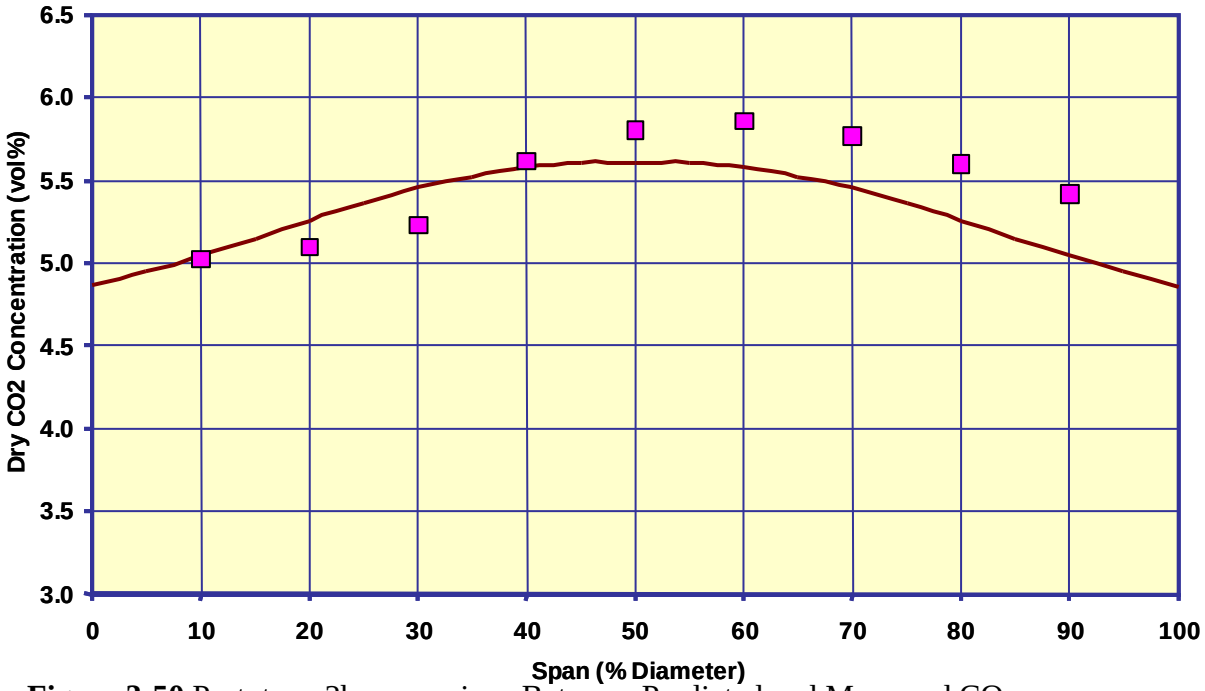

Figure 3-50 Prototype 2b comparison Between Predicted and Measured CO_2 Concentration Profile at Transition Piece Exit

3.3.4 Thermal Modeling

During the initial testing of Prototype 1 it was noted that the temperature of the exit piece was nearly identical to the combustor cavity temperature. It quickly became apparent that not enough cooling air was flowing across the hula seal and exit piece. While the leakage through the hula seal was intended to be 2.0% of the total mass flow, cold flow tests determined that it was approximately 0.65% percent. Only low temperature test points could be run, to minimize the risk of damaging the exit piece.

To improve the exit piece cooling in prototype 2a2 a GE 2-Cool passage system was selected. The 2-Cool system is a production part; the only difference was that our prototype required a smaller diameter roll-up. A custom sleeve was designed for use with prototype 2a2. The geometries of the custom sleeve were based on a 2D heat transfer analysis with the following boundary conditions. A sensitivity analysis was conducted to determine the correlation between wall temperature, passage geometries, and feeder hole size.

The custom sleeve was made from a 0.115" thick rollup with 31 channels milled into the surface. Each channel measured 0.375" wide by 0.025" deep and 3.15" long. The outer sleeve was 0.040" thick and had 31- 0.100" OD feeder holes. These custom sleeves were initially manufactured as a 13.78" ID rollup, by Aero Manufacturing, and then re-rolled to the desired 4.846" ID by the GRC machine shop. Figure 3-51 shows the 2-Cool system hardware assembled.

The thermal design issues of Prototype 1 were addressed in the design of Prototype 2a2. Prototype 2a2 has significant reductions in the effusion air cooling on the cavity outer wall. Prototype 1 experiments indicated that the cavity temperature was well below the design limits, and aero design analysis highlighted the need to reduce flow to the cavity.

The outer wall effusion holes were covered to minimize the effusion air in Prototype 2b. Also, the effusion air to the head end is reduced. For Prototype 1 these temperatures were well below the design limits, so additional air can be removed without penalty to the hardware life. At the center of the main burner there is no effusion air in Prototype 2b. The main burner slots have been extended toward the center of the burner leaving a 0.75" center, which is cooled by conduction of heat away to the slot mixture. The face of the main burner has less cooling air than Prototype 2a2 to accommodate the changes in the assembly. The effusion holes were reduced to four rings of holes in a staggered pattern with 0.020" diameter and 0.160" spacing. Surface temperatures are monitored during the experiments to determine the proximity to temperature limits during operation.

The design of Prototype 2b is shown in Figure 3-52. The forward wall was made in two sections as shown. However, Prototype 2b had problems resulting from thermal deformation during combustion testing. The thermal expansion coefficient differences and temperature profile between the forward wall and the outer ring with the cavity fuel slots caused the forward wall to detach upon cool-down after combustion tests. As an attempted solution, the forward wall was heavily welded to the cavity ring.

Unfortunately this fix resulted in a stress concentration around the forward driver slots, causing cracking through the wall thickness. A Finite Element sub-model of the

forward wall confirmed the high stresses in the same location as the cracking failures. The FEM results indicated the high stress region. Thermal paint was used in the next combustion tests to evaluate the temperatures experienced on the forward wall. The paint test validated the thermal assumptions of the FE model based on classical convection heat transfer correlations with hot side temperatures and velocities from CFD analysis. There was excellent agreement between the thermal paint test and the CFD model of the fwd wall.

The conclusion of the thermal analysis study is that the thermal "fight" between the "hot" main burner and the "cold" outer flange is such to overload the thin wall section between the fwd driver slots. As the main burner grows radially outward it is being "held" by the colder outer flange, the thin fwd driver section develops high compressive stresses (237 ksi based on linear elastic analysis) far exceeding ultimate stress of 65 ksi. During shutdown, as the main burner cools, the plastically yielded section (while in compression during hot conditions) goes into high tensile stresses and cracks during cool-down.

Various geometries were evaluated and parameter sensitivities were performed. The following modifications to the fwd wall were made to minimize thermal strains:

- Increasing the web thickness and length to provide sufficient cross sectional area to carry loading
- Separate the main burner from the outer flange to allow for thermal growth differences, which minimizes the thermal strain. (This design requires a c-seal to minimize leakage into the combustion cavity). A step in the main burner OD reacts the pressure "blow-off" loads which are carried through the outer flange
- Change material from SS316 to the higher strength N-263

Figure 3-53 shows the redesigned forward wall of Prototype-2c. The design incorporates the increased web thickness and separates the main burner from the outer flange. A high temperature material, N-263 was also used for the new main burner. A stress analysis of the new design was performed. The stress around the ports is significantly reduced from 237 ksi to a maximum of 49 ksi.

To help facilitate the vortex strength, a reduction in aft wall cooling was considered. To help in the pre-test evaluation, a Finite Element submodel of the aft region was generated to study the temperature effects of changing the level of cooling.

The criterion is to maintain the temperature of the material to below 1,600 F. An analysis was performed for the aft-wall with 100%, 50%, and 34% of the cooling air. The 34% cooling air case had a peak temperature of 1570 F, which was sufficient to warrant this selection for the design change.

Figure 3-51 Prototype 2a2 2-Cool assembly with hula seal around the combustion liner

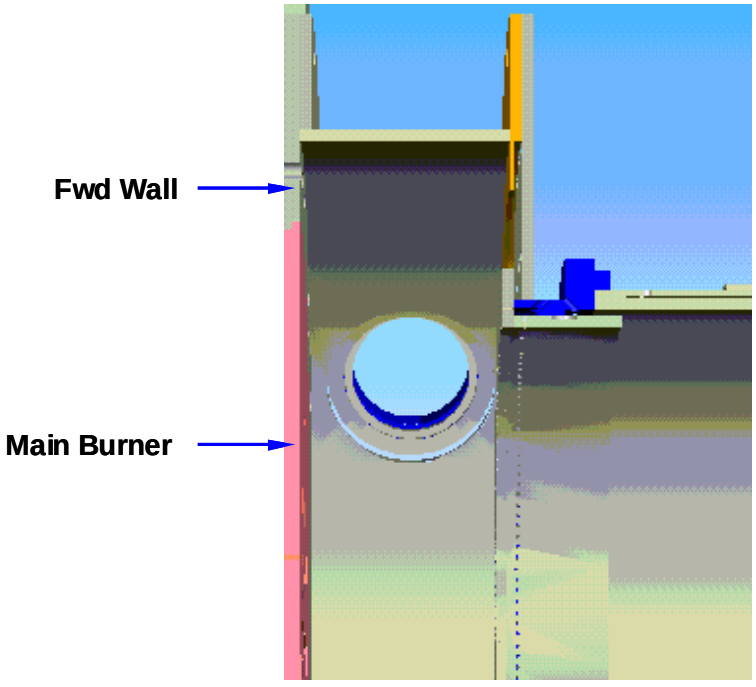

Figure 3-52 Prototype 2b TVC Forward Wall Assembly

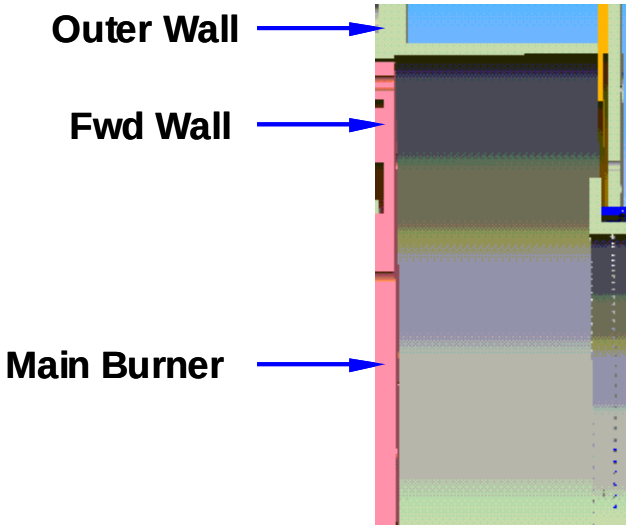

Figure 3-53 Prototype 2c new forward walls

3.3.5 Instrumentation

The Prototype 2 rig, although redesigned in many aspects, had very similar instrumentation as Prototype 1. Temperatures, pressures, and dynamic pressures were measured at similar locations as in the previous tests, with the addition of thermocouple instrumentation on the newly designed 2-cool system. Figure 3-54 is a schematic of the thermocouple instrumentation on Prototype 2 hardware. Emissions were sampled at locations of about 7" and 24" downstream of the face of the forward wall.

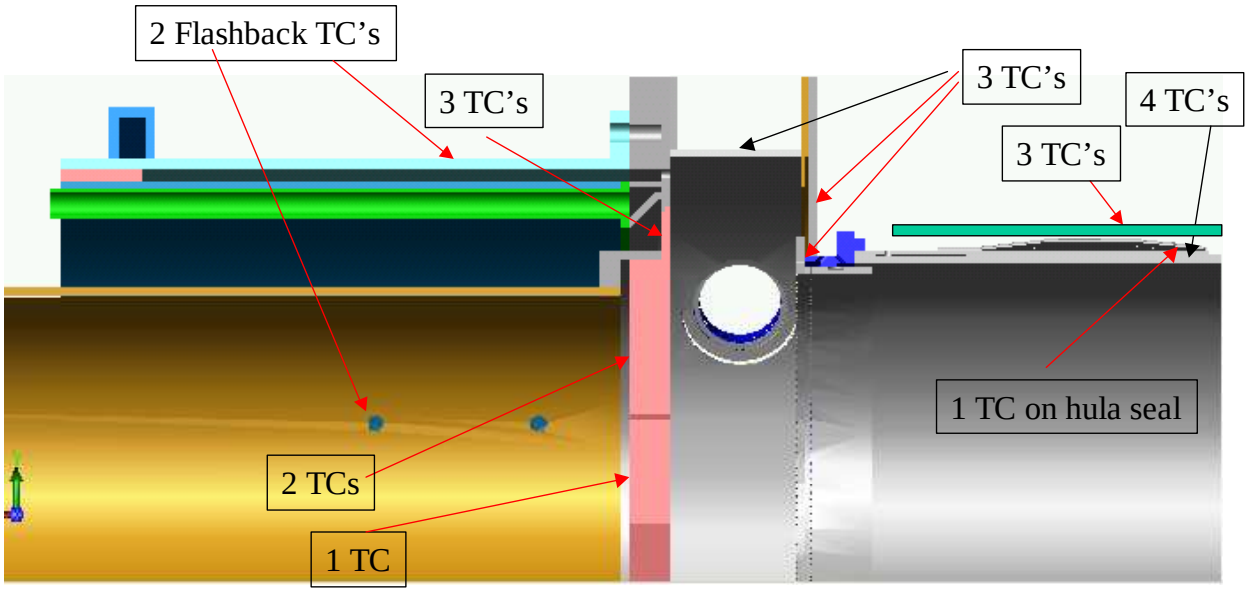

Figure 3-54 Prototypes 2a2, 2b, and 2c thermocouple instrumentation

3.4 Prototype 3

The goal of prototype 3 is to reduce NOx emissions to reach the 50% NOx reduction target, while maintaining low overall pressure drop and low dynamics. To accomplish these goals, a QFD was performed as summarized in Figure 3-55. The design focus efforts are placed on 1) obtaining high premixedness, 2) reducing cavity size, 3) reducing circumferential variation in the cavity, and 4) removing outer wall cooling for the cavity and replacing with an impingement cooled flow sleeve.

Extensive CFD modeling was employed to optimize the combustor cavity size and shape and the percent fuel split between the main and cavity sections. The goal of these studies was to produce the optimal vortex in the cavity and to lower the overall emissions. Also, the geometries of the cavity and main premixer sections were improved with CFD design and Six Sigma methodology in an effort to minimize NOx emissions. Another attempt to decrease emissions was to employ stricter manufacturing tolerances in the cavity premixer section to reduce variations in the fuel/air mixture. Further, the impingement cooling sleeve around the cavity combustor is designed to increase cooling of the cavity walls with minimum pressure drop, and in turn lower NOx production. Further, combustor lifetime was investigated by performing thermal and stress analysis to ensure adequate cooling and to allow for thermal expansion of the forward wall.

Modeling & Experiments to Minimize NOx for 7FA+e	Thermal NOx	Stabilization	Life		Totals
Impingement Cooled Cavity	9		1		10
Ideal Premixing	9	-3			6
Reduced $\sigma_{\phi cavity}$	3	-3			0
Cavity Size	-3	3			0
Cavity Shape	3	3	-9		-3

Figure 3-55 Prototype 3 QFD to improve design for NOx emissions

3.4.1 Component Design

Based on the information from prototype 2c, several components were re-designed. Changes from Prototype 2 to Prototype 3 are summarized in Figure 3-56.

A new cavity premixer was designed to reduce circumferential variability in the fuel/air mixture. The previous design consisted of two concentric rollups. This process did not hold the tolerance on the diameter better than ±0.020". The new design for Prototype 3 was made of a single part and should hold within ±0.002". This is expected to reduce temperature variation along the trapped vortex, thus reducing overall NOx variation.

The main premixing geometry was also modified. Prototype 2C employed a static premixer assembly consisting of two mixing elements constrained in a 3.5" schedule 10 pipe. A transfer function based on published NOx-temperature models in literature [1] was used to determine the variation in fuel/air ratio required to meet the desired NOx tolerance. Upon examination, the Prototype 2c premixer was found to be unable to give sufficient fuel-air homogeneity to hold the targeted NOx tolerances of +/- 0.5 ppm. This resulted in the addition of 5 mixing elements to the main premixer geometry, increasing the overall length of the test rig so that entitlement NOx levels could be evaluated.

The specific geometry of the TVC forward wall was generated based on the flow conditions and premixer characteristics. It was developed through CFD modeling of the design. For the targeted pressure, temperature, and mass flow the holes were sized to distribute the flow according to design targets. The performance of the main and cavity premixers was evaluated under these conditions. The flow distribution was analyzed based on the flow network analysis. Two forward wall geometries were designed and built (Prototype 3-1B and 3-2A) with different overall pressure drops across the holes but with the goal of maintaining the same mass flow distribution. The CFD models described in the following section were used to determine the final configuration of this component.

The construction of the cavity aft-wall was significantly different because of the changes in the cooling scheme. The removal of the cooling slots created the need for a continuous wall. The aft-wall shape was welded directly to the outer-wall and transition piece, and the wall was constructed from 2 sheets welded together. The flat part of the wall was a machined disk; the nose was custom machined. The aft-wall was backside cooled. The shroud cooling hole size and distribution were determined by the local wall heat transfer coefficients. The shroud was offset from as specified by the design analysis.

The outer-wall and transition piece were cooled in the same manner as the aft-wall. The cooling shroud extended from the forward end of the outer wall to the start of the hula seal. The combustion air was directed through cooling holes by designing a seal between the premixers and the reverse flow liner. In this manner air was forced to travel through the cooling shroud before passing into the combustor.

The combustor outer wall was reduced in diameter as per the results of the Flow Field Design CFD. The smaller cavity was easier to cool and reduced the overall size of the combustor. The smaller cavity led to a smaller camera port and a position closer to the combustor center. The camera port equipment was moved to accommodate this change.

Effective area tests were performed to determine the air splits in the regions of the Prototype 3 combustor as shown in Figure 3-57. Region A is leakage air between the hula seal on the combustion liner and the downstream combustion liner (not pictured). Region B is cooling air used to cool the metal wall temperatures of the combustion liner. Region C is air that passes through the cavity premixer and cavity slots into the cavity zone of the combustor. Region D, the majority of the air, passes through the main premixing section and main slots in the main zone of the combustor. Region E is effusion cooling air used to cool the surface of the combustion injector plate, which is also referred to as the forward wall.

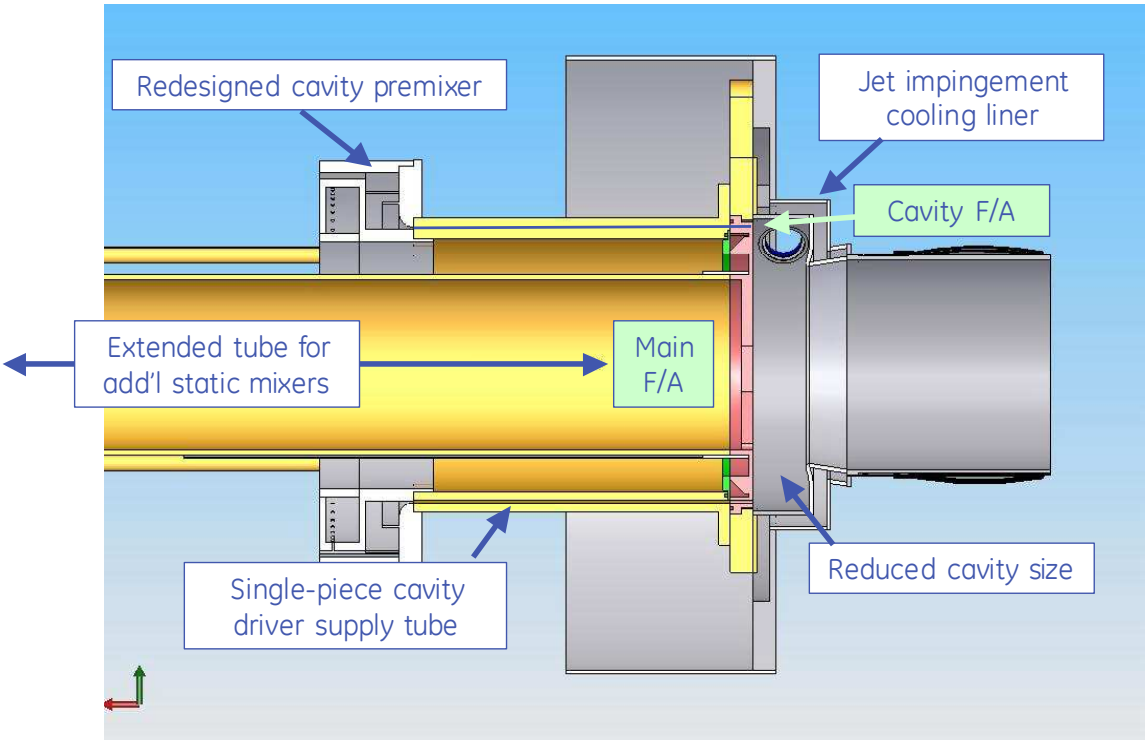

Figure 3-56 Prototype 3 design enhancements

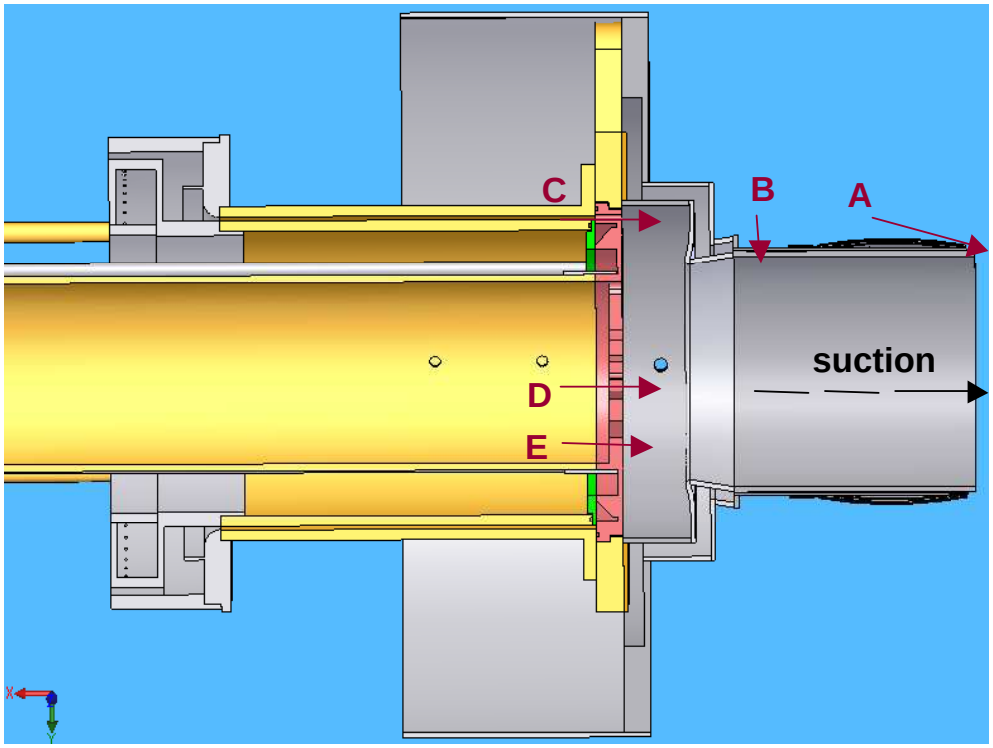

Figure 3-57 Prototype 3 air flow passages

3.4.2 Flow Field Design CFD

The CFD modeling for Prototype 3 was done using commercial Fluent version 6.2.16 software [3]. Two major components were examined using CFD. The first was a reacting flow model of the entire combustor system performed similarly to the methods used earlier in the program. This method was employed in a designed experiment to determine the effect of variations in combustor cavity size and shape on NOx, CO, and temperature. The second area of study incorporated a non-reacting flow model of the cavity premixer geometry to specifically evaluate the spatial steady-state mixedness capabilities of the premixer design. In both cases steady state, compressible turbulent flow was assumed, and a realizable k-ε turbulence model with standard wall function treatment was used. In all cases first-order solutions were used to approach a steady solution, which were switched to second-order solutions to reach model convergence. Air was assumed to be 21% oxygen and 79% nitrogen by volume. Fuel was assumed to be 100% CH4.

For the designed experiment, the combustor geometry employed the features used in Prototype 2c. In the first study cavity size and shape were changed. Two levels of each factor were used to set up a four-run experiment, as shown in the test matrix in Figure 3-58. The cavity shape was changed by varying the radius of curvature of the aft-wall cross-section, resulting in a geometry referred to as a "nose." The cavity size was changed by 50% between the large and small cases. The decrease in cavity size required a corresponding 50% change in flow to the cavity. The geometries can be seen on Figure 3-59. The other boundary conditions were reproduced from Prototype 2C CFD runs. One computational domain was created per test run, resulting in a total of four computational domains, shown in Figure 3-60, with symmetry boundary conditions that were run in Fluent. Inlets were mass-flow inlets with the operating pressure being the combustion cavity pressure of 7FA+e conditions.

For the cavity premixer design, the effect of premixer geometry on mixing performance was studied. The fundamental configuration of the premixer was modified from prototype 2c, which used an annular inlet with transverse fuel injection for mixing the fuel and air. The annular premixer for prototype 3 maintained the same size as 2c to prevent flashback in the mixing chamber. However, for prototype 3 the goal was to study the performance with perfectly premixed fuel & air. To accomplish this a vortex mixer was added upstream of the annular mixing passage. The vortex mixer uses a backward facing step to mix create a recirculation zone. The final design was obtained through an iterative modeling process, with each result prompting continued improvements to the cavity design until premixing levels were satisfactory. The domain includes the cavity premixer and the mixing plenum terminating at the forward wall. The domain was a 4.8° sector model with periodic boundary conditions. It was meshed using commercial ICEM-CFD version 4.3 using a macro-unstructured, micro-structured hex mesh of approximately 2.4 million elements. This final configuration was dependent on the results from the designed experiment CFD. The species model used was a non-reacting species transport, with air and fuel compositions as described above.

The designed experiment run in Fluent yielded a best-case geometry that became the foundation around which the rig hardware was designed. In general, all cases except the first performed well in terms of flow field and predicted NOx and CO emissions. Case 1, which involved the larger cavity and flat nose profile, experienced a hot spot in

the flow resulting in a high NOx prediction. The other cases experience no such flow anomalies and each were predicted to emit <1 ppm NOx at 15% O_2. The best case in terms of flow field was CFD Case 3, which was comprised of a smaller cavity and a flat nose profile. Cases 2 and 4, in which the nose profile was larger, resulted in distorted flow fields in which a strong outer trapped vortex was in general not present. This is largely due to the shape guiding the bulk of the flow out of the vortex cavity by restricting the area of the flow path, while the flat nose allowed the flow to naturally set up a vortex. For these reasons, CFD Case 3 was chosen as the basis for the final prototype 3 design.

There were other factors that needed to be corrected for once this overall configuration was chosen. A flow network had to be analyzed to study the flow distribution throughout the system. Based on the analysis, the forward wall was redesigned and the model was re-run. Two different geometries were selected for final evaluation because of uncertainties in the flow network analysis, termed P3-1b and P3-2a.

The results of this final run of the CFD models predicted a well-developed vortex burning at temperatures similar to those seen in CFD Case 3. These temperatures were predicted to be approximately 2500-2900 degrees in various regions. The flow fields for both cases in the head end region showed an outlet temperature of approximately 2900 degrees F, which is the same as the outlet temp of CFD Case 3. This outlet temperature is approximately 10% higher than that predicted with equilibrium calculations at the specified fuel/air ratio, which was corroborated in the CFD model. The deviation in outlet temperature is believed to be an artifact of the simplified chemical kinetics.

In the cavity premixer analysis, a final design concept for the new non-swirling premixer design was evaluated in terms of homogeneity of concentration of CH4 at the outlet of the domain. In general, larger cavity size with a mid-span baffle produced the best mixing performance. Mixing performance was evaluated by examining the time-averaged spatial distribution of CH4 at each cell in the domain. The mixing performance was quantified using methods based on GE Six-Sigma design practices. Cell concentration values were first weighted individually by mass flow through each cell, and then compared to design requirements in terms of the number of standard deviations to fit within tolerance, i.e., the design's Z-score. In the final case, the design Z-score was 20, which in essence meant perfect premixing. Figure 3-61 shows the spatial distribution of fuel mole fraction at the outlet surface. The low NOx predictions from the CFD of the main flow field, which include combustion, appear to confirm the presence of perfect premixing for this combustor using the cavity premixer geometry, but experimental validation is required to make additional solid claims as to the utility of this design approach.

TVC Prototype 3 CFD Test Matrix		
Run	**Cavity Size**	**Cavity Shape**
1	Hi	Flat
2	Hi	Nose
3	Lo	Flat
4	Lo	Nose

Figure 3-58 Prototype 3 test matrix for CFD-designed experiment for cavity size and shape

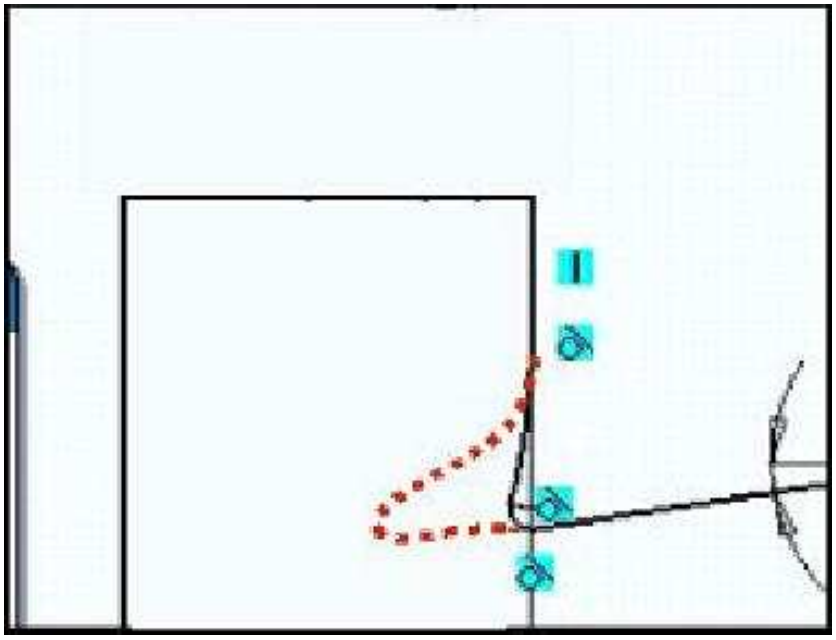

Figure 3-59 Prototype 3 cavity shape geometry with “nose” feature in red dashed line

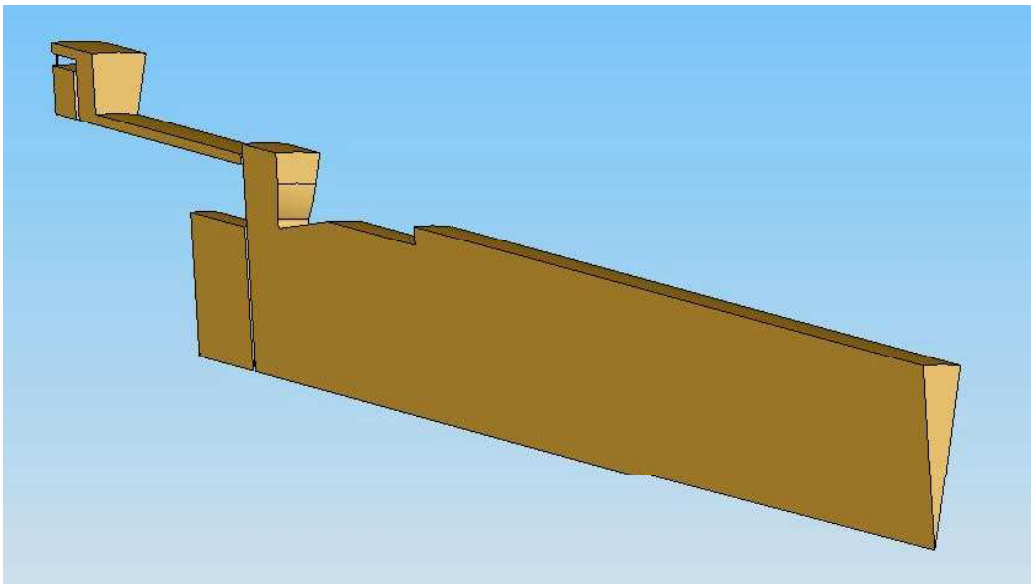

Figure 3-60 Prototype 3 computational domain for an example case in the cavity size and shape designed experiment (Case 3 shown).

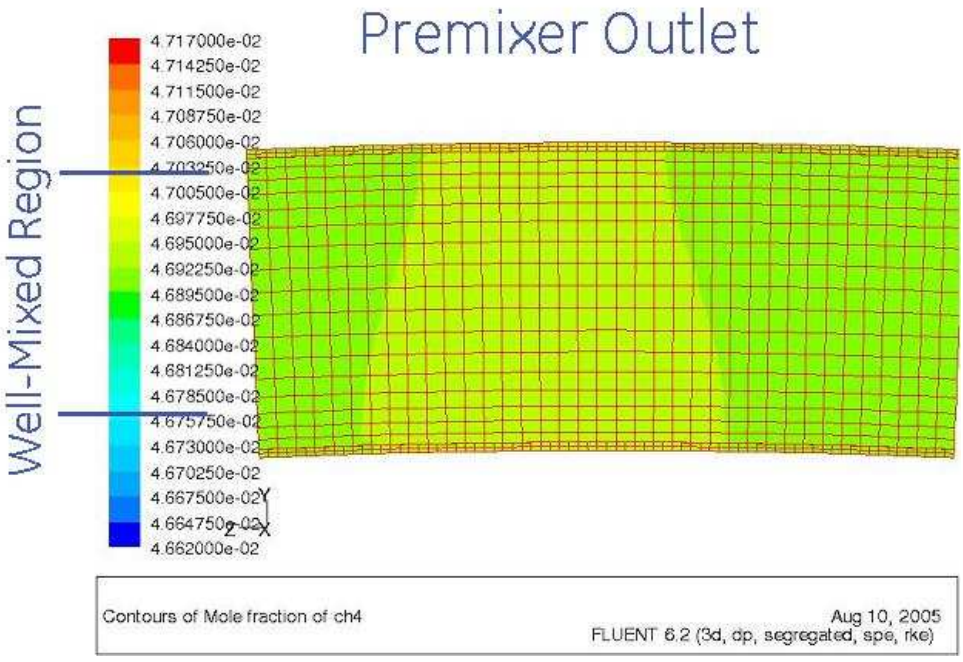

Figure 3-61 Prototype 3 spatial distribution of fuel mole fraction for cavity premixer CFD

3.4.3 Thermal Modeling

The thermal modeling data from prototypes 2b and 2c provided valuable guidelines as to restrictions that needed to be imposed on the forward wall hole geometry in order to tolerate the thermal expansions experienced during firing. The features in prototype 3 were designed to ensure tolerance to thermal expansion by way of large (0.020") clearance gaps on the forward wall diameter, as well as ensuring adequate material present between each outer cavity driver hole. Effusion cooling was used to keep wall temperatures within required limits.

Additional thermal modeling was performed to design an impingement cooling sleeve. This new approach to cooling the combustor was one of the significant changes over prototype 2c. The heat transfer coefficients (HTC) of both the interior of the combustor cavity and the required HTC on the outside to maintain safe operating metal temperatures and associated pressure drop were calculated. Once this HTC was calculated, holes on the sleeve components were sized to provide the correct mass flow through the sleeve. Figure 3-62 shows the basic impingement cooling sleeve for which calculations were made.

The extensive modeling of the combustor wall thermal performance led to the selected design. The heat transfer coefficients and predicted wall temperatures are shown in Figure 3-63. The hot side HTC was shown to range from 145 to 250 $^{Btu}/_{hr\text{-}ft2\text{-}F}$. Four wall temperature curves were plotted against cold side HTC. For safest conditions, a combustor cavity with thermal barrier coating (TBC) is required to withstand the burning regardless of cooling condition. Using a TBC-coated combustor and jet impingement cooling, a cold side HTC of 400 $^{Btu}/_{hr\text{-}ft2\text{-}F}$ or higher is required to maintain safe operating conditions.

Additional design practices authored by GE were used to spec the hole pattern given the geometry in question. A bypass area was specified to reduce the overall pressure drop. This bypass area allowed for approximately 50% of the total flow to be used for impingement cooling, more than an order of magnitude increase from prototype 2c. Pressure drop was predicted to be 0.8% across the new cooling system and bypass area.

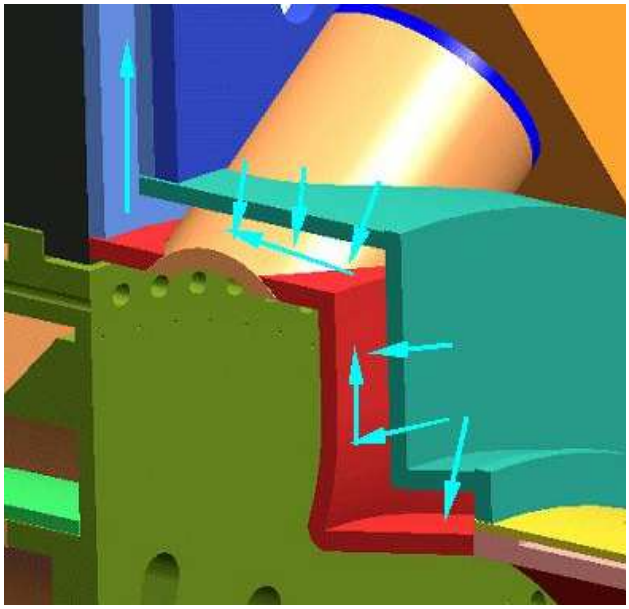

Figure 3-62 Impingement cooling liner geometry prior to heat transfer evaluation for Prototype 3

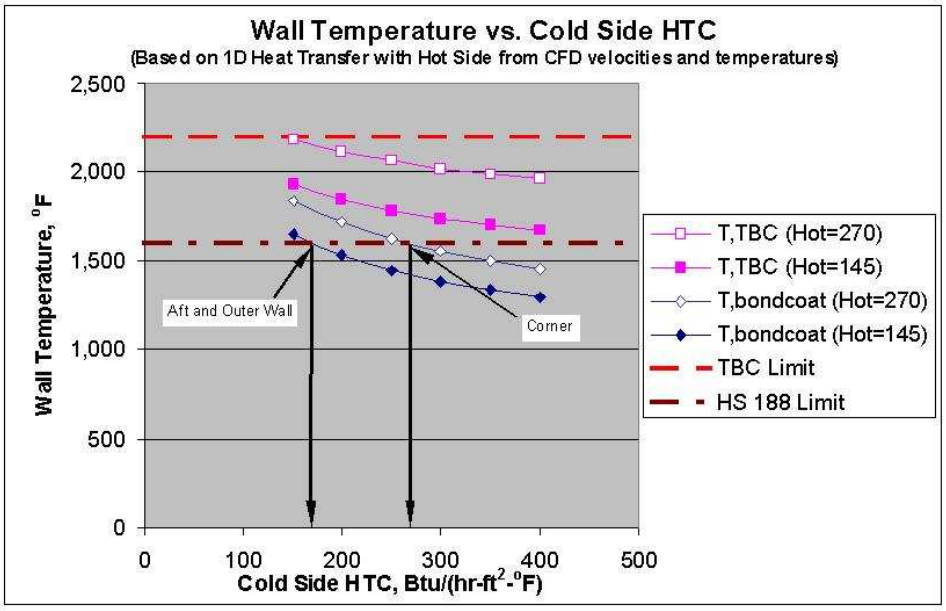

Figure 3-63 Predicted wall temperature vs. cold side heat transfer coefficient (HTC) for various configurations and hot side HTC's for Prototype 3

3.4.4 Instrumentation

Thermocouple and pressure instrumentation locations for Prototype 3 are shown in Figure 3-64 and Figure 3-65. In addition, dynamic pressure measurements were taken at pressure locations numbered 6,7, and 8 in the figure depicting the main combustion region, the cavity combustion region, and the combustion liner region of the test stand.

Figure 3-66 shows a downstream view of the Prototype 3 hardware. This picture shows the exit of the combustor, which is covered with the hula seal that connects to the downstream combustion liner during assembly. Also shown is the cavity impingement cooling sleeve and some of the instrumentation on the exterior of the hardware. Figure 3-67 is a close up of the water-cooled igniter protruding through the impingement cooled liner and placed flush against the wall of the cavity combustor. Figure 3-68 shows instrumentation on the combustor including a cavity pressure tap and thermocouples along the combustor walls.

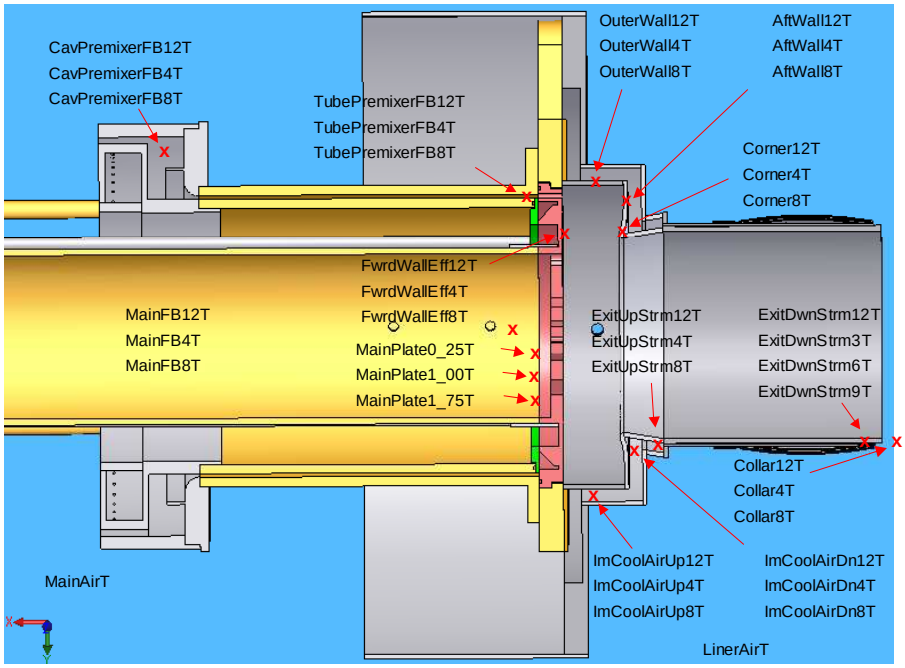

Figure 3-64 Prototype 3 thermocouple instrumentation nomenclature locations

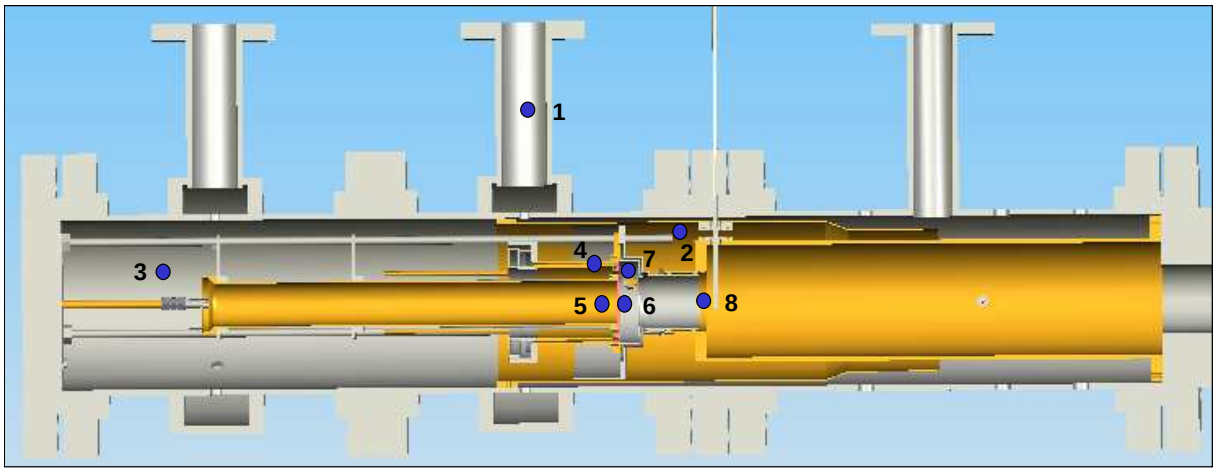

Figure 3-65 Prototype 3 pressure instrumentation nomenclature and locations

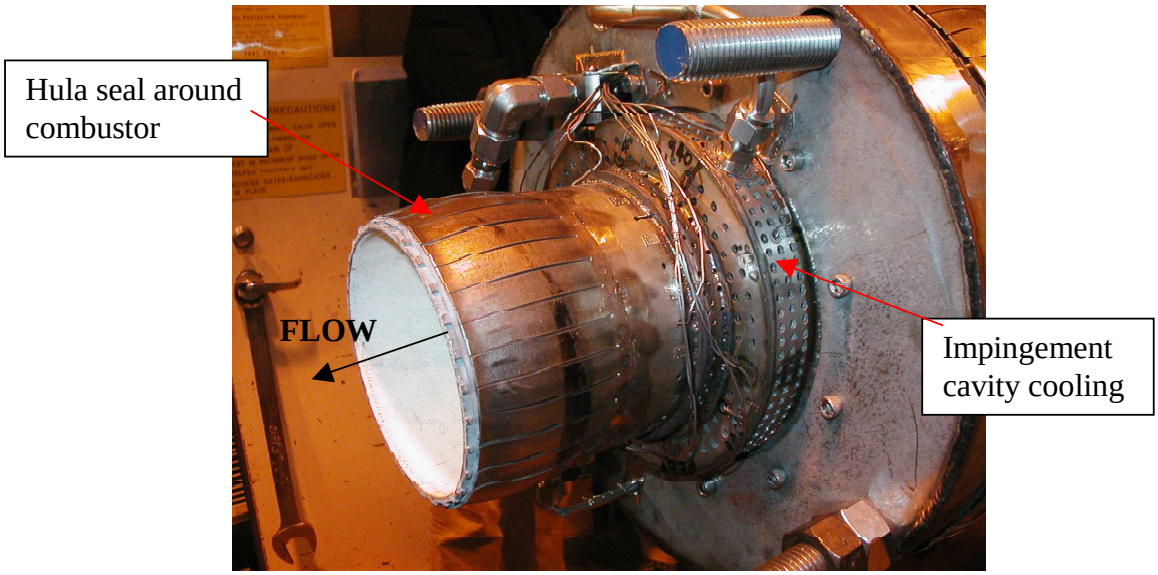

Figure 3-66 Prototype 3 hardware

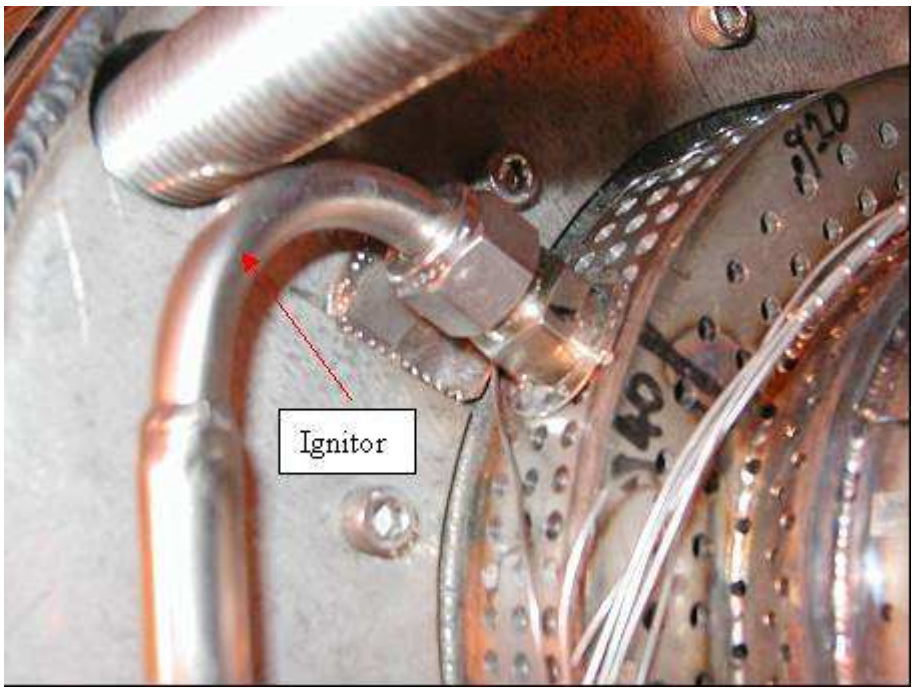

Figure 3-67 Prototype 3 water-cooled, hydrogen spark igniter located through impingement cooling sleeve and aft wall of the combustion cavity section

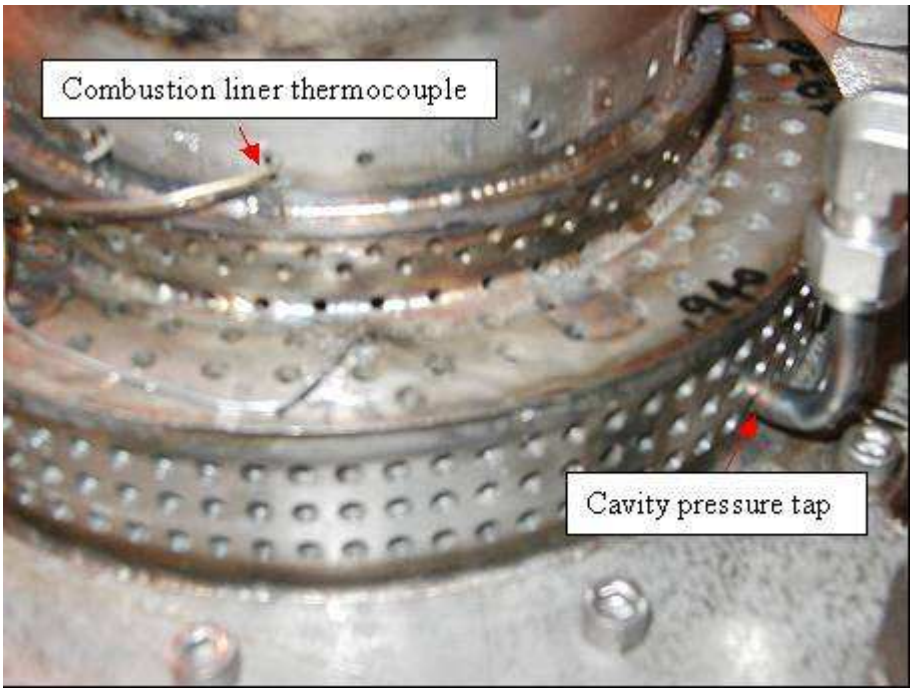

Figure 3-68 Prototype 3 impingent cooling sleeve showing combustion cavity pressure tap and thermocouple instrumentation

4 Results & Discussion

4.1 Atmospheric Combustion Studies

The existing 6" TVC rig was modified for the gaseous (natural gas) fuel injection. Four alternate rig configurations have been designed and fabricated, focused to achieve low emissions. The key features of each configuration can be described briefly as follows. Configuration 1 employs the direct injection of gaseous fuel into the cavity for the primary injector and the premixed injection for the main injector by injecting plain jets of fuel perpendicular into the incoming air upstream. For configuration 2, the premixed primary gaseous fuel injector has been designed by premixing the primary air with fuel, while the main injector design remains the same as for configuration 1. Configuration 3 allows for an improved premixing level in the cavity by premixing both the driver air and primary air with fuel using 4 premixed nozzles on each cavity wall. All the existing driver holes used in configurations 1 and 2 are closed up in order to premix most of the cavity air. For configuration 4 and the final test configuration, the closed fwd and aft driver holes were re-opened up, while fwd, aft, and main premixers remained the same as for configuration 3. For all 4 configurations, emission measurements were performed at the Room 151 facility of Wright Patterson Air Force Base (WPAFB) using a five-element gas-sampling probe.

The testing matrix has been established based on operating conditions of the existing ground-based gas-turbine combustors. The Room 151 facility of WPAFB is limited to the atmospheric operating pressure capability with inlet air temperatures less than 550°F. Since the NOx formation is strongly dependant on the flame temperature, the targeting testing points were determined by matching the reaction-zone and exit temperatures of the existing combustors at their actual operating conditions. It is worth noting that the pressure dependence of NOx is heavily influenced by flame geometry. Based on many studies available in the literature, it has been found that the pressure dependence on the thermal NOx generation is small at flame temperatures less than 2780°F. The testing at the Room 151 facility was performed at atmospheric pressure and an inlet temperature of 450°F with adjusted fuel/air ratios (FARs) matching the reaction-zone and exit temperatures of the existing ground-based gas-turbine combustors. Using the reactor network model, a numerical assessment on the pressure effect is made as part of the study.

The testing was conducted at T3 = 450°F and P4 = 1 atm with a 5% pressure drop for FARs = 0.03136 and 0.0365. The effect of shifting the fuel from the cavity to the main was also investigated for completeness. The measured emission data, NOx (15% O2) and combustion efficiencies, for configuration 1 are shown in Figure 4-1 through Figure 4-3. In general, combustion efficiencies were above 99% for the testing points over a fuel split range from 0.4 to 0.75. Here, the fuel split is defined as the ratio of primary fuel to total fuel. The combustion efficiency at a fuel split of 1 is about 98 % for both FARs. At fuel splits near 0.33 (FAR = 0.03136), the combustion efficiency is down to about 96% due to the low flame temperature in the cavity, close to the lean blowout (LBO), causing insufficient energy transport from the cavity to the main. Thus, the combustion at fuel splits below 0.33 is highly unstable. At fuel split = 0.33 (FAR = 0.03136), ϕ_{c+c} (equivalence ratio of cavity including cooling air) is about 0.47 which is

about the same as the cavity LBO ϕ_{c+c}. Figure 4-1 and Figure 4-2 show that the NOx generation is strongly dependant on the fuel split. At FAR = 0.03136, NOx (15% O2) changes from 8.7 to 21.7 ppm with increasing fuel split from 0.39 to 1.00. At FAR = 0.0365, NOx (15% O2) increases from 15.8 to 25.2 ppm as fuel split increases from 0.43 to 1.00. For both FARs, the lowest NOx (15% O2) was achieved when ϕ_{c+c} and ϕ_{IDIF} (equivalence ratio of main air passages) were about the same. The lowest NOx (15% O2) at FAR = 0.03136 was measured to be 8.7 ppm (ϕ_{c+c} = 0.57 and ϕ_{IDIF} = 0.65) at a fuel split of 0.39, and the lowest NOx at FAR = 0.0365 was 15.6 ppm (ϕ_{c+c} = 0.72 and ϕ_{IDIF} = 0.72) at a fuel split of 0.43. When ϕ_{IDIF} becomes greater than ϕ_{c+c}, NOx (15% O2) emissions increase. The further decrease in fuel split makes the cavity fuel leaner, but makes the main fuel richer. Figure 4-3 shows FAR sweep data for the cavity-only-fuel injection mode. As shown in the figure, NOx (15% O2) increases with increasing FAR, although ϕ_{c+c} increases from 1.18 to 1.69, yielding very rich cavity. It indicates that a Rich-burn/Quick-quench/Lean-burn (RQL) mode has not been achieved over the conditions investigated.

In order to obtain better understanding about the key physiochemical processes responsible for NOx emission, the data reduction and analysis/level 2 (DRA-2) NOx modeling of TVC 6" rig config.1 has been performed using the reactor network simulation (RNS) with the detailed kinetics mechanism. The model was developed for the same testing conditions as for configuration 1 at T3 = 450°F and P4 = 1 atm with a 5% pressure drop for both FARs = 0.03136 and 0.0365. The model consists of five reactors in a series and/or parallel to simulate various combustor regions of the TVC 6" rig as shown in Figure 4-4. The cavity has two reactors: one is the lean blowout (LBO) reactor, the other is the cavity secondary reactor. The cavity flow enters the main dome reactor, and subsequently the main dilution reactor. Lastly, the aft liner cooling wall reactor has been included for completeness. The model uses the constant TAU-PHI approach for the cavity secondary reactor and the constant volume approach for all other reactors. In reactors 1 and 2, ϕ's were fixed to ϕ_{limit} of 0.75 indicating a good mixing level in the cavity associated with flame stretching. The highly turbulent flow structure of the vortex formed in the cavity provides an excellent fuel/air mixing mechanism. The model also shows that the flame stretching (maintaining constant ϕ and residence time) is one of the major physiochemical processes involved in the cavity. As the mass flow rate of fuel injected into the cavity increases from fuel-lean conditions in the cavity, the flame tends to expand within (or beyond) the physical cavity volume and mixes with any additional available air in the cavity (and in the main). Thus, the model was established to allow for the cavity primary reactor volume to vary with the mass flow rate of the cavity fuel by implementing the constant TAU-PHI approach. The measured effect of shifting the fuel from the cavity to main has been successfully reproduced by the model as shown in Figure 4-5 and Figure 4-6. The averaged % difference between the measured NOx (15% O2) and predicted NOx (15% O2) over the operating conditions investigated is 7%. If the constant volume approach is used for the cavity secondary reactor, the maximum NOx (15% O2) will be always predicted at ϕ_{c+c} close to 1.0 instead of fuel split = 1.0. Note that the 6" TVC rig has multiple air inlets in the cavity, including the primary, driver, and cooling air, at different positions. Thus, the flame in the cavity does not behave as a perfectly premixed flame with a single source inlet in a constant reactor volume due to the different residence times involved in the mixing with each different air

inlets. As explained in the discussion part of the configurations 2, 3, and 4 emission data, it does indeed show that configuration 1 achieves an excellent mixing level in the cavity.

By extending the DRA-2 model, the pressure effect on the TVC 6" Rig emission has been numerically investigated for the best performing conditions at both FARs = 0.03136 and 0.0365. The overall FAR was adjusted as T3 and/or P4 increase in order to have the combustor exit temperature the same as the cases for T3 = 450°F and 1 atm at both FARs = 0.03136 and 0.0365. In this analysis, several different cases were studied with a combination of the higher P4 (P4 = 277 and 450 psia) and the higher T3 (T3 = 800 and 1005°F) in order to simulate the actual operating conditions of the existing lean-premixed gas turbine combustors. For the case of FAR = 0.03136, the maximum increase was about 12% (from 8.3 ppm to 9.3 ppm) at P4 = 450 psia and T3 = 450°F. For the higher temperature case (FAR = 0.0365), the maximum increase was about 16% at P4 = 277 psia and T3 = 450°F (from 15.2 ppm to 17.7 ppm). The dependence of T3 on the NOx generation was relatively small. Less than 6% increase in NOx (15% O2) is predicted for both cases studied at higher T3. For the actual operating conditions, about 7% increase in NOx (15% O2) was predicted for the lower temperature case, while about 17.2% increase in NOx (15% O2) was obtained for the higher temperature case. In general, the pressure dependence on the NOx generation can become small if a good fuel/air mixing is achieved in the fuel-lean cavity and main.

For configuration 2, the cavity primary injector has been designed to premix the primary air with fuel prior to injection into the cavity, while the main injector design remains unchanged from configuration 1. The air split distributions of configurations 1 and 2 are about the same. The emissions testing for configuration 2 has been performed at the same operating conditions as for configuration 1. The performance of configuration 2 was similar to (or slightly worse than) that of configuration 1 over the operating conditions investigated as shown in Figure 4-7 and Figure 4-9. For FAR = 0.03136, the lowest NOx (15% O2) of configuration 2 is about 3% higher than that of configuration 1. However, for FAR = 0.0365, the lowest NOx (15% O2) of configuration 2 is about 25% higher than that of configuration 1. The combustion efficiencies at these conditions are about the same. It is indicating the cavity mixing of configuration 1 is better than that of configuration 2. It can be attributed to the differences in the injection characteristics of the 2 different injector designs. The primary fuel direct injector of configuration 1 has 4 small fuel holes and 18 small primary air holes. Configuration 2 design utilizes premixers and inject the air/fuel mixture into the cavity as one single mixture jet. A strong incoming fuel/air flow from the premixers of configuration 2 may disturb the cavity vortex generated by the forward and aft driver air. Since the cavity vortex is the key mixing mechanism of TVC, the cavity mixing is strongly dependant on the vortex strength. The primary air is less than 10% of the total air. Thus, the premixer is typically highly fuel rich over the operating condition range investigated. The fuel still needs to mix with other available air in the cavity in order to have a stable burning. In addition, the 4 fuel holes and 18 air holes of the primary injector of configuration 1 allows the fuel and air to mix better because a number of small jets encounter more shear/turbulent interaction compared to one big jet. The LBO performance of configuration 1 (ϕ_{c+c} = 0.45) was also slightly better than that of configuration 2 (ϕ_{c+c} = 0.50). It is no surprising, since the penetration depth of direct fuel injection of the configuration 1 may not be sufficient at low fuel flow rates due to the relatively low fuel

velocity at the fuel nozzle tip. The injectors were not designed for this extreme condition. Thus, diffusion-type flame can be achieved locally near the fuel injectors at low fuel flow rates. For configuration 2, since the all the fuel is premixed with the primary air in the premixed injectors, some degree of premixing level at the extremely low fuel mass flow rate condition helps the local mixing near the injectors.

Configuration 3 achieves an improved premixing level in the cavity by premixing most of the cavity air, including primary air, forward driver air, and aft driver air, with fuel using 4 premixing nozzles on each cavity wall. Thus, all cavity air is premixed except the cooling air in the cavity. The concepts of the forward and aft premixer designs of configuration 3 are similar to that of configuration 2. In order to keep the air split distribution about the same as configuration 1, configuration 3 has larger air effective areas for the premixers in order to add the driver air to the premixers. Interestingly, the emission performance of configuration 3 was slightly poorer than that of configuration 1 over the operating conditions studied as shown in Figure 4-10 through Figure 4-12. For both FARs = 0.03136 and 0.0365, the lowest NOx (15% O2) of configuration 3 is about 10% higher than that of configuration 1. Configuration 3 also encounters acoustic instability for some of the operating conditions, especially when the premixers are relatively fuel lean or fuel rich. The intent of the configuration 3 design is to utilize the forward and aft premixer jets to drive the vortex in the cavity instead of using smaller driver holes. Thus, all the driver holes, used in configuration 1, were closed up. From the video image, it was clearly shown that the strong cavity vortex, seen in configuration 1, was not formed in configuration 3. Note that acoustic instability was never encountered for any of the operating conditions investigated for either configuration 1 or 2. The stability can be attributed to the strong, stable vortex formed in the cavity in configurations 1 and 2. Because of the strong vortex formation in configuration 1, it also indicates that the mixing level in the cavity of configuration 1 is slightly better than that of configuration 3, although a large amount of the cavity air is premixed in configuration 3.

For configuration 4, the final test configuration, both the closed fwd and aft air driver holes were re-opened up in order to stabilize the flow better in the cavity, while fwd, aft, and main premixers remained the same as for configuration 3. As expected, configuration 4 did not encounter the acoustic instability, occurred in configuration 3, over the operating conditions studied. However, based on the visual observation, the cavity vortex formed in configuration 4 was not strong as the one formed in configuration 1. The premixed jets may still disturb the cavity vortex to a certain degree, and thus the vortex is not as strong (and as stable) as the one formed in configuration 1. In comparison between the configurations 1 and 4 emission data, the configuration 4 data show a 12% reduction in NOx (15% O2) for FAR = 0.03136 and about 27% reduction in NOx (15% O2) for FAR = 0.0365 as shown in Figure 4-13 through Figure 4-15. Since the weaker cavity vortex is formed in configuration 4 compared to configuration 1, this reduction in NOx (15% O2) may not be due to the better mixing, but it can be attributed to the shorter residence time in cavity with a higher air loading cavity for configuration 4. The cavity air is about 22% of the total air for configuration 4 while it is about 17% of the total air for configuration 1.

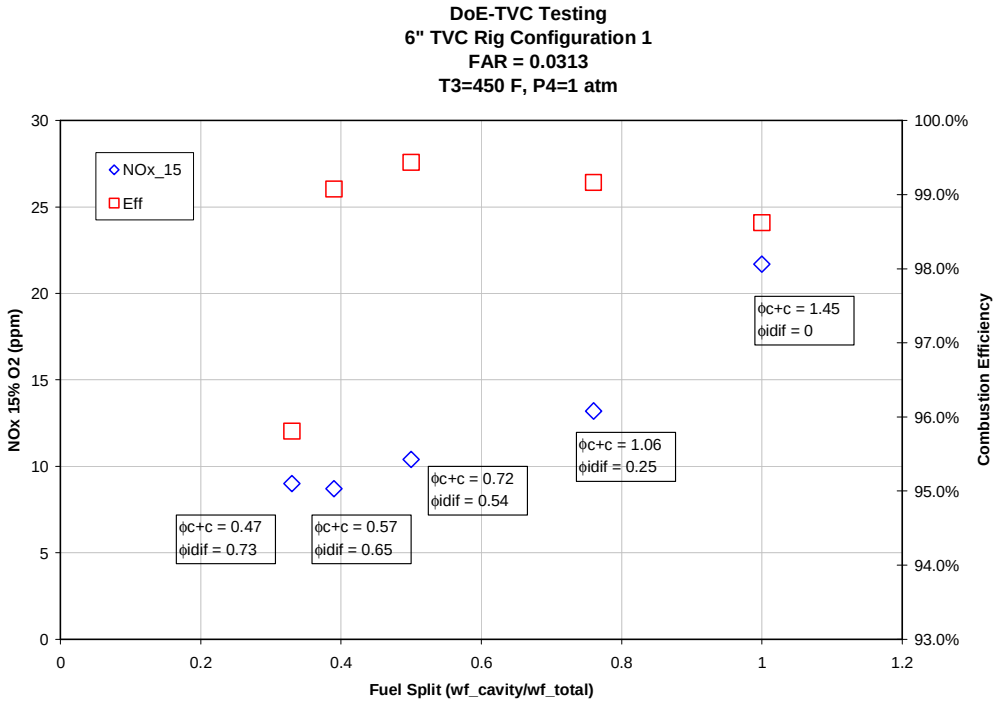

Figure 4-1 Measured NOx 15% O2 (ppm) & Combustion Efficiency at FAR = 0.03136

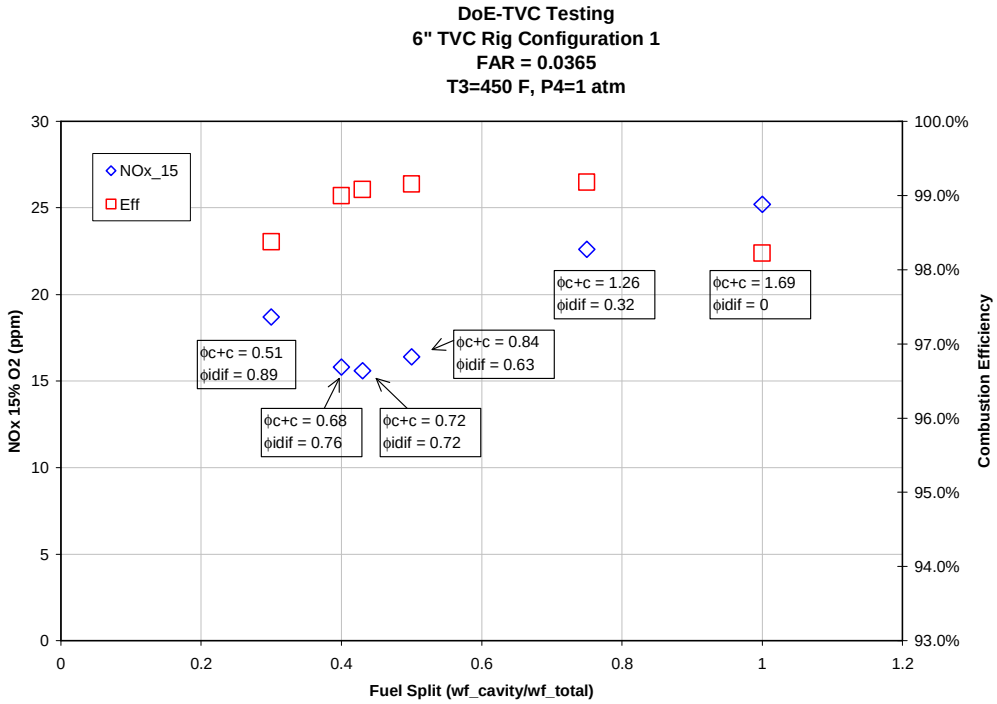

Figure 4-2 Measured NOx 15% O2 (ppm) & Combustion Efficiency at FAR = 0.0365

T3 = 450 F, P4 = 1 atm

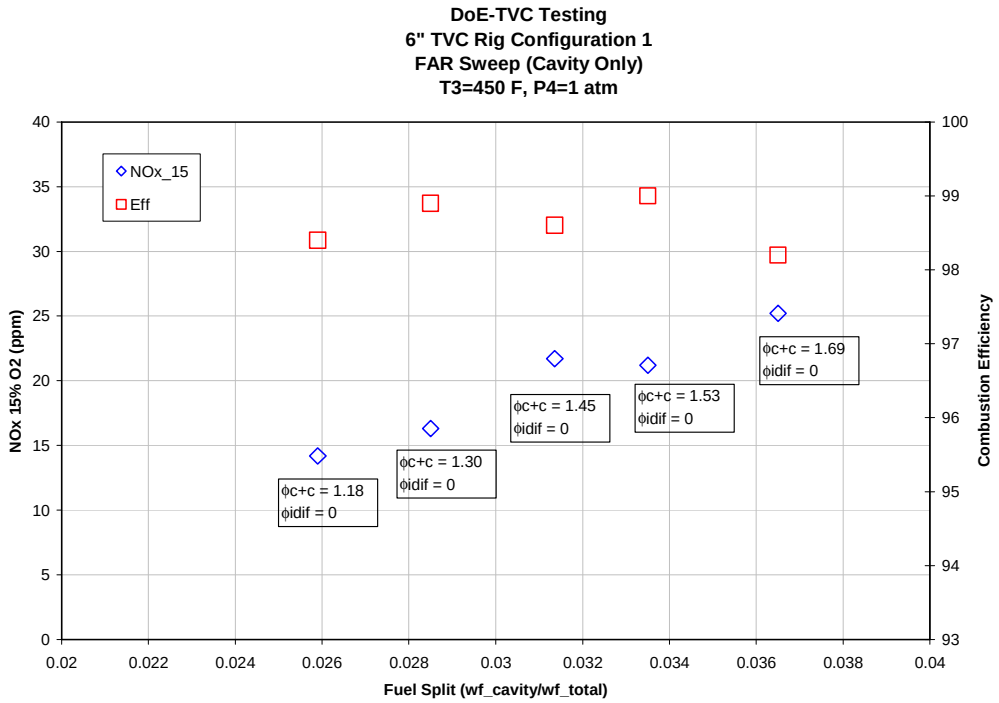

Figure 4-3 Measured NOx for Cavity Only Fuel Injection at Different FARs

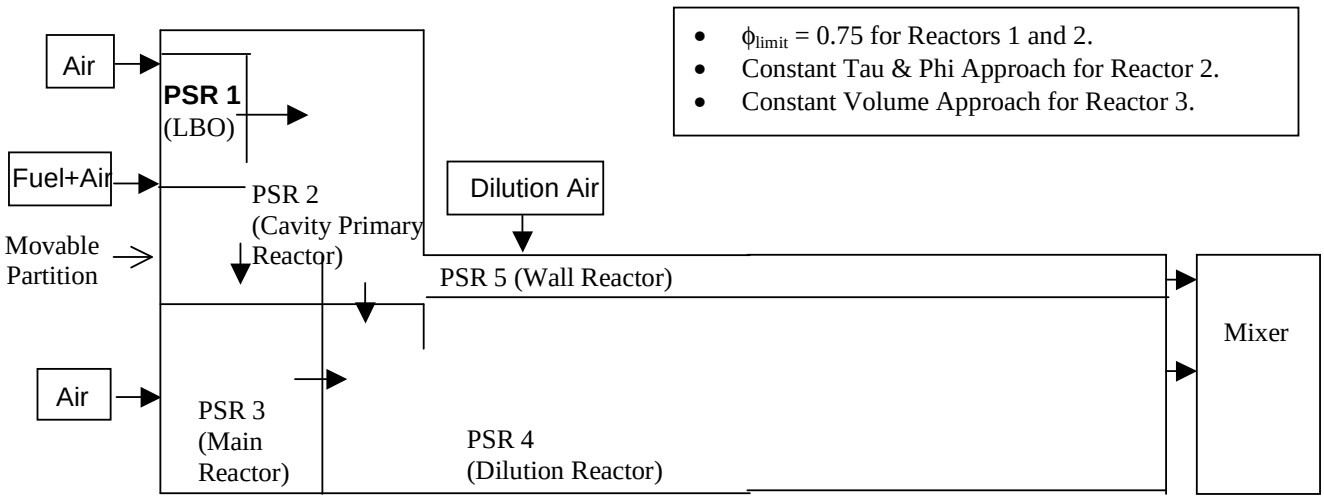

Figure 4-4 DRA-2 (Network Reactor) Model

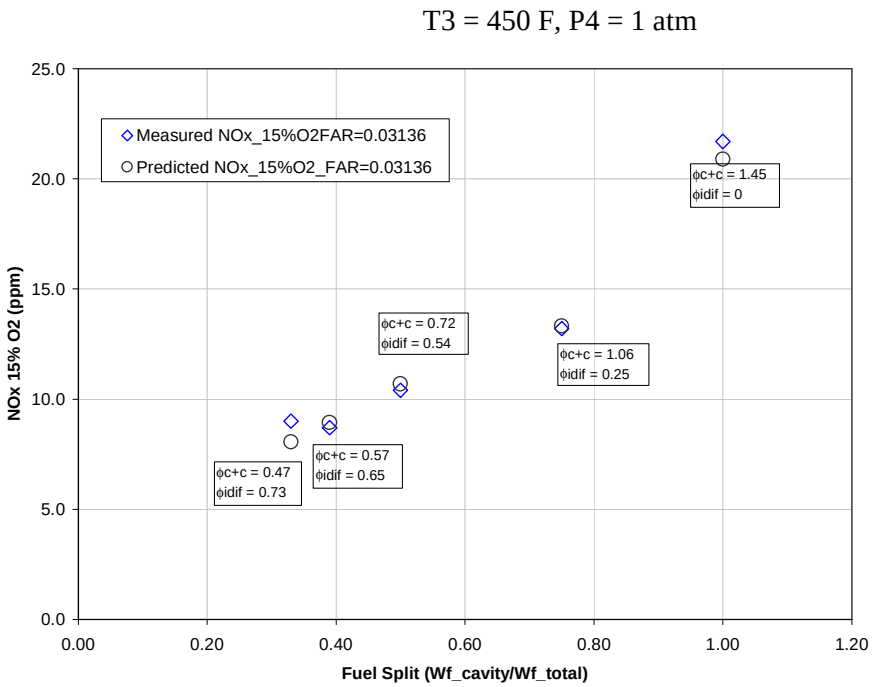

Figure 4-5 DRA-2 Model Prediction for NOx 15% O2 (ppm) at FAR = 0.03136

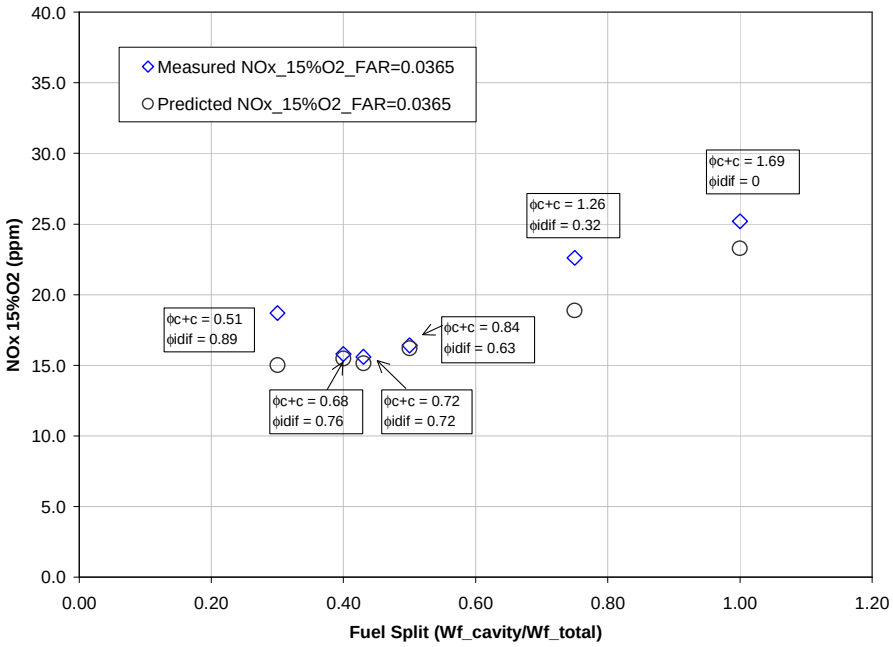

Figure 4-6 DRA-2 Model Prediction for NOx 15% O2 (ppm) at FAR = 0.0365

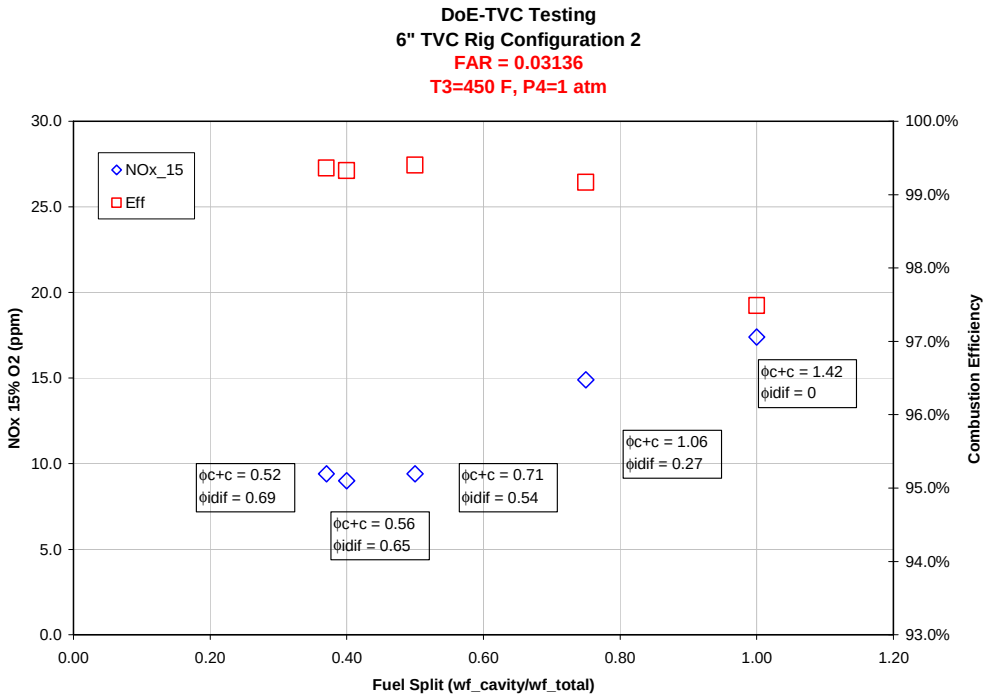

Figure 4-7 Measured NOx 15% O2 (ppm) & Combustion Efficiency at FAR = 0.03136 (Config. 2)

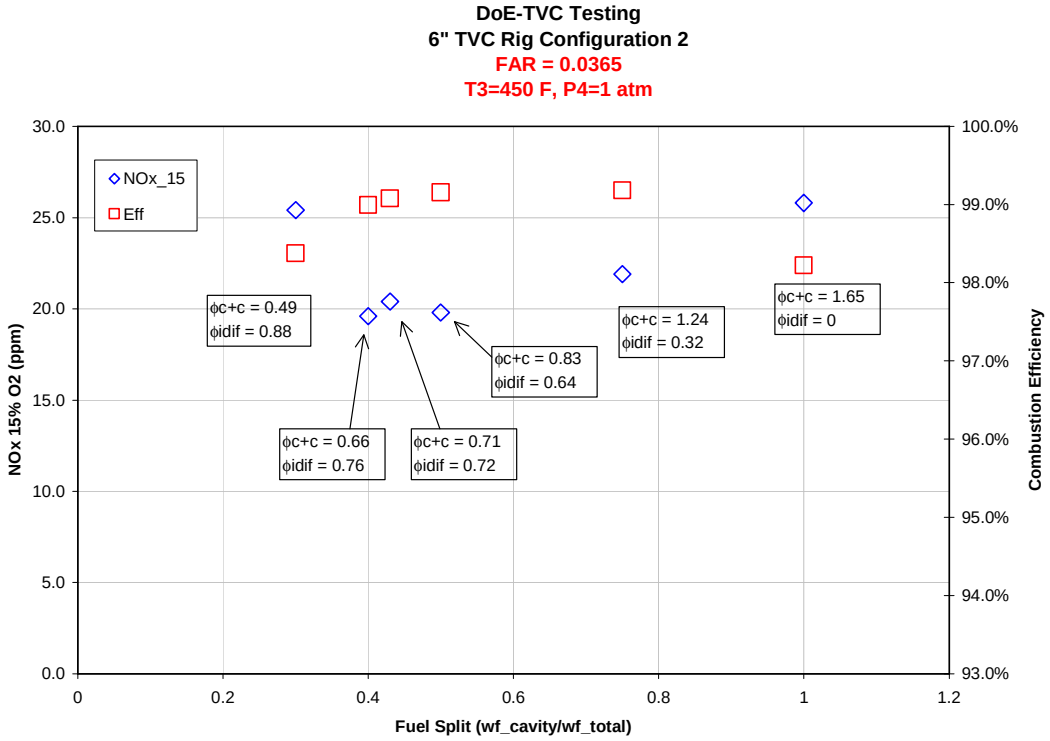

Figure 4-8 Measured NOx 15% O2 (ppm) & Combustion Efficiency at FAR = 0.0365 (Config. 2)

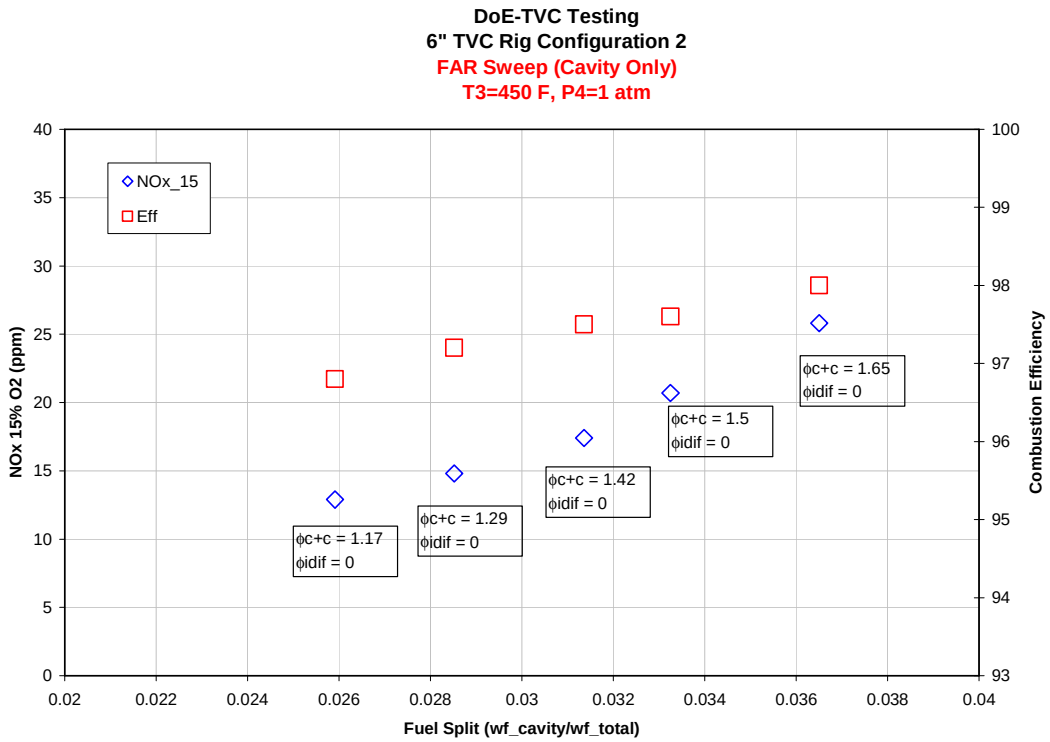

Figure 4-9 Measured NOx for Cavity Only Fuel Injection at Different FARs (Config.2)

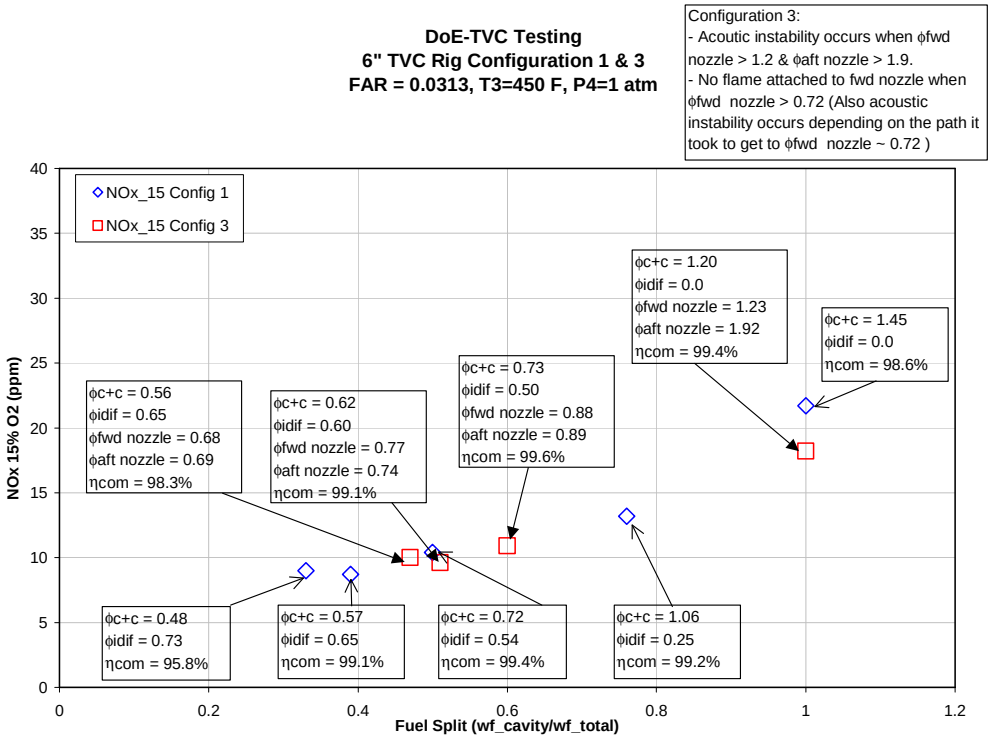

Figure 4-10 Comparison Between Configs. 1 and 3 Measured NOx 15% O2 (ppm) & Combustion Efficiency at FAR = 0.03136

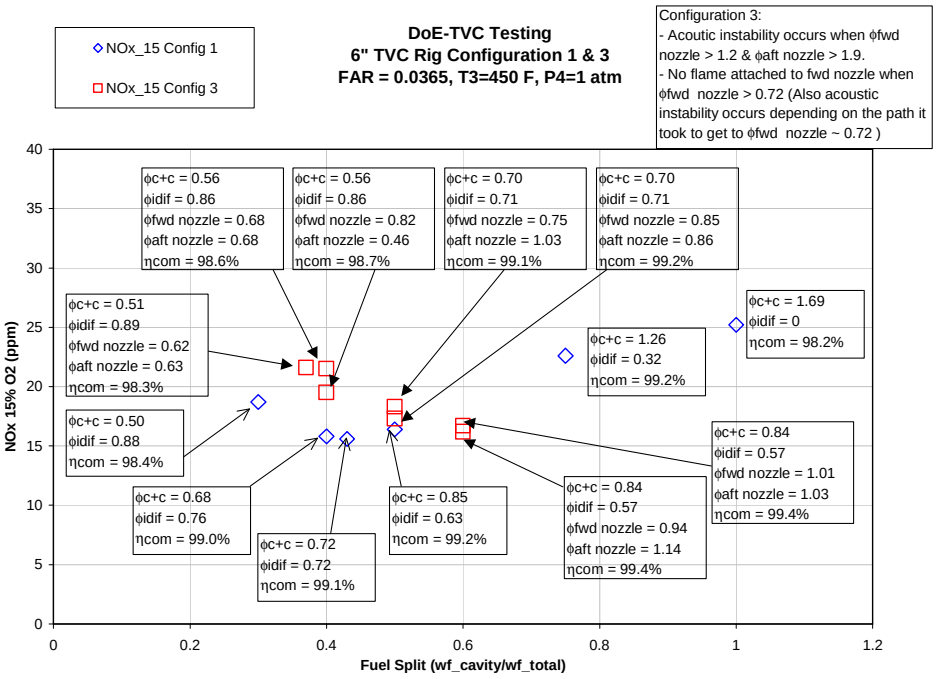

Figure 4-11 Comparison Between Configs. 1 and 3 Measured NOx 15% O2 (ppm) & Combustion Efficiency at FAR = 0.0365

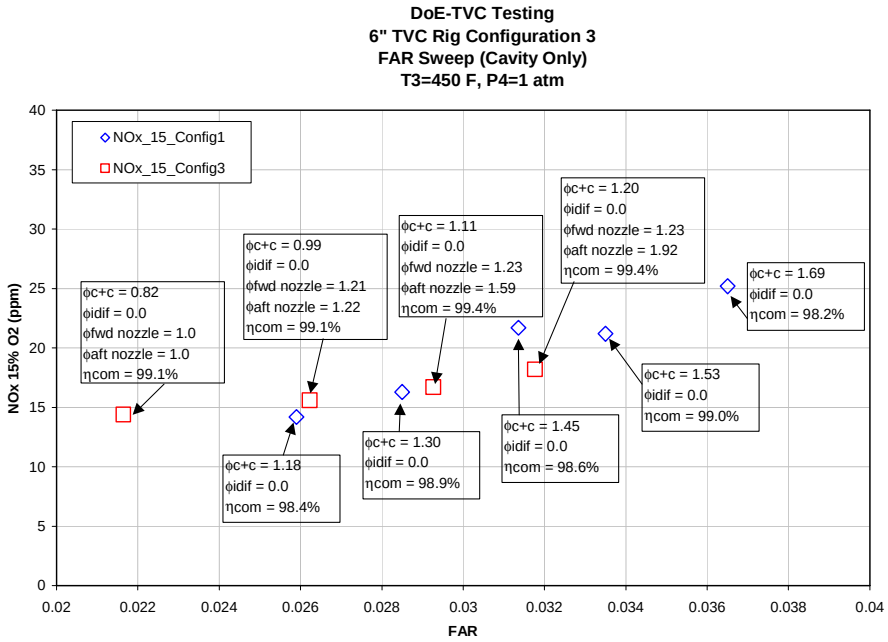

Figure 4-12 Comparison Between Configs. 1 and 2 Measured NOx for Cavity Only Fuel Injection at Different FARs

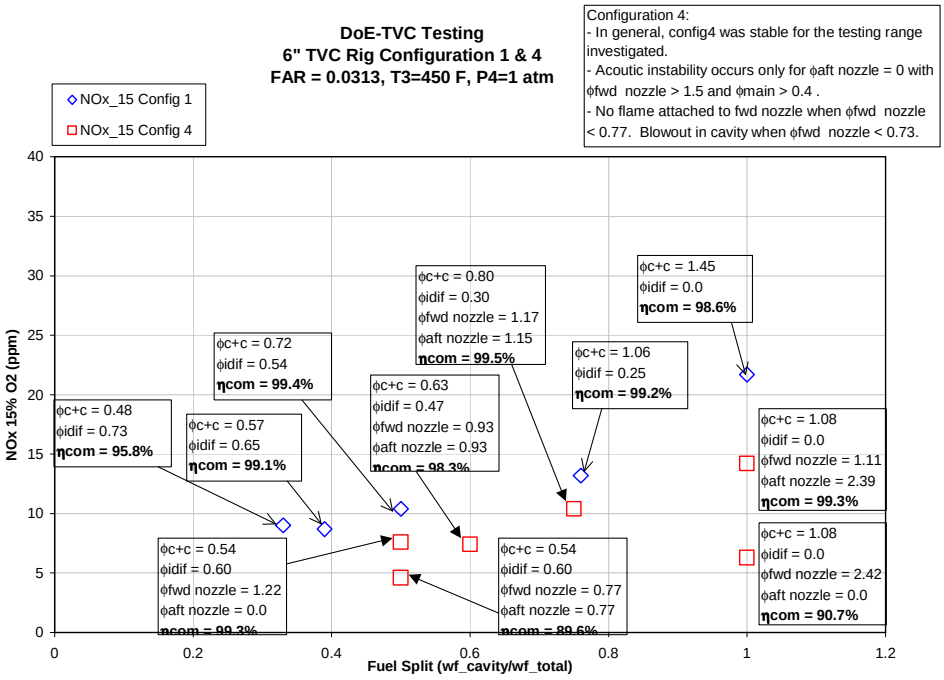

Figure 4-13 Comparison Between Configs. 1 and 4 Measured NOx 15% O2 (ppm) & Combustion Efficiency at FAR = 0.03136

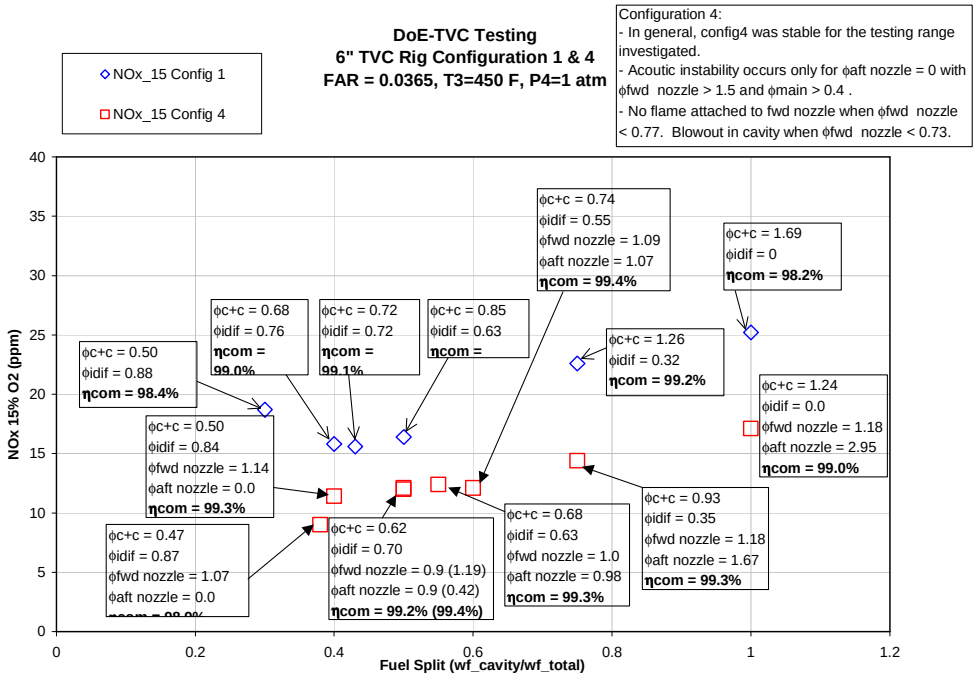

Figure 4-14 Comparison Between Configs. 1 and 4 Measured NOx 15% O2 (ppm) & Combustion Efficiency at FAR = 0.0365

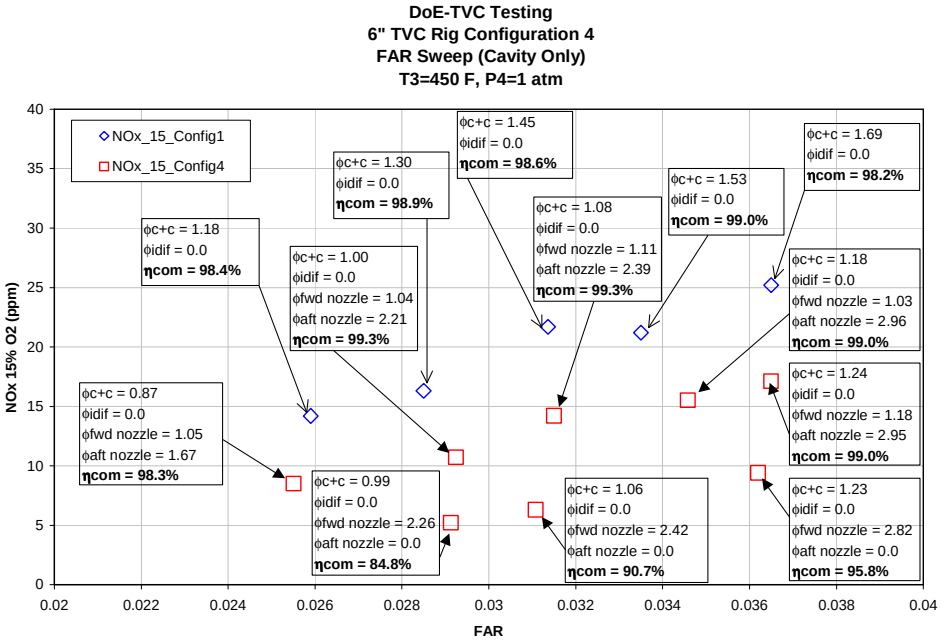

Figure 4-15 Comparison Between Configs. 1 and 2 Measured NOx for Cavity Only Fuel Injection at Different FARs

4.2 Prototype 1

4.2.1 Experimental Results

Following the test matrix in Figure 4-16, the critical design parameters of the combustor were studied. Two different main burners were evaluated. Two injector lengths and two injector orientations were also evaluated. The combustor was operated over a range of test conditions by changing the firing temperature, flow residence time, cavity fuel split, and % diffusion fuel in the cavity.

Emissions data was collected over the range of test conditions. Figure 4-17 shows the NOx performance for prototype-1. Most of the low temperature operation of the combustor was above the target of 50% NOx reduction. However, at least 2 points fell below the target reference demonstrating a NOx emission reduction. The lowest point was more than 25% below the reference line. In a complementary plot of NOx vs. CO emission, Figure 4-18 shows the high NOx performance relative to the CO emission. With a CO target of 10 ppm it is clear that most of the data lies outside of the CO target as well. Figure 4-19 gives a relative performance picture of the NOx & CO emission relative to the temperature dependent NOx curve. The low NOx performance point is shown to have CO emissions at least 50% above the 10 ppm target. The data points with acceptable CO have excessive NOx beyond the scale of the plot. Lower NOx is accompanied by high CO levels.

A surface response formulation of the NOx emission was constructed from the experimental data. Figure 4-20 shows the response data obtained in the analysis. In case A, a coarse fit to the NOx data was obtained using primarily linear terms. The fit showed little improvement for case B with the addition of a quadratic term and the removal of the Main Burner correlation. The best fit of a quadratic system to the response data had R-sq(adj) = 96%. The premixer length, main burner design, and the combustor firing temperature show the strongest influence on the NOx.. The % Cavity fuel had a strong effect on the NOx showing up in the quadratic terms. The injector orientation does not show up as a significant parameter, and the influence of residence time and the % diffusion fuel was weak over the range of study.

The effect of cavity fuel on the NOx emission is shown in Figure 4-21. A clear trend of reduced NOx with increased cavity fuel is demonstrated. The effect of the geometry changes is also shown in the table. Prototype1-4 shows the lowest emission and produced the 50% NOx reduction data. Figure 4-21 demonstrates the ability of the response surface formulation to reproduce the emission data for the various geometries. The fit is within 99% of the actual values.

Name	Run	Date	Main Burner	Injector Premixer Mixing L	Injector Orientation
P1-1	1	9/16/2003	1	Long	+
P1-2	2	9/18/2003	1	Short	X
P1-3	3	9/23/2003	2	Short	+
P1-4	4	9/25/2003	2	Long	+

Figure 4-16 Prototype 1 Experimental test matrix

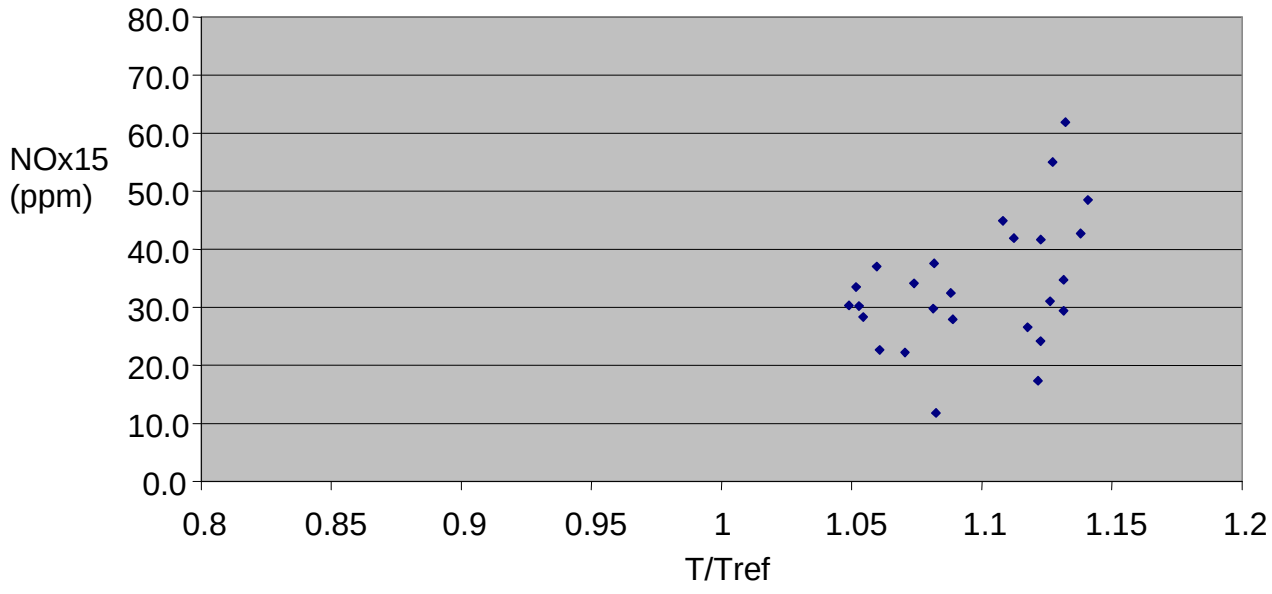

Figure 4-17 Prototype-1 NOx Emission Measurements

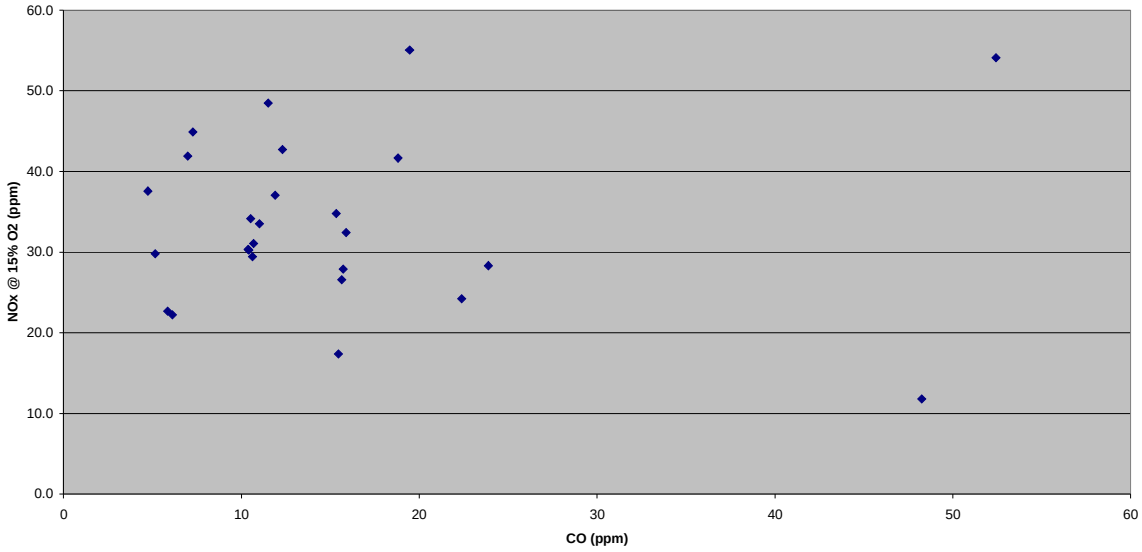

Figure 4-18 Prototype 1 NOx and CO correlations

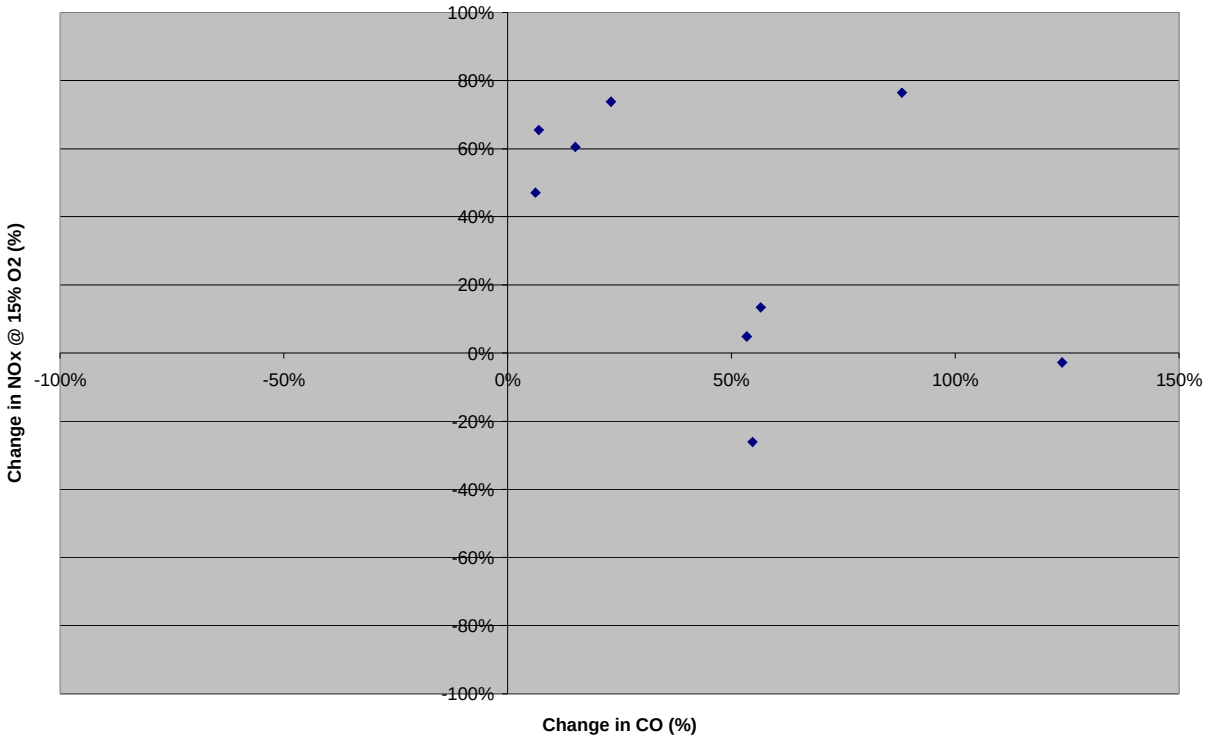

Figure 4-19 Prototype 1 comparison to emissions targets

	A	B	C
Variable	Coded Coefficient	Coded Coefficient	Coded Coefficient
Constant	24.65	22.54774	14.81
MainBurne	-1.40		12.43
InjOrient	-3.63	-3.75327	
PremixL	12.69	12.29086	-20.34
Temp	7.20	7.356314	24.65
%Cav	-7.89	-9.142681	7.20
Tau	6.53	7.141597	-8.22
%Diff	-5.05	-5.013499	-5.20
MainBurner*%Cav			-15.13
PremixL*%Cav			-7.98
PremixL*Tau			26.14
Temp*%Cav			-19.75
Temp*Tau			-11.86
Temp*%Diff			-8.95
%Cav*Tau			-13.03
%Cav*%Diff			-5.47
Temp^2			7.49
%Cav^2		4.516094	20.70
Tau^2			13.77
%Diff^2			3.59
Statistics			
Std Err	5.53	5.207	2.11
R-sq	82.22%	84.26%	0.99
R-sq(adj)	75.31%	78.14%	0.96
R-sq(pred)		67.01%	0.89
Press		1022.734	337.88

Figure 4-20 Prototype 1 response surface model parameters

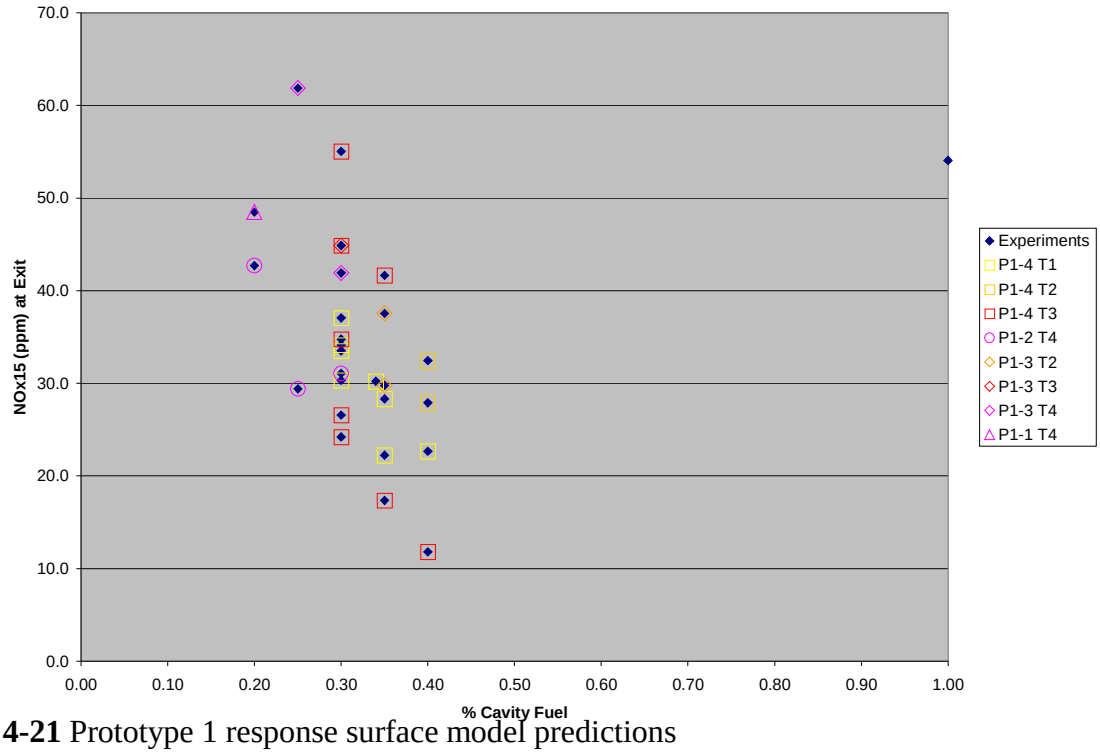

Figure 4-21 Prototype 1 response surface model predictions

4.2.2 Discussion

Prototype 1 demonstrated the ability of the trapped vortex combustor to reduce NOx emission below the target performance curve, but the CO was excessive. The parametric evaluation pointed to a longer premixer and the second main burner design as the best influences on reducing the NOx emission. The NOx response surface was able to give a good prediction of the combustor performance. However, the evaluated parameters did not appear to be able to bring the combustor performance in line with the emission targets.

Increasing the % cavity fuel tended to decrease the NOx. This is indicative of a rich condition in the vicinity of the cavity flame. This corresponds to high CO production as well. A significant amount of NOx is produced by the cavity under these conditions when the rich mixture is leaned out. A significant change in the design with a leaner cavity was proposed.

4.3 Prototype 2

4.3.1 Experimental Results

The poor emission performance of Prototype-1 led to a redesign of Prototype-2a1 with targeted improvements in emission performance. Prototype-2a1 had redesigned forward wall injectors comprised of 75 annular ports, which created a stronger cavity vortex in the CFD models of its performance, but was never tested.

Prototype 2a2 had an annular premixer that feeds the ports with a fuel-air mixture. The design of the main burner also changed to incorporate slot-like ports rather than circular ports. Also, the design improved combustion liner cooling to reduce combustor surface temperatures.

Prototype-2a2 is representative of an approximately 1:10 scale gas turbine can combustor and was evaluated at full load gas turbine conditions. The goal of the redesign effort was to further reduce NOx at lower operating temperatures and improve CO emissions at all temperatures. Figure 4-22 shows the negative shift in NOx performance for Prototype-2 compared to Prototype-1. The lowest NOx emission was still above 10 ppm, but a shift to lower temperatures indicates a decreased performance for this design. Likewise, the high NOx temperature range is shifted to lower temperatures from Prototype-1. These changes are contrary to the NOx emission targets.

On the other hand, the CO emission for Prototype-2a2 is significantly improved. Sub-10 ppm CO emission was obtained for the high-temperature/ high-NOx operating points as shown in Figure 4-23. The good CO burnout is attributed to the improved vortex performance. The CO emission ~ 5 ppm was in line with the CO emission target for the prototype. It was concluded that additional design changes were needed to focus on NOx reduction without increasing the CO.

Further changes were made to Prototype-2a2 to meet the NOx performance targets. In the next revision, Prototype-2b, the premixer was modified, the cavity design was changed, the main burner was redesigned, and outer wall effusion cooling was eliminated. Figure 4-23 shows the low NOx and CO obtained by these prototypes. The CO was consistently below 10 ppm over the entire range of operation; the NOx was as low as 9-ppm.

The TVC combustor is sensitive to the amount of fuel sent to the cavity. The experiments, the percent cavity fuel is varied while maintaining a fixed combustor firing temperature. It appears that a relative minimum appears for the two prototypes. The combustor was found to have lowest NOx emissions at a particular fuel split which was then maintained during the turndown evaluations which follow.

In the Prototype 2c, the NOx emission was further reduced and the thermal life issues were solved. Prototype 2c was able to demonstrate strong emission performance over a very wide temperature range. Emission levels were at or below 9-ppm between 1.0 and 1.04 T/Tef as shown in

Figure 4-24. This was an improvement compared to the DLN combustion system, but fell short of the 50% improvement which is targeted. At temperatures around 1.06 T/Tref emissions were still below 20 ppm. The improvements in Prototype-2c were accomplished by improvements in the thermal design and air handling. The CO emission for Prototype 2c was consistently below 6-ppm over the temperature range of interest, as

shown in Figure 4-25. The good CO performance was even better than had been demonstrated with Prototype-2b. The absence of a high CO regime was indicative of the wide turndown margin potential.

The turndown margin for the combustor was explored in additional experiments. Figure 4-26 shows the NOx emission and turndown margin for Prototype 2c. Below Tref the NOx increases to between 15 and 20 ppm, but no further changes are observed as the combustor is turned down to 0.8 T/Tref. The NOx performance at high temperature is consistent with Figure 4-24. The CO emission with turndown below Tref remained in the single digits until just before the lean blow-out point at 0.8 T/Tref as shown in Figure 4-27. This demonstrates a strong turndown characteristic for the combustor. Just before lean blow out the CO emission rises to nearly 100 ppm. At temperatures above Tref the CO emission is consistent with Figure 4-25.

A network emission model was developed to try to simulate the emissions of the TVC combustor. Earlier work focused on trying to do this for the atmospheric combustor rig, but the predicted lean blow out point and high temperature emissions showed large discrepancies with experimental data. The effort was revisited for prototype-2c, which nearly met the emission goals. The kinetics network consisted of a series of PSR's & PFR's representing the different reaction regimes of the combustor. The model was anchored based on the physical characteristics of the design and lean blow out performance. The remaining parameters were tuned to match the combustion characteristics. Figure 4-26 shows the strong agreement between the reactor network predictions and the measured experimental performance, demonstrating the ability of the reactor network to simulate the TVC combustor performance over the full range of operating conditions. The fit is strongest for T > Tref, but captures the trends at lower temperatures as well. Figure 4-27 shows the CO predicted by the network model in comparison to experimental measurements. The rise in CO near the lean blow out point is predicted, and the rise above 10 ppm is predicted 75 degrees above the actual crossover temperature. The low CO performance is predicted at the design point, but the model inaccurately predicts high CO levels at higher temperatures.

The combustion dynamics of Prototype 2c were also measured over the range of operating temperatures including turndown. Figure 4-28 shows the peak-to-peak fluctuation in combustion pressure at full-pressure conditions. The dynamic pressure could be as high as 9 psi p-p just above Tref, the lowest NOx condition. However, it was also demonstrated that combustion dynamics could be reduced in that regime through a trade-off with NOx performance. Near the lean blow-out condition combustion dynamics remained below 2 ppm.

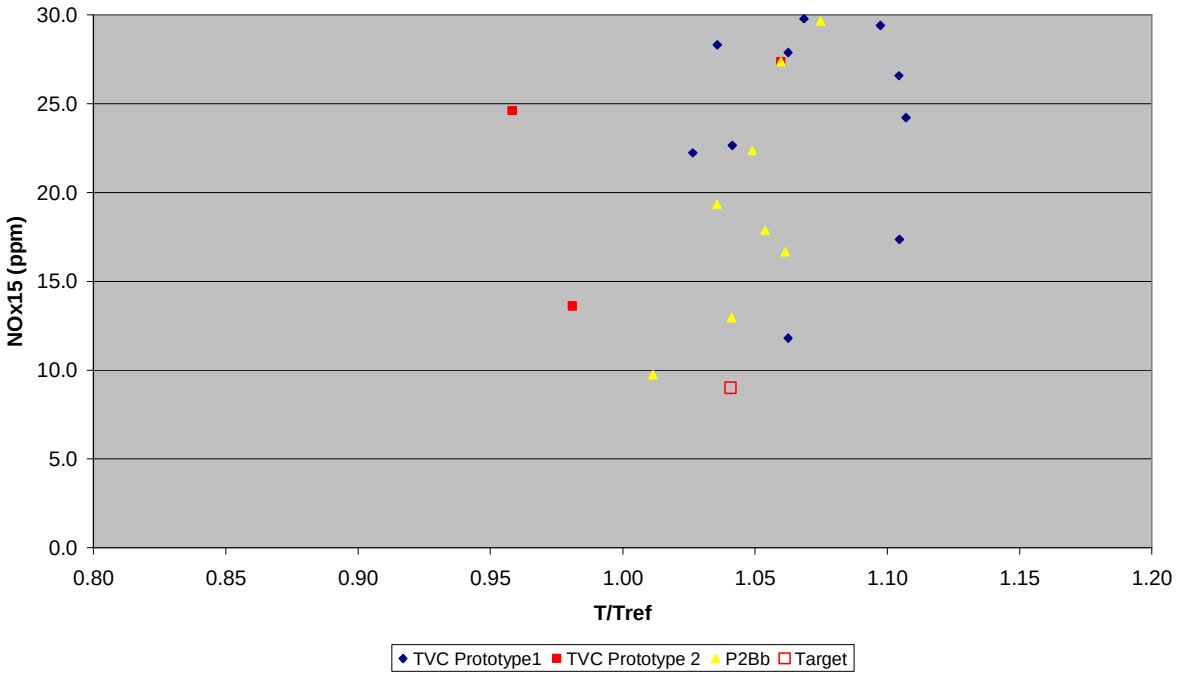

Figure 4-22 TVC Prototype 2a2 and 2b NOx emissions

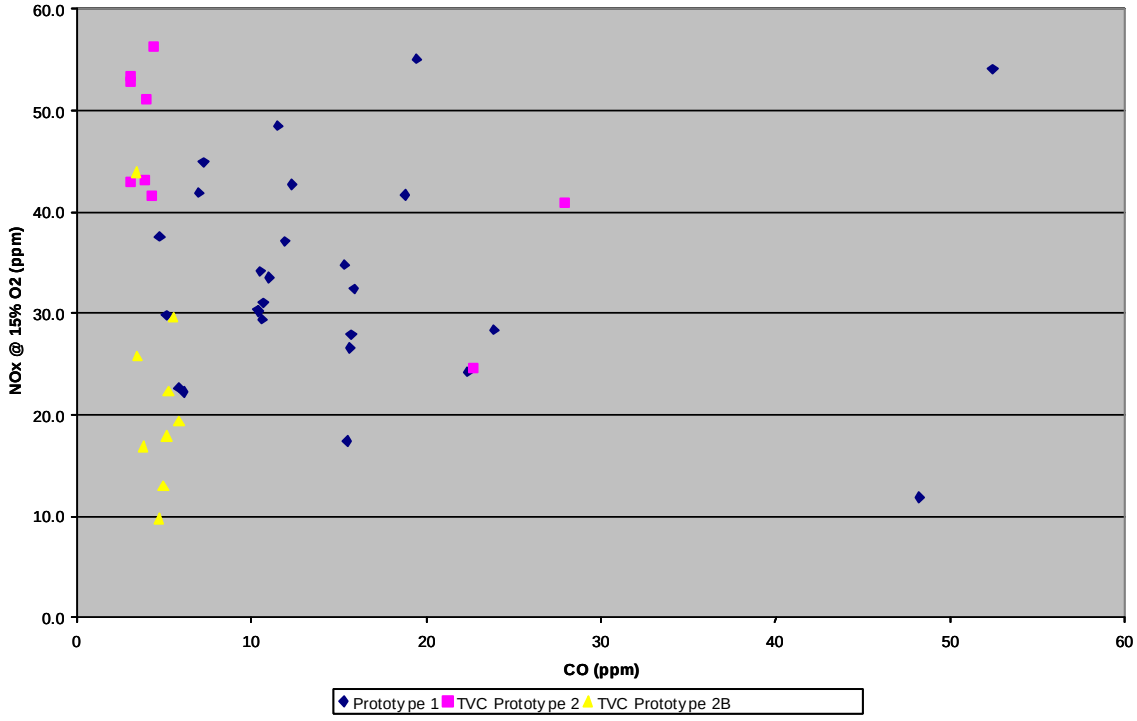

Figure 4-23 TVC Prototype 2a2 and 2b NOx vs. CO emissions

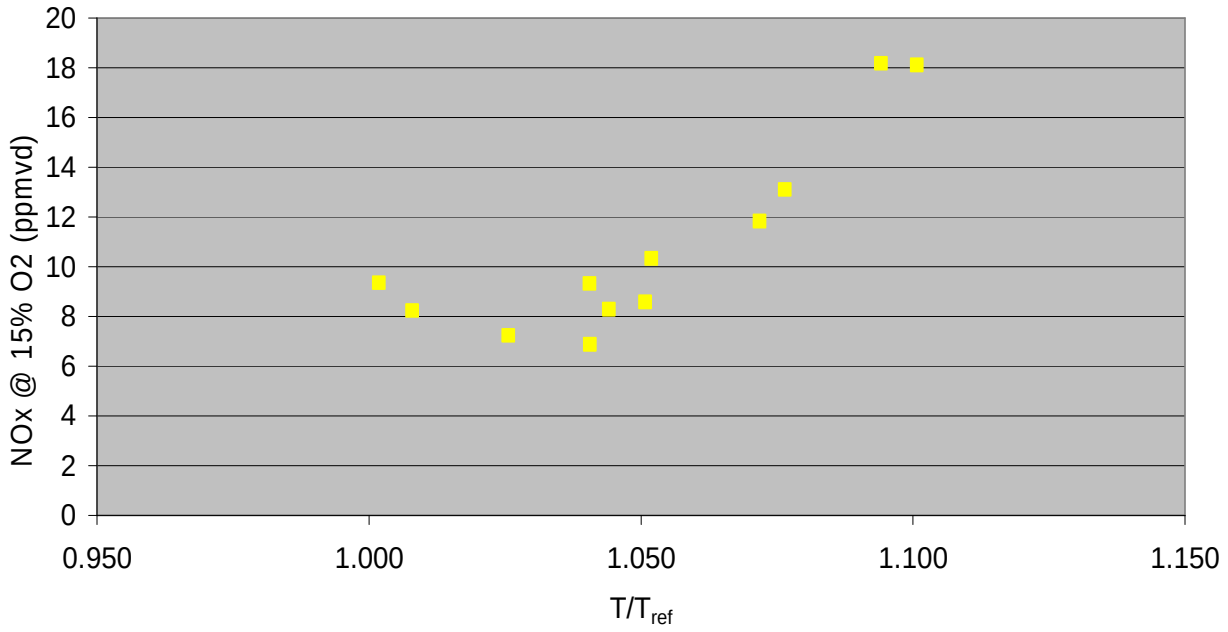

Figure 4-24 Prototype 2c NOx emissions

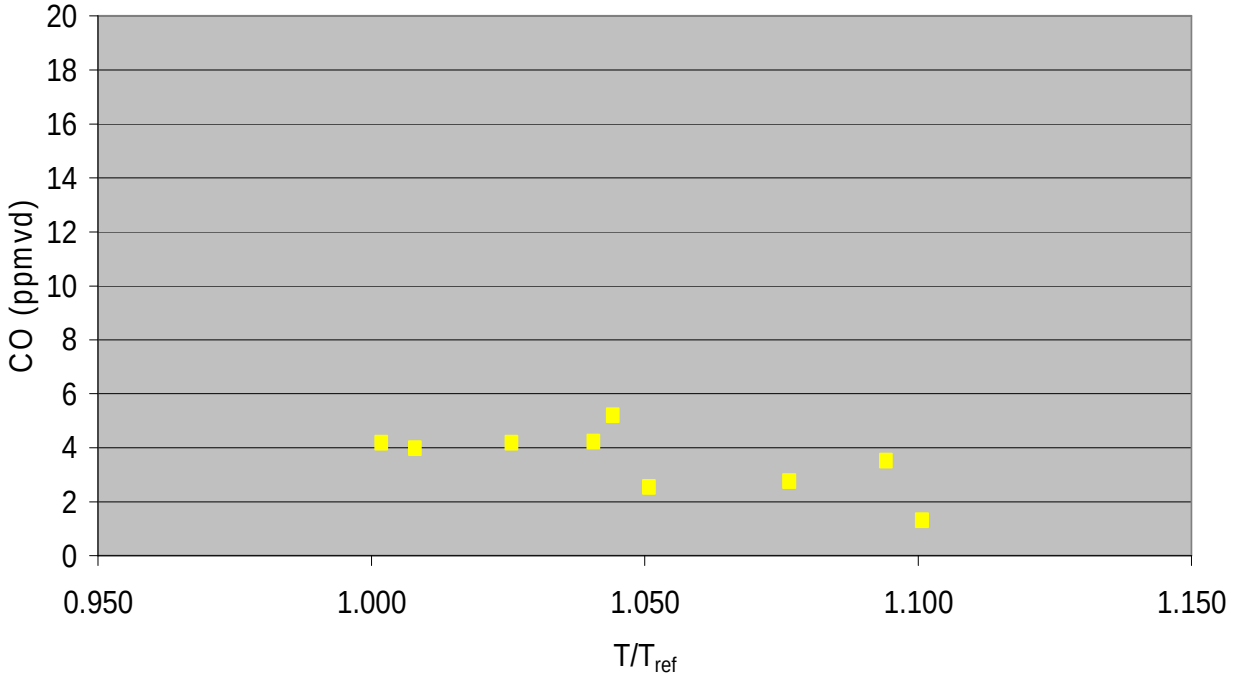

Figure 4-25 Prototype 2c CO emissions

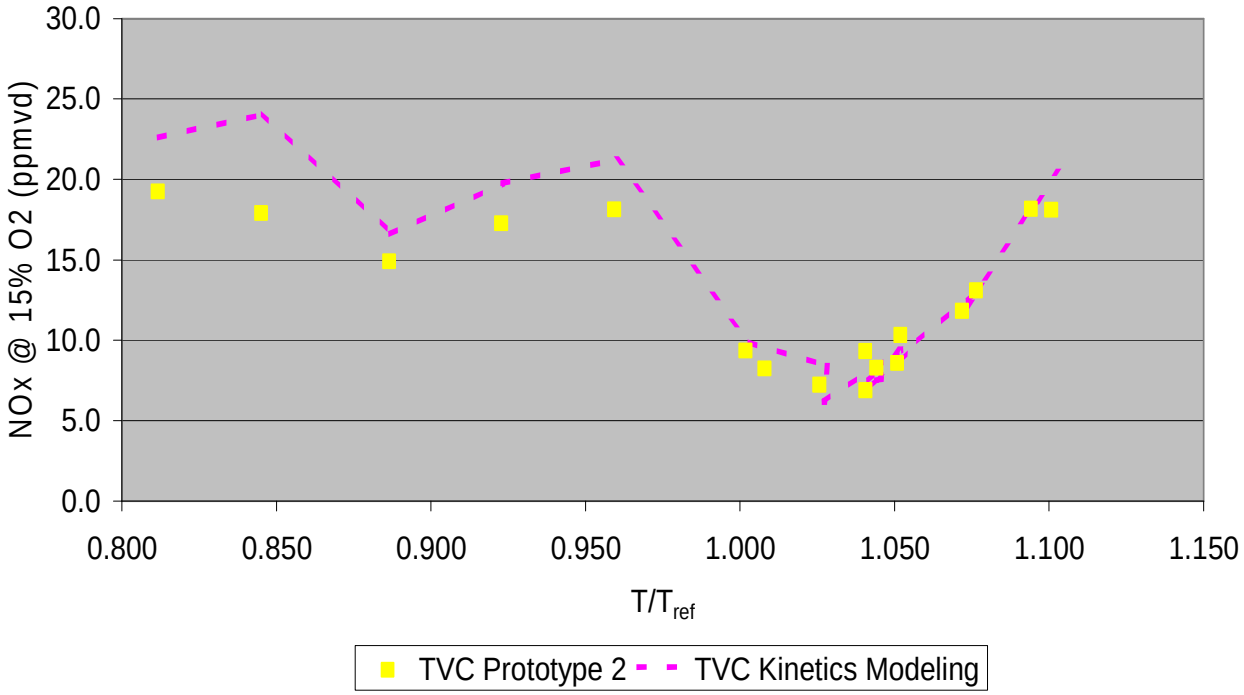

Figure 4-26 Prototype 2c NOx emissions and turndown

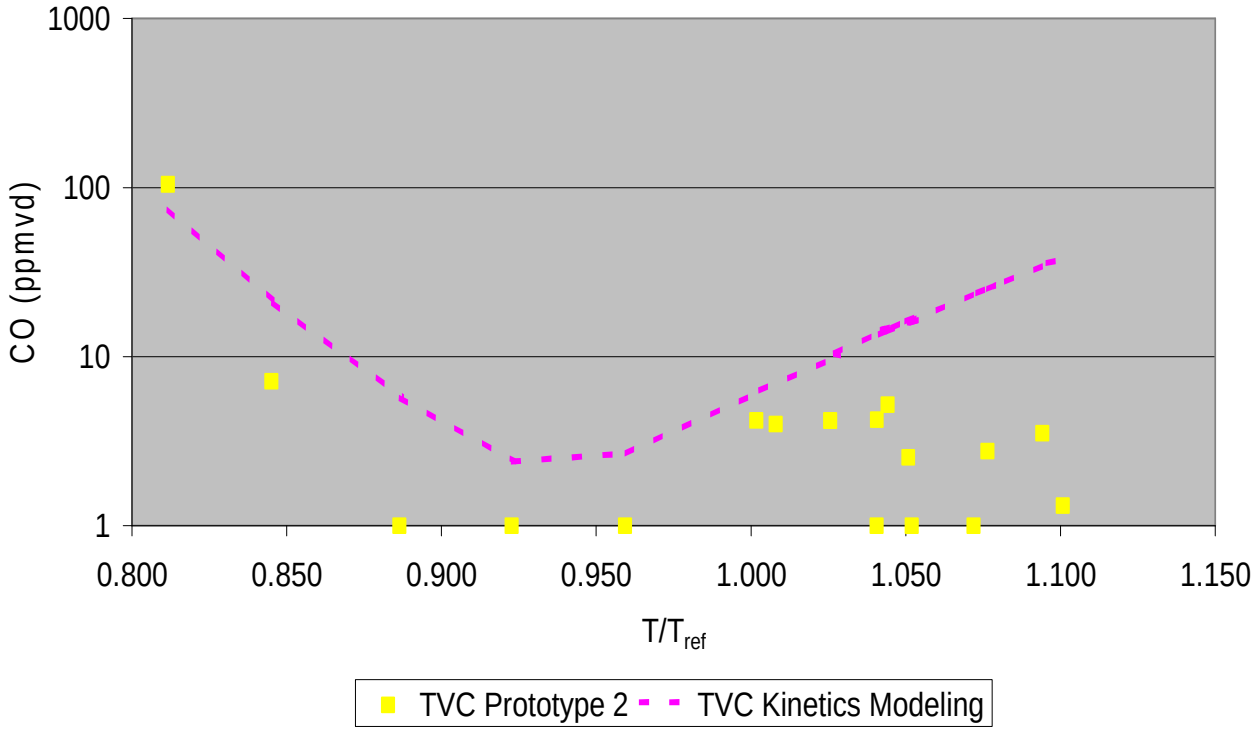

Figure 4-27 Prototype 2c CO emissions and turndown

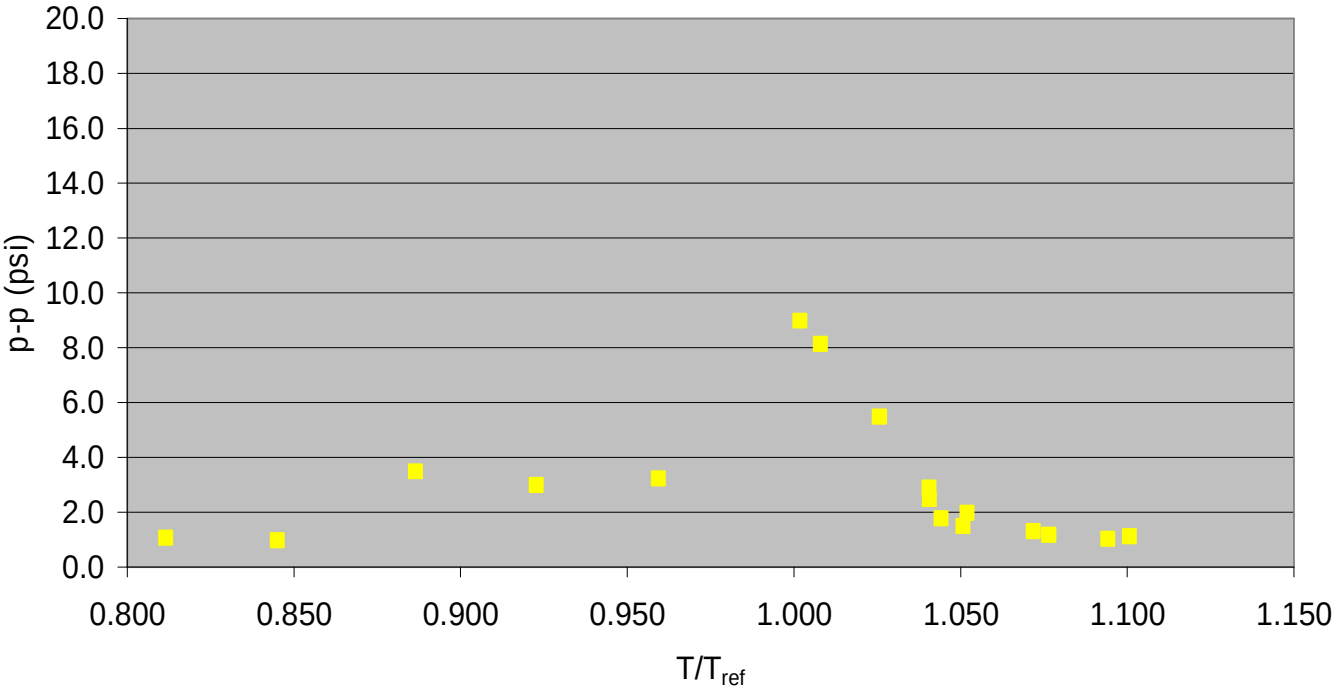

Figure 4-28 Prototype 2c dynamic response

4.3.2 Discussion

The prototype-1 data gave a clear indication that a significant redesign was needed to approach the targeted NOx & CO levels. The additional effort of redesigning the combustor eventually led to promising results. Prototype 2a2 showed significant reductions in CO. The NOx levels however remained above acceptable limits. Changing the air distribution and improving the premixer performance all had a demonstrated benefits in prototype 2b. Further modifications to the main premixer and air distribution in 2c reduced the NOx even further while maintaining the low CO. An assessment of the design indicated that premixer performance remained below ideal levels, and the design could be further modified for performance improvements. These discoveries justified the need for a third prototype, Prototype 3, with which to evaluate the emissions entitlement for the design.

Prototype 2c had several noteworthy performance features. The NOx emissions were below the 9 ppm target by as much as 24%, and the CO was well below the 10 ppm limit in the range of 1 to 5 ppm. Further reductions are desired, but the demonstrated capabilities of the prototype make the outlook promising. The combustor could be turned down nearly 20% below the reference condition while maintaining relatively low NOx and CO emissions. Additionally, the dynamics performance was excellent, and the region of high dynamics could be controlled. The prototype demonstrated good performance across various design features and would be the starting point from which to design a combustor to demonstrate the emissions entitlement.

The network model was able to predict the emissions performance of Prototype 2c with good fidelity. The NOx prediction followed the experimental values within 15% and fared better at or above T_{ref}. The model showed a surprisingly strong ability to predict CO emission which is typically much more difficult. At high temperatures the model tended to over predict the CO, but the ultra-low emission regime was captured by the model. The model was anchored by the geometry, flow conditions, and lean blow out performance and had only a few tuning parameters. The ability of the model to represent the combustor performance gives credence to the modeling approach which was based on understanding the combustion phenomena.

4.4 Prototype 3

4.4.1 Experimental Results

Two variations of the forward wall design were manufactured & evaluated and are named Version P3-1b and P3-2a. Combustion testing of Version P3-2a produced high dynamics as shown in Figure 4-30 at moderate flame temperatures. Therefore, the hardware was changed to install the P3-1b forward wall. All data presented are with this version. Tests were performed over a range of flame temperatures and cavity/main fuel splits to capture emissions and dynamics behavior. Two sets of data are taken with the conditions given in Figure 4-29, referred to as FA and FB conditions.

To determine the effectiveness of the thermal design of the impingement cooling sleeve, temperature measurements were made around the combustion cavity in the cooling zone. Figure 4-31 shows the combustor wall temperatures at full preheat and pressure conditions over the range of test points examined. The aft wall of the combustor cavity section experienced the highest temperatures over a broad range of flame temperatures, around the allowable temperature limit, Tref. This is an expected result since the fuel and air exiting the cavity slots impinge directly on this wall and burn nearby. The corner, or nose of the cavity between the cavity and main section, experienced cooler temperatures. This section of the combustor is directly where the hot cavity vortex and main flame streams interact. The outer wall, or annulus of the cavity combustor, experienced cool wall temperatures. Future work will include reducing the aft wall and corner temperatures more as this is a limiting condition for burning at higher equivalence ratios in the cavity zone.

Emissions data are averaged over 15 seconds at each data point and are post processed using a weighting factor according to position across the combustor. Five positions are compiled for one data point (10%, 30%, 50%, 70%, and 90% of span). The profile across the combustion liner span is skewed as shown in

Figure 4-32 and Figure 4-33 with an increase of up to 0.15 seen across the span. In general there was a “sweet spot” between the cavity/main fuel split that yielded the best the best performance. Also since samples at two probe locations were taken, about 16 in and 25 in downstream of the combustor, clear trends with residence times are noticed.

At a FA conditions, the lowest NOx15 recorded was 8.6 ppm with about 20% cavity fuel split at the 16 inch probe location as shown in Figure 4-34. This is on par with the typical NOx rating of 9 ppm for an FA machine. The CO at this condition was high, but further downstream the CO dropped to significant levels. At higher and lower percentages of cavity fuel splits, NOx15 increases. The trend of CO emissions was inversely related to NOx15. At 25 in downstream, the NOx15 emissions increased by about 4.5 ppm and CO was reduced to nearly zero. The dynamics data over the same test conditions is given in Figure 4-35. The dynamics levels fell within an acceptable range around 2 psi peak to peak. The highest dynamics occurred near a 19% cavity fuel split at just over 2 psi peak-to-peak with a frequency of about 58 Hz.

For the FB condition, NOx15 emissions were minimized with a high cavity fuel split. The fuel split was raised to 19% and the NOx emission was only 8 ppm. This represents a greater than 60% reduction in the NOx emission for an FB gas turbine which

is typically rated for 25 ppm NOx15 emission. At FB conditions the CO emission was well below the 10 ppm target at the low NOx condition as shown in Figure 4-36. CO emissions followed a similar profile with NOx15 emissions initially rising and then decaying as the % cavity fuel was increased. As with the FA condition the lowest CO emission was with high cavity fuel split. Further downstream in the combustor the CO emission was nearly zero over the full range of operation. Over the full range of fuel splits at FB conditions the combustion dynamics did not exceed 2 psi peak to peak with frequencies ranging from 25 to 55 Hz as shown in Figure 4-37.

A summary of the NOx15 and CO emissions from all data points is plotted in Figure 4-38, Figure 4-39, and Figure 4-40. At high temperatures the low NOx performance represents a significant improvement over current technology. The lowest CO levels are consistently with the longer combustor length. The tradeoffs between residence time and emission performance are evident from the results. Variation in the cavity fuel split accounts for the rest of the scatter in the data. The data shows regimes of high and low dynamics, where generally the dynamics are low at high flame temperatures.

	FA	FB
Preheat temperature, T3 (F)	745 - 760	755 - 820
Flame temperature (F)	2603 - 2675	2800 - 2910
Combustion Pressure (atm)	14.9 - 15.3	14.8 - 15.7

Figure 4-29 Prototype 3 experimental test conditions

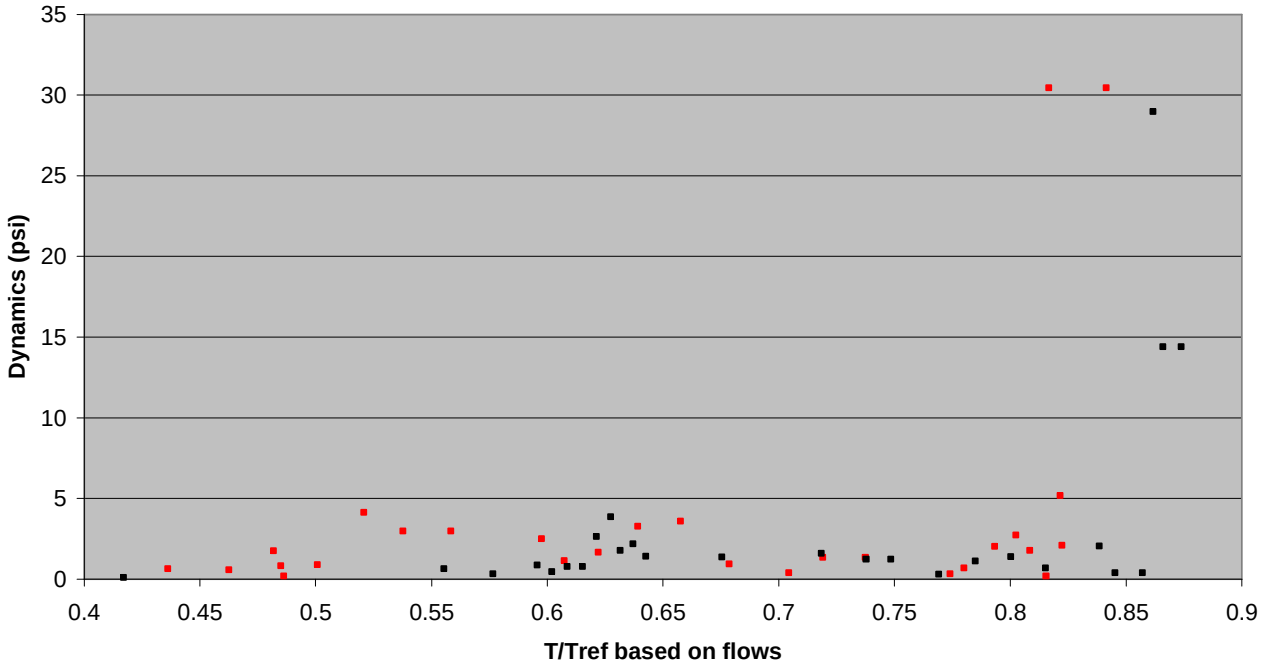

Figure 4-30 Prototype 3 dynamic pressure oscillations of forward wall Version P3-2a

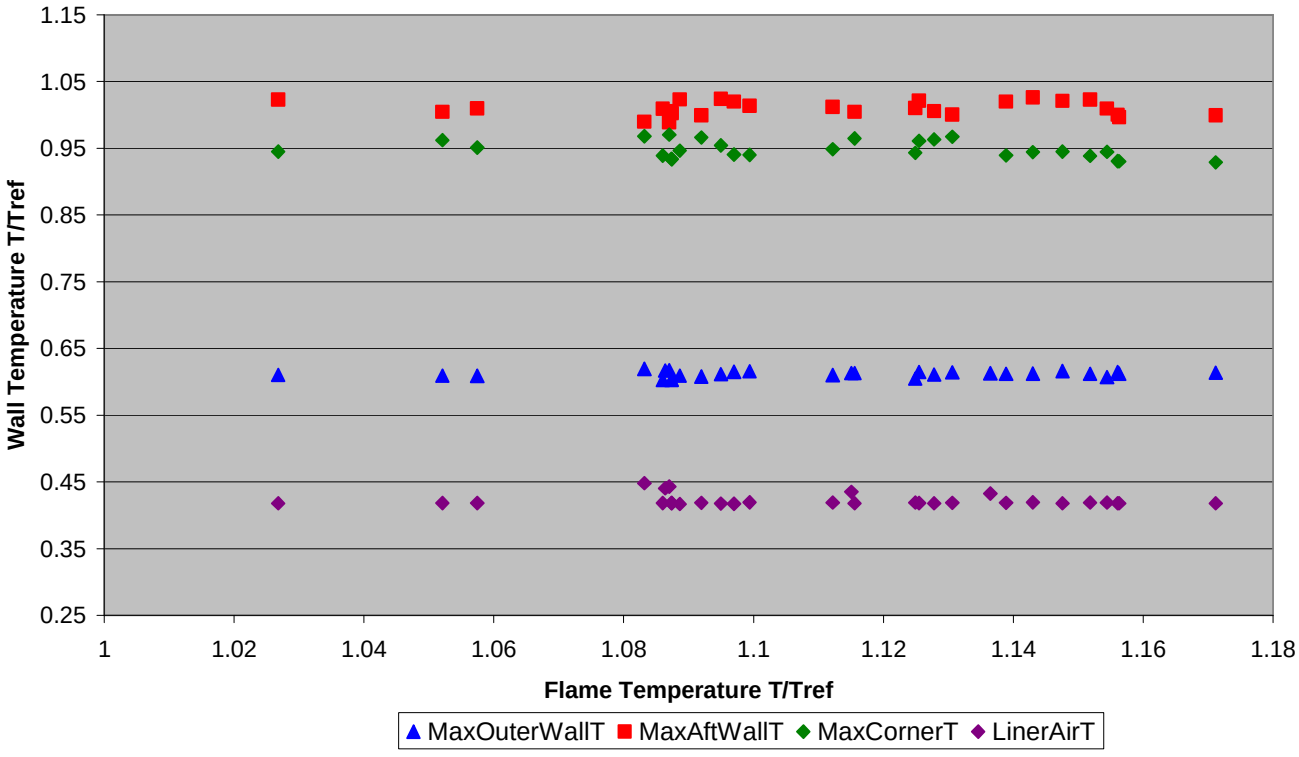

Figure 4-31 Prototype 3 combustor metal wall temperatures versus combustion flame temperature

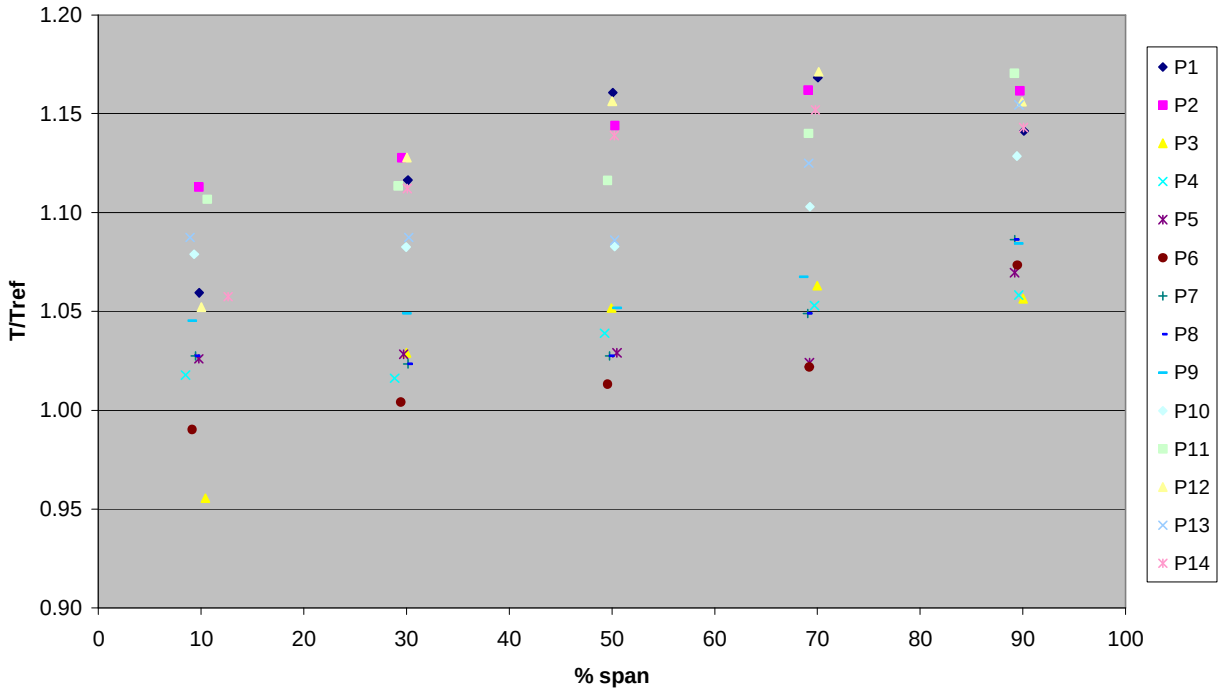

Figure 4-32 Prototype 3 combustion temperature based on O2 emissions as a function of span across combustor

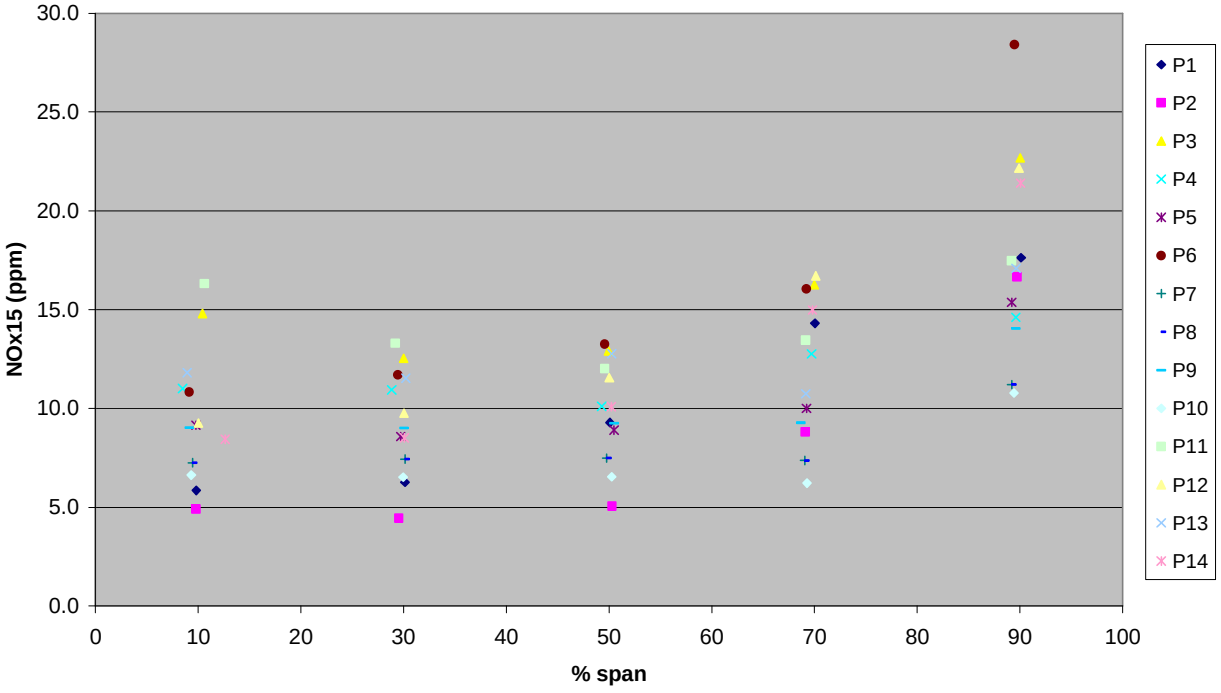

Figure 4-33 Prototype 3 NOx15 versus span position across combustor

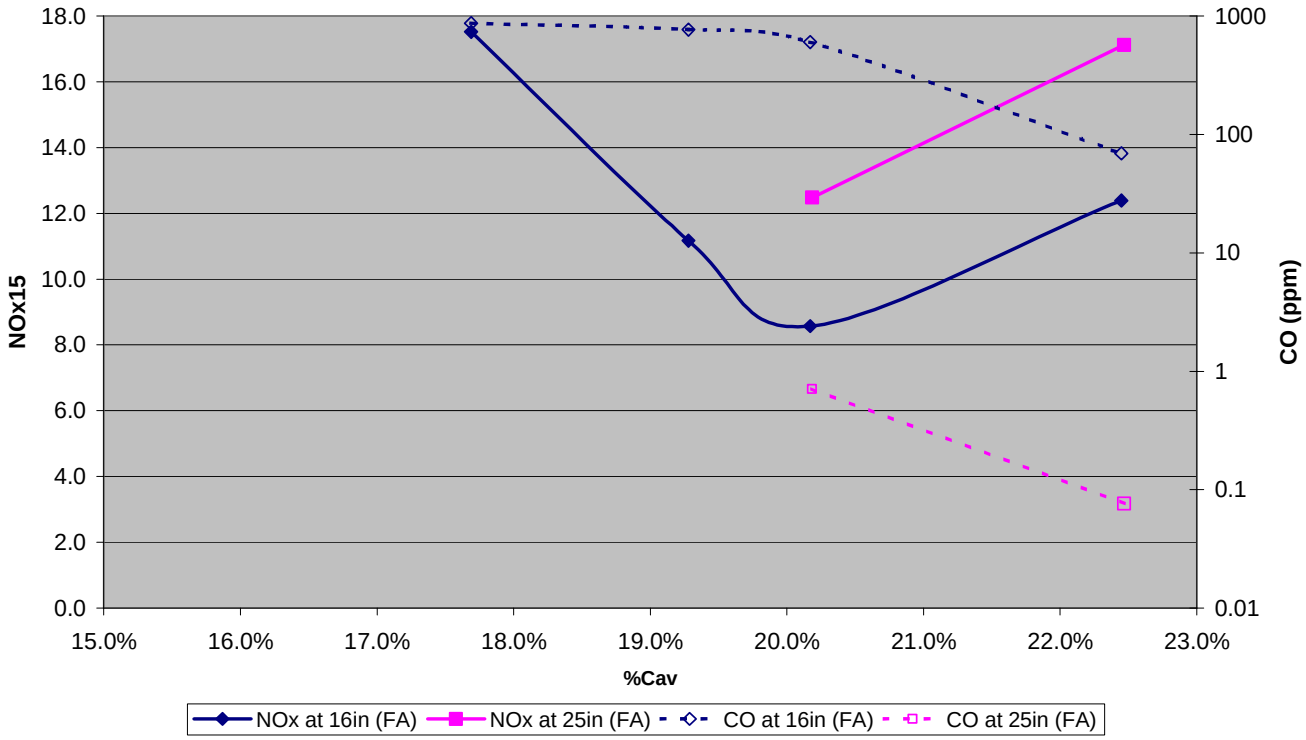

Figure 4-34 Prototype 3 NOx15 versus %cavity fuel split for two sample probe locations at FA conditions

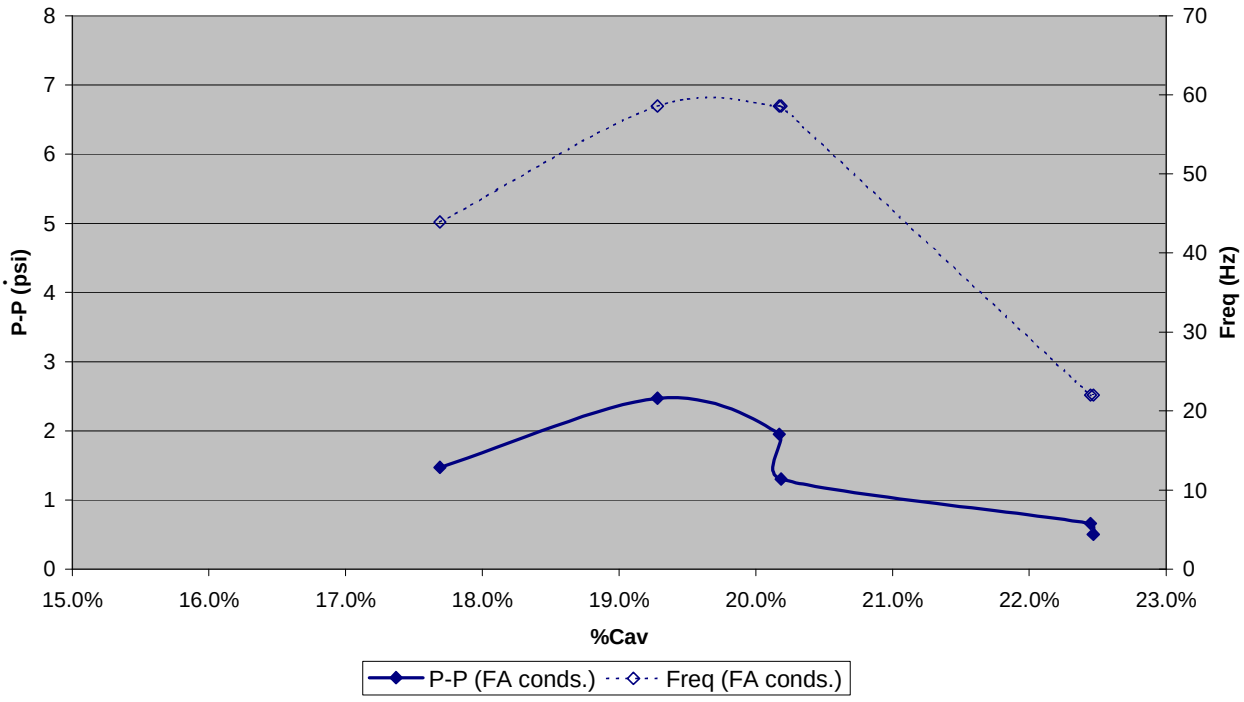

Figure 4-35 Prototype 3 combustor dynamics versus %cavity fuel split at FA conditions

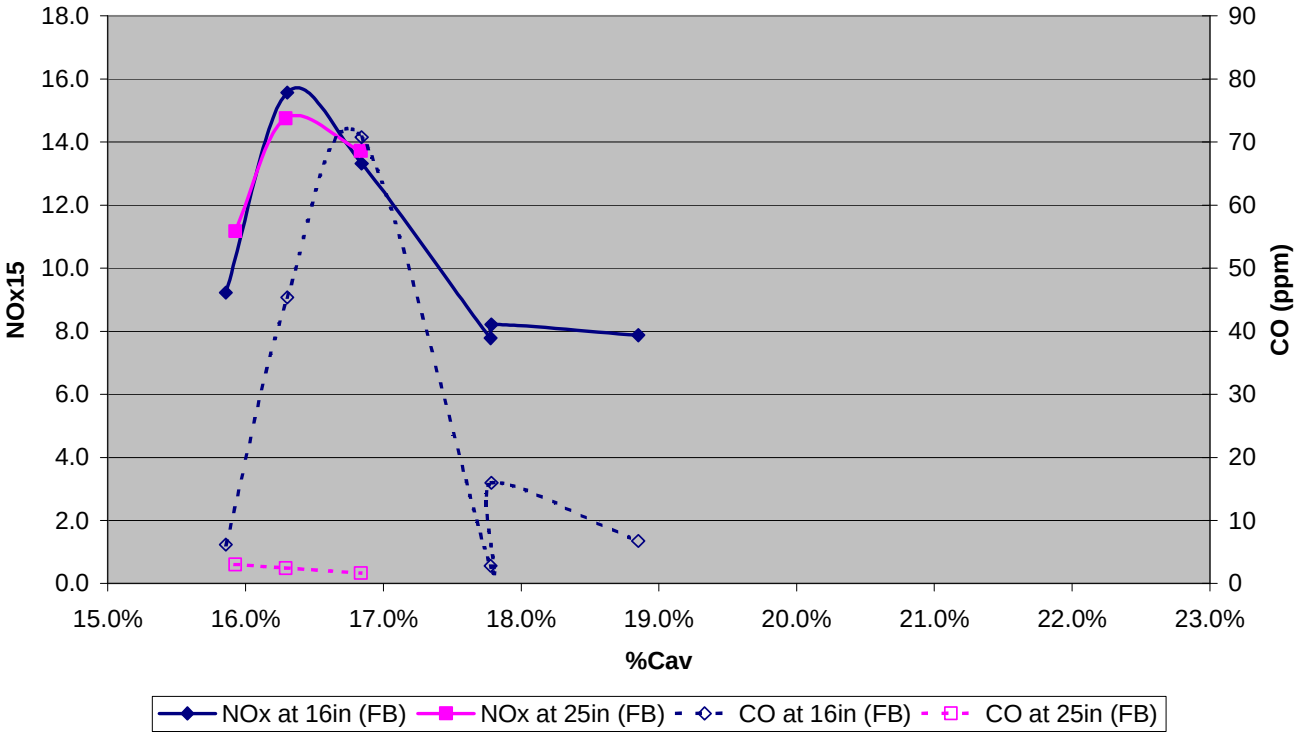

Figure 4-36 Prototype 3 NOx15 versus %cavity fuel split for two sample probe locations at FB conditions

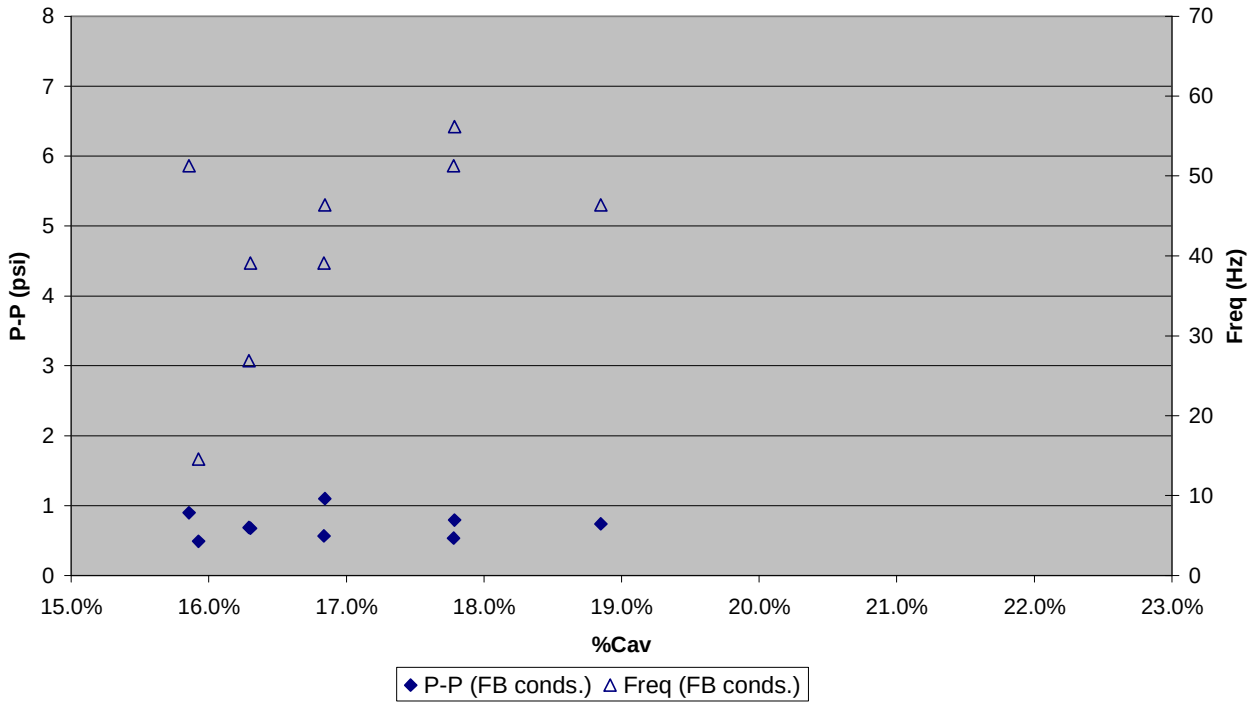

Figure 4-37 Prototype 3 combustor dynamics versus %cavity fuel split at FB conditions

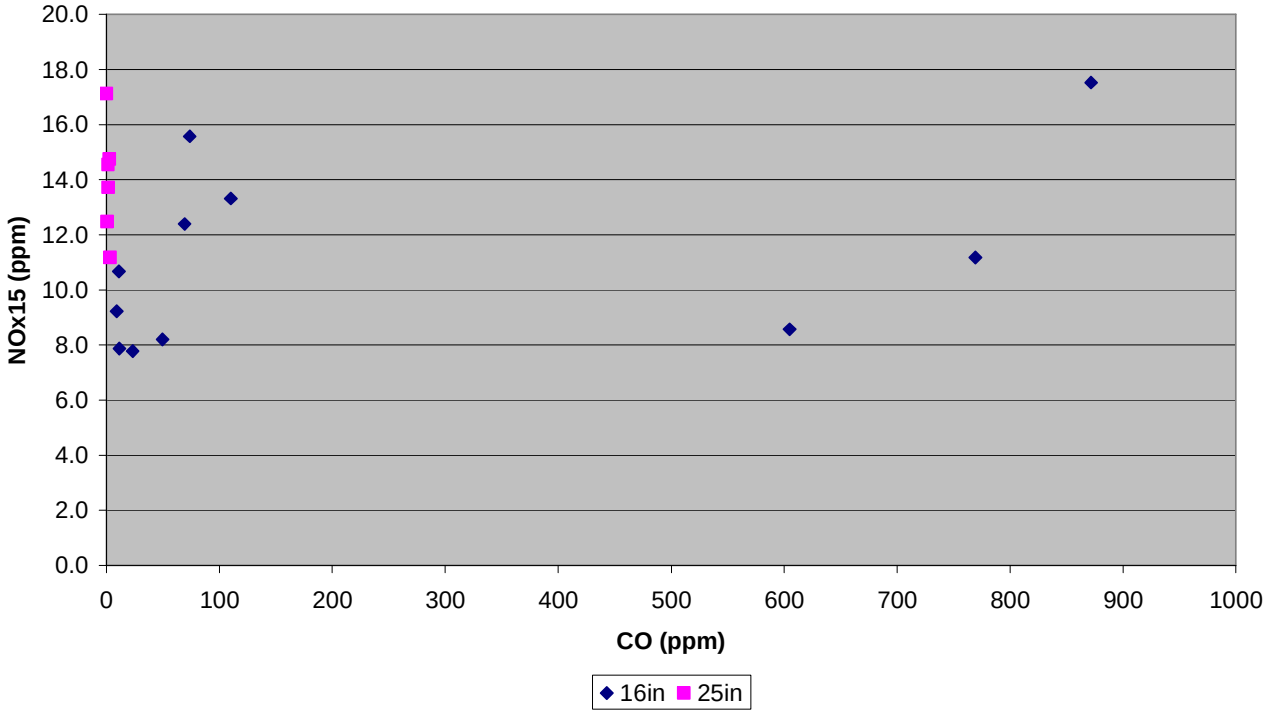

Figure 4-38 Prototype 3 NOx15 versus CO for all data points including combustion temperatures at FA and FB

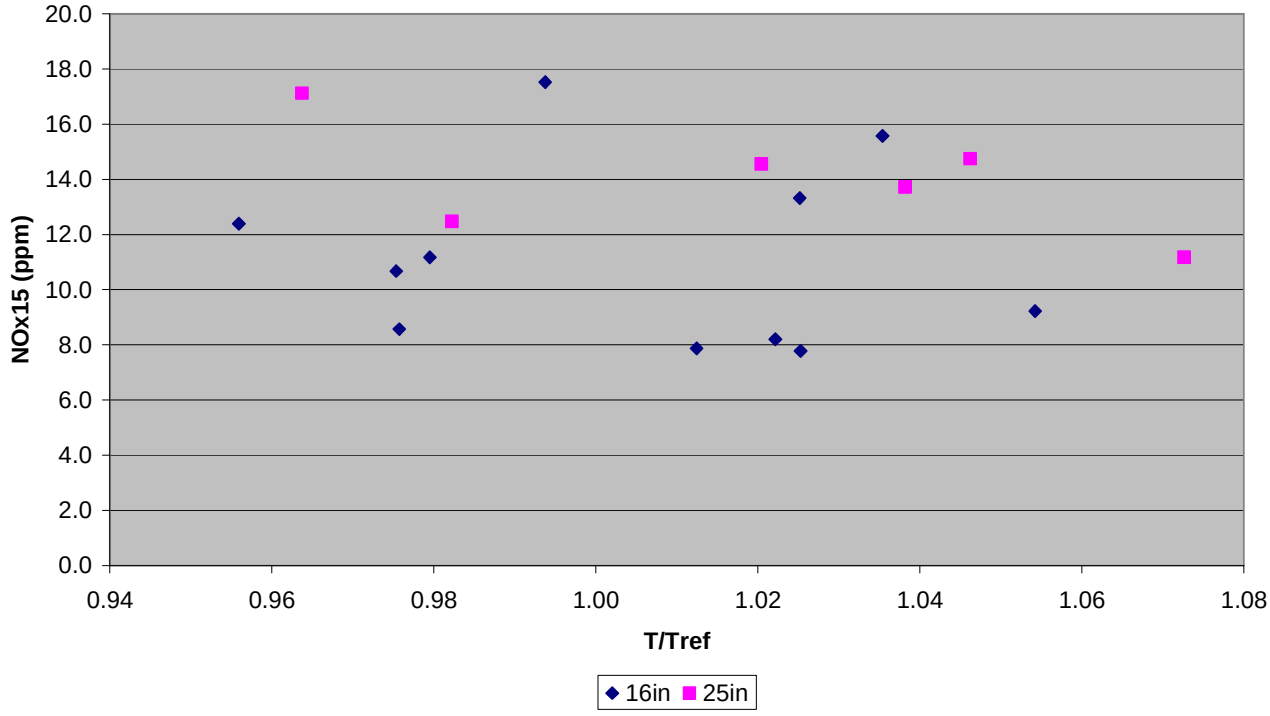

Figure 4-39 Prototype 3 NOx15 versus combustion temperature based on O2 concentration for all data points

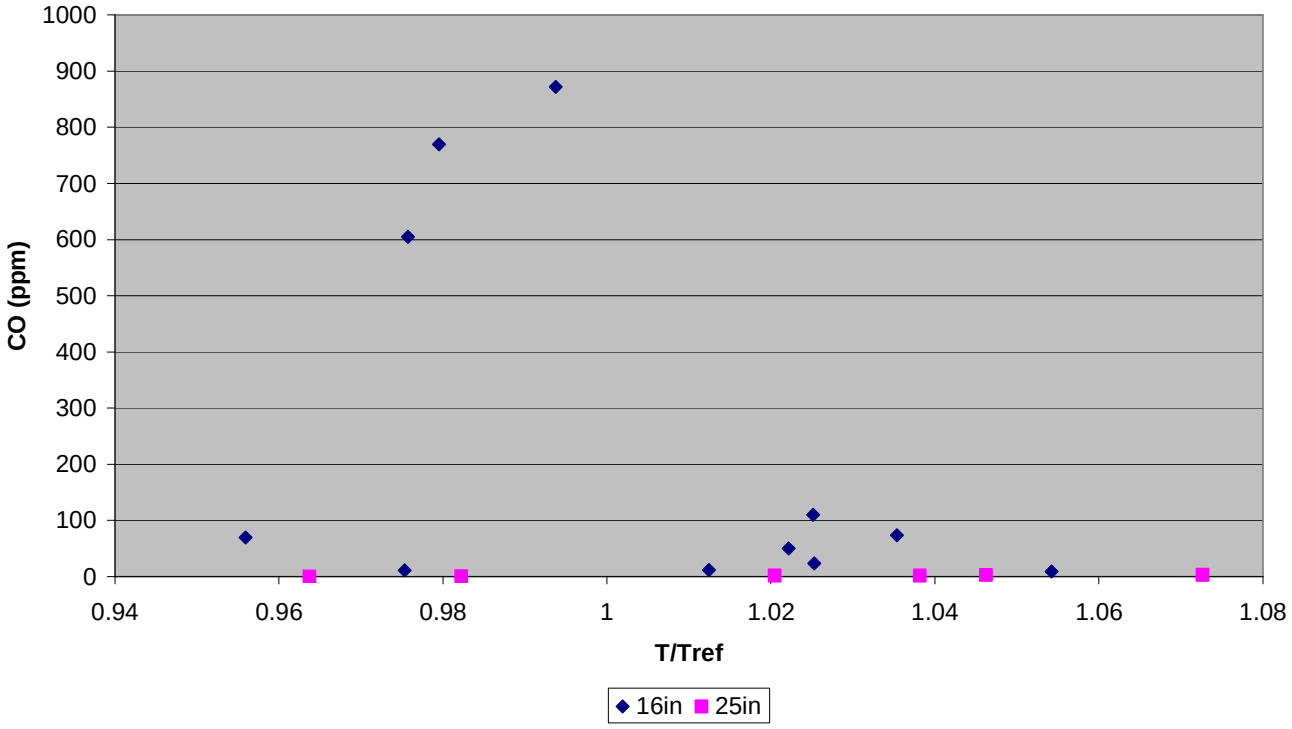

Figure 4-40 Prototype 3 CO versus combustion temperature based on O2 concentration for all data points

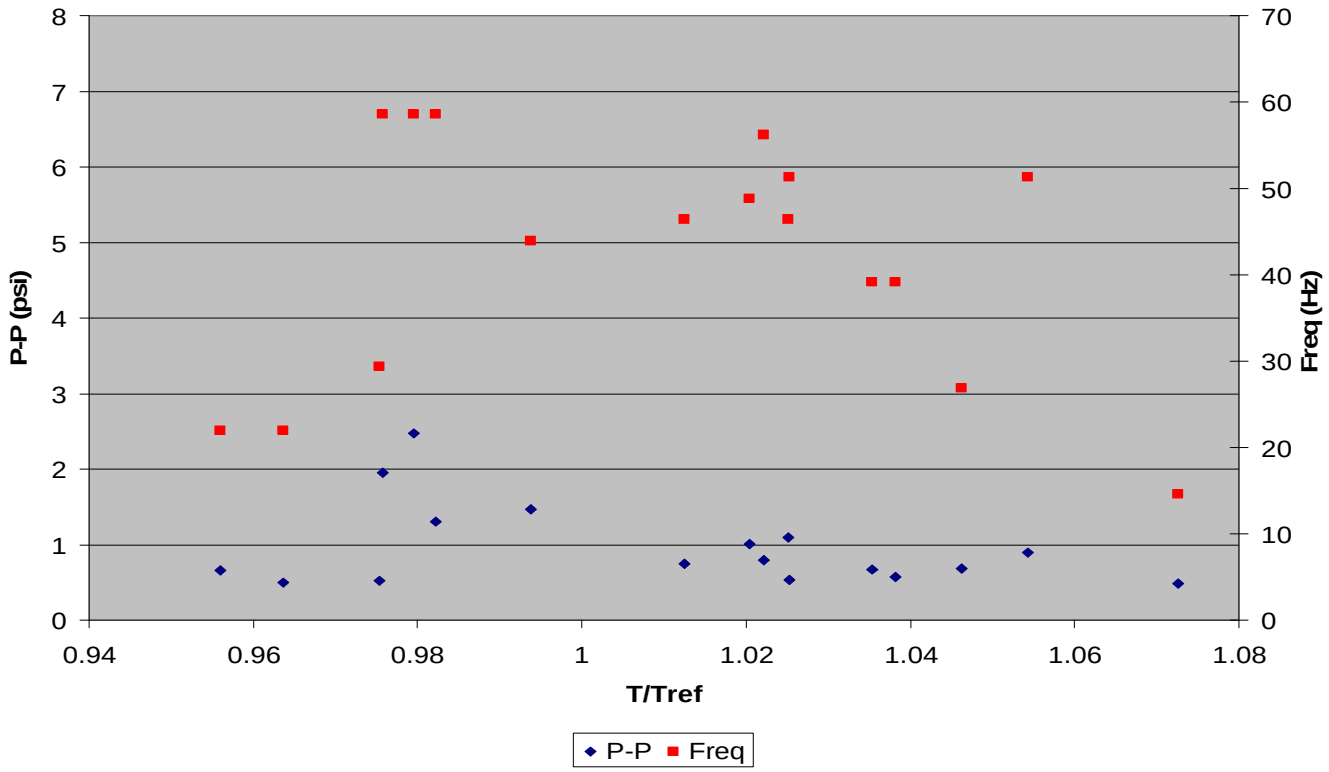

Figure 4-41 Prototype 3 dynamics versus combustion temperature based on O2 concentration for all data points

4.4.2 Discussion

The NOx performance for Prototype 3 exceeded the 50% NOx reduction goal at FB conditions while maintaining single digit CO emissions but the improvements were not evident at FA conditions. The biggest factors in emissions performance include cavity fuel split, radial sampling location, and flame temperature. For the data at FA conditions, a "sweet spot" is observed over the range of cavity fuel splits where dynamics is minimized. At low cavity fuel splits, the main section environment is hotter and susceptible to producing more NOx. Since this is where the majority of the mass flow burns, the overall combustor NOx increases. At very high cavity fuel splits, more NOx may be produced due to the very hot products in the cavity section.

CO burnout was generally good at high flame temperatures, and can be adjusted with combustor length. With a longer combustor the CO was easily burned out and emissions fell below 10 ppm at both conditions. With a shorter combustor high CO levels accompanied the 8 ppm NOx at the FA condition, and 10 ppm could be surpassed at the FB test condition. The optimal NOx vs. CO point taken in this set of experiments yielded 7.8 ppm NOx and 3 ppm CO at FB conditions.

A linear temperature profile is observed over all operating regimes. This profile suggests non-uniformity from the combustor exit section. This may be a result low mixedness in the main burner, leaks in the combustor, or damage to the rig. A flatter emissions profile would lessen NOx emissions even further.

With this prototype the combustion dynamics were very low. The peak dynamics levels fell below 3 psi p-p and the associated frequencies were below 100 Hz. Dynamics could be minimized with fuel split, but the effects were small because the dynamics levels were low.

5 Conclusions

5.1 Atmospheric Combustion Studies

The liquid fueled trapped vortex rig was successfully modified for natural gas injection. Four configurations were examined and tested based on fuel injection strategy. Also, a chemical kinetics model was developed, showing that the NOx generation can become small if a good fuel/air mixing is achieved in the fuel-lean cavity and main sections. The best performing configuration resulted in a 27% reduction in NOx.

5.2 Prototype 1

Prototype 1 demonstrated the mechanical viability of the TVC design and gave some hint of the low emission potential. The best performance was a 25% reduction in NOx, however CO was excessive at low levels of NOx. At the low NOx data points, the CO was at least 50% above the target. Changing the fuel injection scheme, and cavity air, and the main floor area were concluded to be necessary to improve the performance.

5.3 Prototype 2

Several design changes were performed in Prototypes 2a2, 2b, and 2c. Design changes planned for Prototype 2a1 was determined not to be able to meet the NOx reduction target in the modeling design phase. For Prototype 2a2, the incorporation of annular premixing ports in the cavity section, and improved combustor surface cooling resulted in lower NOx and CO as compared to Prototype 1. For Prototype 2b, the cavity premixer and cavity designs were modified, the main burner was redesigned, and outer wall effusion cooling was eliminated. Prototype 2c was further improved to account for thermal stresses on the previous prototypes. The NOx emissions for Prototype 2c were an improvement on DLN combustion system levels, but fell short of the 50% improvement that is targeted.

Also in this design phase, a robust modeling tool was developed which captures the main flow field characteristics and provided design guidance on emission performance. The modeling results indicate that improvements to the premixer performance and aft wall injection air can improve emission performance.

Strong emission performance, turndown, and dynamics performance by prototype 2c made the goal of 50% NOx reduction appear within reach. Strategic incremental changes in the design were able to reduce the NOx while maintaining low CO. Further improvements require more drastic changes to demonstrate the entitlement capabilities of the design. The modeled performance reinforces confidence that the low emission performance is grounded on sound physical principals.

5.4 Prototype 3

Prototype 3 incorporated several design enhancements in an effort to reach emissions targets. Extensive CFD and thermal modeling was performed to aid in this analysis, in addition to Six Sigma design practices. The design changes incorporated better premixing, reducing the cavity size, reducing circumferential variation in the cavity

premixer, and replacing combustor cavity wall cooling with an impingement cooled flow sleeve.
The NOx emissions for Prototype 3 exceeded the 50% NOx reduction goal at the FB condition, and showed lesser improvement at FA conditions. The combustion dynamics with this prototype were even lower than Prototype 2C. CO burnout was generally good at high flame temperatures producing single digit emission levels. At lower temperatures, the preference was toward a longer residence time for low CO.

6 References

[1] Hsu, K-Y, Goss, L.P., Roquemore, W.M. “Characteristics of a Trapped-Vortex Combustor,” Journal of Propulsion and Power, 14 (1): 57-65, 1998.

[2] Sturgess, G.J., Hsu, K-Y, “Entrainment of Mainstream Flow in a Trapped Vortex Combustor,” AIAA 97-0261, 35th AIAA Aerospace Sciences Meeting, Reno, NV, 1997.

[3] Bowman NOx model from 24th symposium